

Alterations of Plant and Bacterial Sulfate Assimilation Pathway Affect Immunity and Pathogenicity

Inaugural - Dissertation

zur

Erlangung des Doktorgrades

der Mathematisch-Naturwissenschaftlichen Fakultät

der Universität zu Köln

2023

vorgelegt von

M.Sc. Li Chen

Aus Xiantao, China

Berichterstatter/in:

Prof. Dr. Stanislav Kopriva

Prof. Dr. Alga Zuccaro

Tag der Promotion:

Abstract

Sulfur is an essential component for the biosynthesis of primary and secondary metabolites for all organisms. Camalexin and glucosinolates that share a common precursor Indole-3-acetaldoxime (IOAx), are important sulfur-containing secondary metabolites and play a crucial role in mediating sulfur-induced resistance against pathogens in Arabidopsis. It has been reported that pathogens deficient in cysteine biosynthesis have decreased virulence. However, it is still unclear how changes in the sulfur assimilation pathway and modulation of overall sulfur metabolism affect bacterial virulence and plant susceptibility. In this study, we used the rice pathogen *Burkholderia glumae* PG1 strain (wild type) and the model plant *Arabidopsis thaliana* (Col-0) to bilaterally investigate the effects of regulation of the sulfate assimilation pathway. We examined not only its influence on the pathogenicity of *B. glumae*, but also the effects of changes in plant sulfur metabolism on susceptibility and immune response to pathogens. As a non-host pathogen of Arabidopsis, *B. glumae* is able to colonize Arabidopsis and induce high camalexin accumulation. Its mutants *cysH* and *cysM*, are deficient in reducing 3'-phosphoadenosine 5'-phosphosulfate (PAPS) to SO_3^{2-} and in converting thiosulfate to S-sulfocysteine respectively. Mutants *cysH* and *cysM* were less virulent than PG1 because they had attenuated pathogenic properties such as less plant growth inhibitory effect, less camalexin induction and triggering weaker hypersensitive response in Arabidopsis. The colonization result indicates that the ability of the pathogen to proliferate inside plants and acquire nutrients from the host plant are reduced when its sulfate assimilation pathway is impaired. Various Arabidopsis sulfur metabolisms mutants were investigated as well. Different camalexin accumulation patterns elicited by PG1, *cysH* and *cysM* at Col-0, *myb28 myb29* and *slim1-1* indicate that the regulation of sulfur metabolism in Arabidopsis has an impact on its response to pathogens, highlighting the complex sulfur flux between camalexin and glucosinolates in different Arabidopsis genotypes. Furthermore, it was found that SLIM1, a well studied transcription factor related to sulfur deficient response, is involved in the regulation of plant defense response because PG1 and bacterial mutants induced camalexin in *slim1-1* at the same level, and SA accumulation in *slim1-1* was significantly lower than in Col-0. This is the first research attempt that combines both bacterial and plant mutants to manipulate levels of sulfur metabolites and ability to use sulfur compounds to investigate effects

of sulfur metabolism on plant-pathogen interactions and shed light on the comprehensive regulation of sulfur metabolism under pathogen attack.

Table of contents

Abstract	I
1 Introduction	1
1.1 The importance of sulfur	1
1.2 The sulfate assimilation pathway of <i>Arabidopsis thaliana</i>	2
1.3 The sulfate assimilation pathway of bacteria	5
1.4 Plant-pathogen interactions and integrated defense response	7
1.5 Sulfur-induced resistance	9
1.6 Glucosinolates and camalexin.....	11
1.7 Nutrient acquisition strategies employed by bacteria	14
1.8 Aim of the thesis	15
2 Materials and Methods	17
2.1 Plant materials.....	17
2.2 Bacterial strains and culture conditions	18
2.3 Bacterial growth in different sulfur sources	18
2.4 Co-cultivation of Col-0 and bacteria strains	21
2.5 Leaves infiltration	22
2.6 Chlorophyll measurements.....	22
2.7 12-well hydroponic system	23
2.8 Visualization of H ₂ O ₂ with the DAB staining method.....	23
2.9 Bacterial growth in media containing shoot metabolites	24
2.10 Bacterial concentration quantification	26
2.11 Metabolites analysis	28
2.11.1 Isolation & quantification of camalexin.....	28
2.11.2 Isolation & quantification of glucosinolates	28
2.11.3 Isolation & quantification of low-molecular weight thiols	29
2.11.4 Determination of Pipecolic acid and salicylic acid	30
2.12 Gene expression analysis	30
2.13 Data analysis	32
3 Results	33
3.1 The bacterial <i>cysH</i> mutant is deficient in consuming oxidized sulfur sources	33

3.2 <i>cysH</i> and <i>cysM</i> mutants have less severe growth inhibitory effect on <i>Arabidopsis thaliana</i>	34
3.3 PG1 elicits stronger hypersensitive response on <i>Arabidopsis</i> leaves than <i>cysH</i> and <i>cysM</i> mutants	36
3.4 PG1 triggers stronger initial immune response in <i>Arabidopsis</i> than <i>cysH</i> and <i>cysM</i> mutants	38
3.5 <i>B. glumae</i> PG1 induces higher level of the phytoalexin camalexin.....	39
3.6 Exogenous cysteine restores pathogenicity of <i>cysH</i> and <i>cysM</i> mutants.....	40
3.7 PG1 harbours more robust colonization ability than <i>cysH</i> and <i>cysM</i> mutants.....	43
4 Results	45
4.1 Modulation of sulfur assimilation in <i>Arabidopsis</i> has an impact on immune response to <i>B. glumae</i>	45
4.2 Contents of sulfur-containing metabolites in <i>Arabidopsis</i> Col-0, <i>myb28 myb29</i> and <i>slim1-1</i> do not change upon microbial infection.....	49
4.3 <i>SLIM1</i> is potentially involved in immune response triggered by <i>B. glumae</i>	53
4.4 <i>cysH</i> grows slower than PG1 and <i>cysM</i> when fed with shoot extracts of <i>myb28 myb29</i> and <i>slim1-1</i>	57
5 Discussion.....	60
5.1 Sulfur assimilation pathway affects virulence of <i>cysH</i> and <i>cysM</i>	60
5.2 Reduced nutrition acquirement and bacterial proliferation in plant niches partly explain attenuated pathogenicity of mutants <i>cysH</i> and <i>cysM</i>	62
5.3 Differences between the <i>cysH</i> and the <i>cysM</i>	64
5.4 Regulation of sulfate assimilation pathway in <i>Arabidopsis</i> affects camalexin induction pattern by <i>B. glumae</i>	67
5.5 <i>SLIM1</i> is involved in the regulation of <i>Arabidopsis</i> defense response.....	69
5.6 Camalexin, glucosinolates and pipercolic acid demonstrated different accumulation pattern following bacterial infection	71
5.7 Conclusions and outlook	73
References	75
Supplemental data	89
List of abbreviations	91
List of tables and figures	93
Acknowledgement.....	95
Erklärung.....	97
Curriculum Vitae.....	98

1 Introduction

1.1 The importance of sulfur

Sulfur is a crucial macronutrient for all organisms. Sulfur is present in nature in both inorganic and organic forms. Sulfur can change its oxidation state from the most oxidized form (+VI redox state) to the most reduced form (-II redox state). Sulfur's property of changing its oxidation state leads to its frequent occurrence in a number of important compounds including the amino acids cysteine (Cys) and methionine (Met), vitamins (biotin and thiamin), a wide variety of coenzymes, prosthetic groups (Fe-S clusters) and other primary and secondary metabolites (Sekowska et al., 2000; Nakai and Maruyama-Nakashita, 2020). Sulfur is an essential element for all organisms due to its biochemical versatility. In plants and microbes, these sulfur-containing metabolites have multiple functions (Sekowska et al., 2000). For example, sulfur-containing compounds play an important role in plant resistance against biotic stress. Reduced glutathione (GSH) is considered to be one of the most important scavengers of reactive oxygen species (ROS) and play an important function in redox homeostasis. The ratio of GSH:GSSG (oxidized glutathione) is used as a marker of oxidative stress in plants, which causes profound alterations in structures of proteins, nucleic acids, lipids and cellular membranes (Spoel and Loake, 2011; Rahantaniaina et al., 2013). Glutathione is also important for bacteria. It is one of the most abundant nonprotein thiols in cyanobacteria and proteobacteria, plays a protective role under conditions of oxidative stress, low pH and osmotic stress. It is also a post-translational regulator of protein function by the direct modification of proteins via glutathionylation (Masip et al., 2006). Iron-sulfur clusters are simple inorganic structures that are bound to many enzyme complexes and play versatile roles in multiple fundamental biological processes, including DNA repair, ribosome biogenesis, photosynthesis, and gene expression regulation (Frazzon and Dean, 2003; Xu and Møller, 2011; Imsande, 1998). Glucosinolates (GLS) and indole-type phytoalexins are two highly diversified sulfur-containing secondary metabolite groups that have been shown to act in plant immunity (Bednarek, 2012; Chhajed et al., 2020). In addition to the defensive function, sulfur is closely related to crop yield and quality as well (Gutierrez Boem et al., 2007; Malhi et al., 2007).

Sulfur nutrition is particularly important not only for plants themselves but also for humans as sulfur deficiency affects the growth, development, disease resistance, and performance of plants

and also has a great impact on the nutritional quality of crops, from which we obtain our primary source of the essential Cys and Met. Several studies have demonstrated that sulfur deficiency affects biomass production, chlorophyll content and morphological parameters, yield, and nutritional value of the plants (Houhou et al., 2018; Yu et al., 2021b). It has been reported that sulfate deficiency leads to decreased assimilation rates of CO₂ and eventually results in retarded synthesis of carbohydrates and chlorosis of wheat young leaves (Gilbert et al., 1997). It was also reported in rice plants (*Oryza sativa* L. cv. IR72) that an increase of sulfate concentration in the medium resulted in a significant increase in the relative growth rate, leaf blade and leaf sheath (Resurreccion et al., 2001).

1.2 The sulfate assimilation pathway of *Arabidopsis thaliana*

In nature, the most common form of sulfur is the oxidized inorganic sulfate (SO₄²⁻), but most functional bioorganic compounds of primary and secondary metabolism contain the reduced form of sulfur. Therefore, plants and microorganisms must reduce sulfate to sulfide and incorporate it into organic metabolites to perform its biological functions. The sulfur transport from soil to plant and the assimilation pathway within the plant have been extensively studied and reviewed by Kopriva et al., 2009, Takahashi et al., 2011 and Gigolashvili and Kopriva, 2014.

To successfully consume sulfur nutrition, plants first transport sulfate from the environment into roots. There are 12 characterized sulfate transporter genes (*SULTR*) in *Arabidopsis*. These genes have been subdivided into four groups based on sequence, which have distinct roles in sulfate uptake and allocation (Buchner et al., 2004). The root-specific genes *SULTR1;1* and *SULTR1;2* belonging to group 1 are dominant genes that facilitate sulfate uptake from the soil into the roots. *SULTR1;1* plays a major role when a plant suffers from sulfate starvation. On the other hand, *SULTR1;2* is more pronounced with sufficient sulfur supply (Rouached et al., 2008).

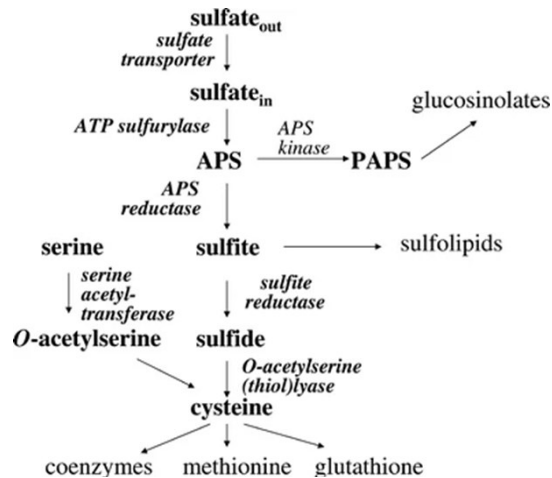


Figure 1.1 Scheme of plant sulfate assimilation

Transporters and enzymes are indicated in each steps (Kopriva et al., 2009).

Once taken up by plants, sulfate is activated, reduced and eventually incorporated into a diversity of bioorganic compounds via the sulfate assimilation pathway (Fig. 1.1). The sulfate is activated into adenosine 5'-phosphosulfate (APS) by ATP sulfurylase (ATPS). There are two branches emanating from APS in the sulfur assimilation pathway. In the first branch of the pathway, traditionally referred to as primary sulfate assimilation, APS is reduced by APS reductase (APR) to sulfite, then further reduced to sulfide by sulfite reductase (SiR), and consequently incorporated into the amino acid backbone of *O*-acetylserine (OAS) by *O*-acetylserine(thiol)lyase (OASTL). Cys is the first product of primary sulfate assimilation and can be used for the synthesis of methionine (Met), glutathione and a large number of important sulfur-containing biomolecules. In the second branch, APS is phosphorylated by APS kinase (APK) to form 3'-phosphoadenosine 5'-phosphosulfate (PAPS), which is a donor of activated sulfate for many sulfated metabolites, such as glucosinolates.

Sulfate assimilation is an essential process in plants, a deficiency in it leads to considerable modifications in sulfur metabolism and plant phenotypes. For example, experimental evidence shows that disrupting the function of APK1 and APK2 in *Arabidopsis* reduces glucosinolates levels. The double mutant *apk1 apk2* shows a remarkably visible semidwarf phenotype compared to wild-type (WT) plants (Mugford et al., 2009a). Depletion of SiR showed a similar result: the *A. thaliana* T-DNA insertion line *sir1-2* has only 14% SiR transcript levels compared to the WT and

is early lethal to seedling. *sir1-1* seedlings have 44% SiR transcript levels and are severely growth-retarded (Khan et al., 2010).

Sulfur assimilation is under complex regulation according to sulfur availability and environmental conditions. The control of sulfur assimilation occurs not only at the transcriptional level, but also at post-transcriptional level, such as the regulation of sulfate transporters and APR (Leustek et al., 2003; Yoshimoto et al., 2007; Scheerer et al., 2010). Several metabolites also play a role in regulating sulfate assimilation. For example, OAS is an important intermediate in the Cys biosynthetic pathway. Global expression profiling of sulfur-starved Arabidopsis revealed that OAS was a positive regulator of sulfur deficiency-response genes including *APR2* (Hirai et al., 2003). In contrast, the reduced form of glutathione (GSH) negatively regulates the sulfate uptake and the activity of ATP sulfurylase (Lappartient et al., 1999). The stress-related phytohormones jasmonate, abscisic acid and salicylate are also involved in the regulation of sulfate assimilation (Fodor et al., 1997; Harada et al., 2000; Koprivova et al., 2008; Li et al., 2021). Other transcriptional sulfur regulators worth highlighting here are SLIM1 and MYBs (Fig. 1.2). Sulfur Limitation 1 (SLIM1), is a critical regulator of sulfur assimilation under conditions of sulfur deficiency. It is involved in the upstream of assimilation pathway and affects the accumulation of sulfur-containing metabolites during sulfur limitation. RNAseq analysis showed that SLIM1 is intensely involved in the regulating the response to sulfur-deficiency in roots, with 83% of different expressed genes (DEGs) related to the sulfur-deficiency response being regulated by SLIM1, including sulfur compound transport and glucosinolates synthesis (Dietzen et al., 2020; Ristova and Kopriva, 2022). MYB transcription factors are important positive regulators of glucosinolates biosynthesis. Glucosinolates are sulfur-rich secondary metabolites found in plant order Brassicales, hydrolysis products of which play an important function in growth inhibition to a wide range of plant enemies. Glucosinolates can be classified into three categories based on their precursor amino acids: compounds derived from Ala, Leu, Ile, Met, or Val are called aliphatic glucosinolates, those derived from Trp are called indolic glucosinolates, those derived from Phe or Tyr are aromatic glucosinolates (Fahey et al., 2001). MYB transcription factors are divided into two categories: MYB28, MYB29 and MYB76 from group 1 which induce the biosynthesis of methionine-derived aliphatic glucosinolates (Gigolashvili et al., 2007b; Hirai et al., 2007); whereas MYB34, MYB51, and MYB122 are responsible for the regulation of indolic glucosinolates (Celenza et al., 2005; Gigolashvili et al., 2007a). Transgenic lines expressing each MYB gene

illustrate the functions of individual MYBs: MYB28 mainly activates the synthesis of short side-chains glucosinolates, whereas neither MYB28 nor MYB29 can induce long-chain AGSL accumulation. The function of MYB76 is dependent on the expression of *MYB28* and *MYB29* (Li et al., 2013a). MYB34, MYB51, and MYB122 function distinctly to regulate biosynthesis of indolic glucosinolates in *Arabidopsis*. MYB34 acts mainly in roots, while MYB51 in shoots and MYB122 play an accessory role (Frerigmann and Gigolashvili, 2014).

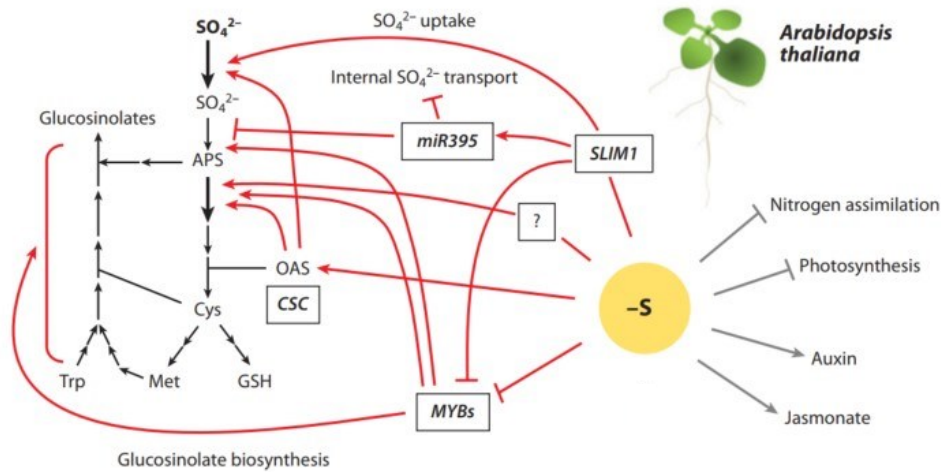


Figure 1.2 Regulatory pathways and components under sulfur deficiency condition of *Arabidopsis*

Red line indicates pathways that regulate sulfate uptake and metabolism. Gray lines indicate pathways that are affected by sulfur limitation (Takahashi et al., 2011).

1.3 The sulfate assimilation pathway of bacteria

Also, for bacteria, extracellular sulfate transport and reduction followed by cysteine biosynthesis is a major pathway of sulfur assimilation. In the model bacteria *Escherichia coli*, similar to plants, sulfate is activated to APS by an ATP sulfurylase, which is encoded by genes *CysD* and *CysN* (Fig. 1.3). Next, APS is converted to PAPS, catalyzed by an APS kinase encoded by *CysC* gene with the involvement of an ATP molecule. Then PAPS is reduced to SO_3^{2-} (sulfite) by PAPS reductase which is encoded by *CysH*. Sulfite is reduced by NADPH-sulfite reductase to sulfide which is incorporated into the OAS skeleton for the biosynthesis of Cys. The OAS is synthesized from L-serine and acetyl-CoA by serine acetyltransferase (SAT), encoded by the *CysE* gene. Sulfite reductase comprises two subunits which are encoded separately by *CysI* and *CysJ*. The biosynthesis of L-Cys from sulfide and OAS is catalyzed by O-acetylserine (thiol)-lyase-A and -

B encoded by genes *CysK* and *CysM* respectively (Sekowska et al., 2000). In addition to the OAS pathway, a thiosulfate pathway for L-Cys biosynthesis exists in *E. coli*. In this pathway, S-sulfocysteine (SSC) is produced from OAS and thiosulfate ($S_2O_3^{2-}$) catalyzed by OAS (thiol)lyase B (*CysM*). SSC is next transformed to L-cysteine and sulfite through involvement of several reductases. The sulfite generated from the SSC reduction reaction is a suitable sulfur source for additional L-Cys biosynthesis (Nakatani et al., 2012a).

Unlike *E. coli*, many pathogens are unable to assimilate sulfate because reduced organosulfur metabolites are accessible in the host during infection. For example, *Staphylococcus aureus* is a gram-positive human pathogen. *S. aureus* SH1000 strain lacks genes required for the uptake and reduction of sulfate, sulfite and sulfonate in the Cys biosynthetic pathway. However, *S. aureus* SH1000, can take up thiosulfate, sulfide, or glutathione as the sole sulfur source (Lithgow et al., 2004). The Cys transporter is another important way for bacteria to get sulfur nutrient, especially for Cys auxotrophic bacterial species. *Legionella pneumophila* is such Cys auxotroph, confirmed by the absence of activities of two key Cys biosynthetic enzymes (serine acetyltransferase and cysteine synthase). A high affinity and a low affinity energy-dependent Cys transporters were identified in *L. pneumophila*, which help the bacterium to acquire Cys from the host and support its proliferation.

Many studies have shown that alteration of sulfur assimilation leads to incomplete functioning of bacterial cells. For instance, the Cys biosynthesis pathway influences the physiology of an opportunistic pathogen *Serratia marcescens* - the cysteine auxotroph of *S. marcescens* is unable to differentiate into hyperflagellated and elongated swarmer cells. Furthermore, the *S. marcescens* cysteine auxotroph displays reduced level of transcription of the putative virulence factors flagellin genes, phospholipase and hemolysin (Anderson et al., 2019). *Pseudomonas fluorescens* strain SS101 (*Pf. SS101*) promotes growth of *A. thaliana* and induces systemic resistance (ISR) in plants to counter against the bacterial pathogen *Pseudomonas syringae* pv. *tomato* (*Pst*). Cheng et al. (2017) demonstrated experimentally that the *cysH* mutant of *Pf. SS101*, which is deficient in reducing APS to sulfite, lacks the ability to induce lateral root formation and ISR against *Pst*. In addition, transcription data indicated that *cysH* treated Arabidopsis exhibited lower level of biosynthetic processes associated with sulfur compounds, particularly serine, Cys and glucosinolates, compared to plants treated with the *Pf. SS101*.

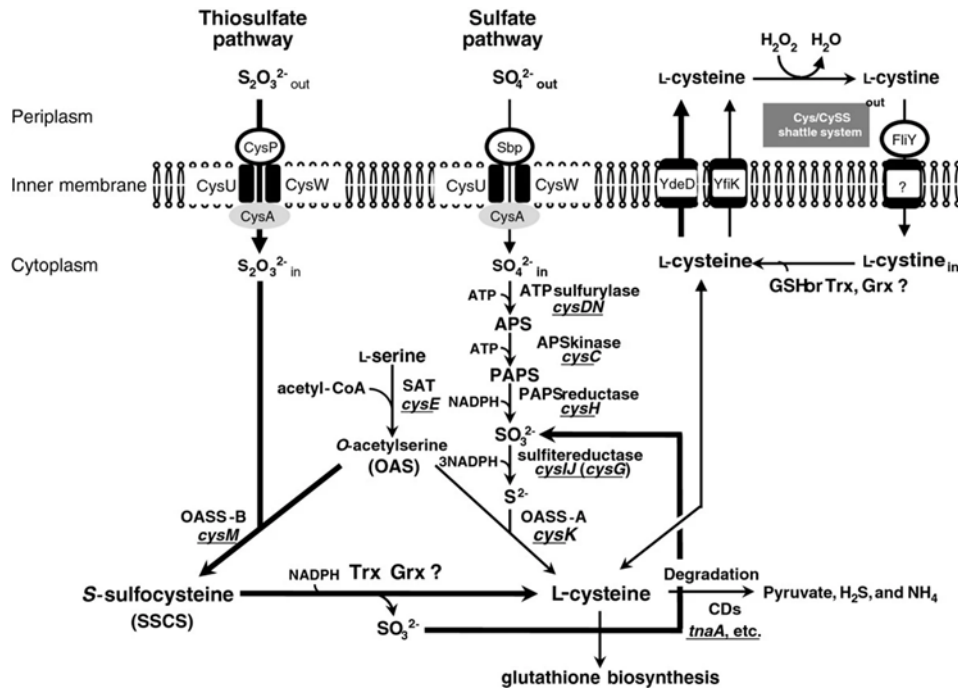


Figure 1.3 Sulfur assimilation and L-cysteine biosynthesis pathway in *Escherichia coli*

E. coli has two pathways for Cys biosynthesis: starting from sulfate or from thiosulfate. Genes involved in the enzymatic activities are shown (Nakatani et al., 2012).

1.4 Plant-pathogen interactions and integrated defense response

Sessile plants are subject to constant attack from numerous harmful microorganisms and insect pests. Therefore, they developed comprehensive defense systems to protect themselves and maintain a healthy life. Phytopathogens are divided into three categories according to their lifestyle in the host. Biotrophs feed on living cells, whereas necrotrophs kill host tissues and absorb nutrients released from the dead tissue; those that initially require living plant tissue for establishing itself and taking up nutrients, but kill the host cells in later stages of infection and derive nutrients from dead tissues are hemibiotrophs (Mendgen and Hahn, 2002; Horbach et al., 2011).

The first line of active defense in plants is the recognition of conserved elicitors known as microbe- or pathogen-associated molecular patterns (MAMPs/PAMPs). Plants sense the presence of these elicitors through a class of pattern recognition receptors (PRRs) located on the plant plasma membrane (Trdá et al., 2015). MAMP/PAMP-induced heteromerization of PRRs is the first activity in PAMP-triggered immunity (PTI), which allows plant switch from growth and

development to a defense mode. The PTI response includes the production of reactive oxygen species (ROS, also named oxidative burst) and reactive nitrogen species such as nitric oxide (NO), alterations in the plant cell wall, induction of biosynthesis of pathogenesis-related (PR) proteins, and antimicrobial compounds that eventually restrict pathogen population (Chun and Chandrasekaran, 2019; Escudero et al., 2019; Ferelli et al., 2020). The most extensively studied PAMP is the small peptide flg22, a 22 amino acid (aa) peptide with a highly conserved domain in the N-terminal part of bacterial Flg.

The second line of active plant defense is to sense effectors in the cytoplasm injected by pathogens that successfully attenuate PTI and consequently result in effector-triggered immunity (ETI). Plants recognize effectors via plant resistance (R) proteins in a direct or indirect way (Martin et al., 2003). Upon activation by effectors, R proteins elicit a rapid ROS burst, an accumulation of salicylic acid (SA), jasmonic acid (JA), and ethylene (ET) in and around infected cells, increased expression of PR genes, and programmed cell death (PCD) which is known as the hypersensitive response (HR) (Iwai et al., 2006; Nomura et al., 2012; Wu et al., 2014).

In addition to PTI and ETI induced locally or near the site of infection, plants induce a global systemic defense response in the distal parts of plants, usually several days after PTI or ETI. This long-lasting protection and broad-spectrum disease resistance mechanism is referred to as systemic acquired resistance (SAR) (Durrant and Dong, 2004). SAR requires the signal mobile molecule SA. The SA is produced at the infected site as methyl-SA (MeSA) and can move from cell to cell via plasmodesmata or through the phloem to untreated tissues of the plant (Park et al., 2007). Intensive studies have been conducted to elucidate the function of SA, including affecting tolerance to various abiotic stresses such as salinity, drought and cold (Miura and Tada, 2014), inducing resistance to biotic (pathogen-associated) stress (Chaturvedi and Shah, 2007), and regulating plant growth and development (Hayat et al., 2010).

In addition to SA, lysine (Lys) derivative pipecolic acid (Pip) and *N*-hydroxy-pipecolic acid (*N*-OH-Pip) are also mobile molecules initiating SAR signal transduction in Arabidopsis. Pip accumulates in inoculated leaves of Arabidopsis as well as in leaves distal from the site of inoculation. The mutant *ald1* is defect in biosynthesis of Pip and suffers from reduced basal resistance to bacterial pathogens (Návarová et al., 2012). It has been demonstrated that FLAVIN-DEPENDENT MONOOXYGENASE 1 (FMO1) is not only a key regulator of SAR-associated defense priming, but also can synthesize *N*-OH-Pip from Pip. Exogenous *N*-OH-Pip enhances the

SAR and triggers a faster hypersensitive response of *Arabidopsis* to *Pseudomonas syringae* pv. *tomato* DC3000 (*Pst*) (Chen et al., 2018).

1.5 Sulfur-induced resistance

Due to reduced sulfur emissions from industry, the awareness of the importance of sulfur in plant immunity and resistance against diverse pathogens raised. This reduction was beneficial to the environment overall, but had unintended consequences on the yield and quality of agricultural plants because some high-sulfur-demanding crops became more susceptible to disease. This susceptibility was attenuated by the application of sulfur fertilizer, leading to the development of the concept of sulfur-induced resistance (Bloem et al., 2014; Wang et al., 2022). Mounting evidence has shown that sulfur nutritional status, sulfur assimilation pathway and sulfur metabolism are able to influence plant-pathogen interactions. For example, resistant genotypes of *Theobroma cacao* accumulated a high amount of elemental sulfur only in cells and structures in potential contact with the vascular pathogen, for the first time linking elemental sulfur in a plant with a resistance response as a potent fungicide (Cooper et al., 1996). Expression profiling of metabolic genes in response to methyl jasmonate as one potent inducer of defense reactions in *Arabidopsis* revealed that sulfur related genes were by far strongest affected, including genes encoding key reactions of sulfate reduction as well as of Cys, Met and glutathione synthesis. Besides, the observed rapid changes of sulfur metabolism related pathway were different from the sulfur deficiency response, documenting for the first time the comprehensive connection between the regulation of sulfur-related genes and plant defense (Jost et al., 2005).

Extensive research over the past few decades has revealed the pivotal role of sulfur-containing metabolites in plant pathogen defense, strongly supporting the concept of sulfur-induced resistance. These sulfur metabolites can be constitutively produced or induced upon infection. Phytoanticipins are low molecular weight antimicrobial compounds that are constitutively produced in plants before they are attacked by pathogens. Thus, active defensive compounds can be synthesized immediately from such inactive precursors already present in the plants without expenditure of energy (Vanetten et al., 1994). Allicin (diallylthiosulfinate) from garlic is an important example of phytoanticipins. When the garlic is crushed, punctured, or injured, the previously cytosol-held precursor alliin and vacuolar enzyme alliinase are released for the synthesis of allicin (Borlinghaus et al., 2014). Other sulfur compounds related to plant defense are H₂S and well-known ROS

scavenger glutathione (GSH). Field experiment showed that application of sulfate to the soil as fertilization significantly increased the contents of total sulfur, sulphate, organic sulfur, cysteine, glutathione and reduced activity of L-cysteine desulphydrase (LCD) in *Brassica napus* L. LCD releases H₂S during cysteine degradation, the activity of which increased together with Cys and glutathione contents in response to infection with fungal pathogen *Pyrenopeziza brassicae*, indicating that crops are able to react to a fungal infection with the release of H₂S (Bloem et al., 2004). Glutathione (reduced form GSH; oxidized form GSSG), a S-containing thiol tripeptide, is an established antioxidant that plays a central role in maintaining cellular redox homeostasis and has been implicated in detoxification reactions, reduced sulfur storage and regulation of sulfur metabolism in plants (Kopriva, 2006; Dubreuil-Maurizi and Poinssot, 2012; Noctor et al., 2012). Furthermore, GSH is also a well recognized central regulator of plant signaling during plant–pathogen interactions (Gullner et al., 2017; Zechmann, 2020). GSH supplied to suspension cultured cells of bean (*Phaseolus vulgaris* L.) stimulates transcription level of defense genes including those that encode cell wall hydroxyproline-rich glycoproteins and the phenylalanine ammonialyase (PAL) (Wingate et al., 1988).

In addition to the metabolites mentioned above, sulfur containing amino acids (SAAs) Cys and Met are involved in plant disease resistance as well. It has been demonstrated that two enzymes involved in Cys biosynthesis and degradation affect disease resistance of *A. thaliana* to the hemibiotrophic *P. syringae* pv. *tomato* DC3000 (*Pst*) and the necrotrophic *B. cinerea* (Leustek et al., 2003). Arabidopsis ONSET OF LEAF DEATH3 (*old3-2*) mutants lacking functional OASTL in the cytosol show increased susceptibility to the *Pst* DC3000 (Tahir et al., 2013). Cys also has a direct antifungal effect on the mycelial growth and the spore germination of the fungal pathogens *Phaeoconiella chlamydospora* based on a concentration-dependent manner. Met treatment triggers generation of hydrogen peroxide (H₂O₂), a key signalling molecular in plant immunity response, and upregulates the expression of defense-related genes in grapevine (*Vitis vinifera*). Similar to Cys, Met possesses direct antifungal activity, however, this activity is moderate as compared to Cys under in vitro and in vivo (Boubakri et al., 2013). Met treatment also drastically reduces disease severity caused by *Sclerospora graminicola* infection (Sarosh et al., 2005).

1.6 Glucosinolates and camalexin

Glucosinolates and camalexin are sulfur-containing plant secondary metabolites mainly found in Brassicales plants such as broccoli, cabbage, and *Arabidopsis*. They are important compounds involved in sulfur-induced resistance due to their antimicrobial activity (Madloo et al., 2019; Poveda et al., 2020; Nguyen et al., 2022a).

The well-characterized glucosinolates phytoanticipins are divided into aliphatic, indolic and aromatic glucosinolates depending on their amino acid precursor (as described in subsection 1.2). Although intact glucosinolates are biologically inactive, they can be hydrolyzed by myrosinases to produce various chemically active compounds, including isothiocyanates, nitriles, epithionitriles, and cyanides, which are toxic to pathogens (Fahey et al., 2001). Glucosinolates are stored in the vacuole of so-called S-cells, while myrosinases are localized in the cytosol of protein-accumulating myrosin cells in intact plants. These two components mix together upon tissue damage. This glucosinolate–myrosinase defense system is known as “mustard oil bomb” (Koroleva et al., 2000; Andréasson et al., 2001). Aliphatic or indolic glucosinolates and hydrolysis products can be induced by a variety of bacterial and fungal pathogens. For example, Isothiocyanates (ITCs) are generated by the enzymatic hydrolysis of glucosinolates in Brassicaceae vegetables and show in vitro growth inhibitory effect against various bacterial pathogens including *Agrobacterium tumefaciens*, *Erwinia chrysanthemi*, *Pseudomonas cichorii*, *Pseudomonas tomato*, *Xanthomonas campestris*, and *Xanthomonas juglandis* (Aires et al., 2009). The fungus *Sclerotinia sclerotiorum* causes severe white mold disease on Brassica crops worldwide. Infection of cabbage with *S. sclerotiorum* induced expression of glucosinolates biosynthesis genes, increasing simultaneously contents of the aliphatic glucosinolates and the indolic glucosinolates, which was linked to white mold resistance in cabbage (Abuyusuf et al., 2018). Furthermore, the in vitro growth assay of two bacterial (*Xanthomonas campestris* pv. *campestris* and *P. syringae* pv. *maculicola*) and two fungal (*Alternaria brassicae* and *Sclerotinia sclerotiorum*) Brassica pathogens on 17 glucosinolates, their hydrolysis products and leaf methanolic extracts of different Brassica crops indicates that the biocidal effects of the different glucosinolates compounds and hydrolysis products were dependent on the species and race of the pathogen (T. et al., 2015).

Camalexin (3-thiazol-2-yl-indole) is a well-known sulfur-containing phytoalexin identified in *Arabidopsis* and other Brassicaceae species with antimicrobial activity (Browne et al., 1991;

Bednarek et al., 2011). In contrast to phytoanticipins, phytoalexins with antimicrobial activity are synthesized *de novo* and accumulate in plants only at the site of infection. The distinction between phytoalexins and phytoanticipins is based on their mode of synthesis, but not their chemical structure. Camalexin can be induced under a wide range of biotic and abiotic stresses such as infection by pathogens *P. syringae* and *Botrytis cinerea*, plant cell wall derived oligogalacturonides, the bacterial flagellin peptide Flg22, oxidative stress and heavy metal ions (Zhao et al., 1998; Qutob et al., 2006; Gust et al., 2007; Denoux et al., 2008; Kruszka et al., 2020). Camalexin can be induced in *Arabidopsis* and secreted via pleiotropic drug resistance (PDR) transporters PEN3 and PDR12 by the infection of *B. cinerea*. The double mutant *pen3 pdr12* exhibits dramatically increased susceptibility to *B. cinerea*, indicating the importance of camalexin accumulation and transportation in resistance to fungal invasion (He et al., 2019). The antimicrobial activity of camalexin was tested on the necrotrophic fungus *B. cinerea*. (Kliebenstein et al., 2005; Nafisi et al., 2007). More specifically, *B. cinerea* has genetic variation in its ability to tolerate camalexin. The camalexin-insensitive isolate of *B. cinerea* produced similar sized lesions on WT and camalexin-deficient *Arabidopsis cyp79B2/B3* and *pad3*, whereas camalexin-sensitive isolates produced larger lesions on camalexin-deficient *Arabidopsis* genotypes than on the WT. Camalexin not only exhibits direct antimicrobial activity, but also contributes to induced systemic resistance (ISR) against a broad spectrum of pathogens. It has been reported that the beneficial bacterium *Bacillus subtilis* could prime *Arabidopsis* plants for enhanced accumulation of camalexin and its biosynthetic gene *CYP71A12* after pathogen challenge by *B. cinerea* and *Pst* DC3000. Phytoalexin-deficient mutants *pad3* and *cyp71A12* were more susceptible to *B. cinerea* and *Pst* DC3000, indicating the importance of camalexin accumulation in ISR (Koprivova et al., 2019a; Nguyen et al., 2022b). Koprivova et al., (2019) reported that camalexin exuded by *Arabidopsis* roots is important for the plant growth promotion effects of the beneficial bacterium *Pseudomonas* sp. CH267.

Biosynthesis of glucosinolates consists three independent stages: (i) side chain elongation of certain aliphatic and aromatic amino acids by inserting methylene groups, (ii) formation of the core glucosinolates structure by modifications of the amino acids, and (iii) secondary modifications of the amino acid side chain (Sønderby et al., 2010). Constructing the glucosinolate core structure with precursor amino acids is catalyzed by cytochromes P450 of the CYP79 family: CYP79B2 and CYP79B3 both metabolize Trp (Hull et al., 2000; Mikkelsen et al., 2000),

CYP79A2 metabolize Phe (Wittstock and Halkier, 2000), CYP79F1 converts all chain-elongated Met derivatives (Hansen et al., 2001), while CYP79F2 only converts the long-chained Met derivatives (Chen et al., 2003). The biosynthesis pathway of camalexin and indolic glucosinolates share some common precursors since they both originate from Trp. CYP79B2 and CYP79B3 convert Trp into indole-3-acetaldoxime (IAOx), from which camalexin and indole glucosinolates are synthesized (Fig. 1.4). The transcription factors MYB34, MYB51, and MYB122 regulate the generation of IAOx (Frerigmann et al., 2015). However, even though indolic glucosinolates were strongly reduced in *myb34/51/122* plants, gene induction and accumulation of camalexin upon infection of necrotrophic fungal pathogen *Plectosphaerella cucumerina* was not compromised in *myb34/51/122* mutants (Frerigmann et al., 2016). CYP71B15 encoded by *PAD3* (camalexin-deficient phytoalexin deficient 3) catalyzes the final step in camalexin biosynthesis with dihydrocamalexic acid downstream of IAOx as substrate. (Schuhegger et al., 2006).

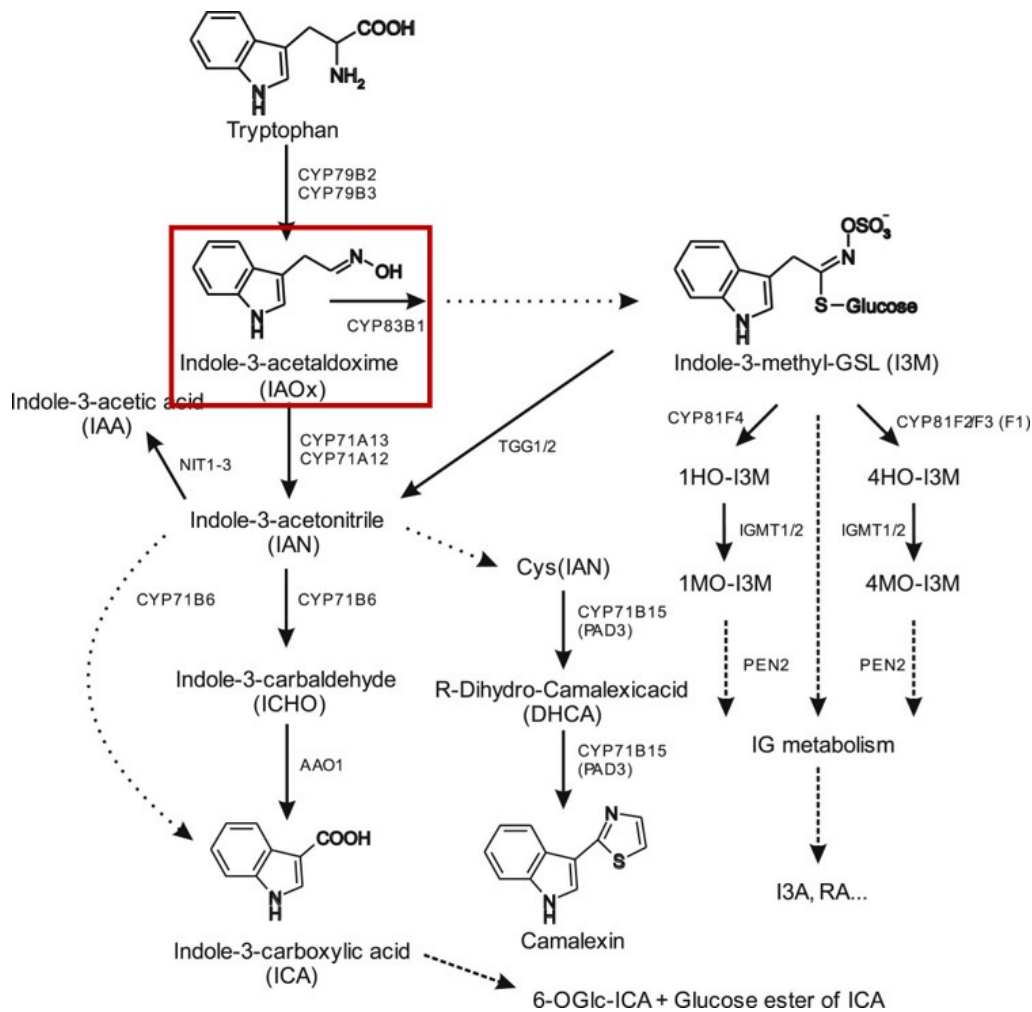


Figure 1.4 Biosynthesis pathways of indole glucosinolates and camalexin are closely connected

Indolic glucosinolates and camalexin are Try-derived secondary metabolites, constituting key components of sulfur-induced resistance in *Arabidopsis*. Highlighted in the red box is the branching point of glucosinolates and camalexin biosynthesis pathway, their precursor IAOx (Frerigmann et al., 2016).

1.7 Nutrient acquisition strategies employed by bacteria

A colonizing bacterial pathogen must acquire essential nutrients from the host plant to support its life. Sulfur-containing metabolites available to bacteria are abundant within the host–pathogen interface. However, different plant tissues harbour different concentration or categories of sulfur-containing metabolites that bacteria are able to catabolize. To overcome this challenge, bacteria employ multiple elegant acquisition strategies for various sulfur metabolites, including inorganic and organic sulfur sources (Lensmire and Hammer, 2019; Kies and Hammer, 2022).

In nature, pathogens initially colonize the plant surfaces, namely the phyllosphere and the rhizosphere and obtain nutrients. Later, majority of them gain access to the host plant's interior tissues, including phloem, xylem, leaf apoplast, root apoplast and cell organelles to obtain more nutrients. Pathogens employ different strategies to acquire desirable nutrients. First of all, transporters play an important role in nutrient acquiring during bacterial colonization. For example, a culture-independent metaproteogenomic analysis demonstrated that the alphaproteobacterial genera *Sphingomonas* and *Methylobacterium* are prominent bacterial species on the phyllosphere of soybean, clover, and *Arabidopsis thaliana* plants. These species express a remarkably wide variety of TonB-dependent outer membrane receptors which are involved in transporting a vast variety of carbohydrates (Delmotte et al., 2009). To survive inside host plants, the bacteria evolved different strategies to obtain nutrients in planta. *Ralstonia solanacearum* is a model destructive microorganism that succeeds in colonizing the water-conducting plant xylem tissue in tomato, which is considered to be a nutrient-poor environment. However, this bacterial wilt pathogen is well adapted to this niche. Compared with bacterial gene expression in pure culture, transcriptome data of *R. solanacearum* in plant xylem showed that several primary metabolic pathways including sucrose uptake and catabolism were highly expressed during early tomato bacterial wilt pathogenesis. Besides, about 12% of their transcriptomes significantly changed in the host planta versus in pure culture (Jacobs et al., 2012). Not only can bacteria regulate their own metabolism, but also, they are able to manipulate the plant cell machinery based on nutrition requirement. For

example, the plant pathogen *Pst* can use the virulence factor coronatine to actively open stomata to entry into host tissue, which is a critical first step in causing infection (Melotto et al., 2008). In the field of human pathogens, numerous studies successfully demonstrated that pathogens are able to utilize sulfur nutrients from host cells. Inorganic sulfur sources such as sulfate, thiosulfate and organic sulfur sources such as Cys, oxidized Cys (referred to as cystine), methionine, or glutathione in host cells are attractive nutrition sources for bacterial pathogens (Lensmire and Hammer, 2019). As described above, sulfate is an established *in vivo* sulfur source for bacteria as they are able to transport and reduce it to sulfide, that can be easily used for Cys synthesis (Gebhardt et al., 2015). Thiosulfate is a substrate of OAS sulfhydrylase in certain bacterial species and is directly involved in the production of Cys (Lithgow et al., 2004). In addition to inorganic sulfur sources, certain bacteria can also utilize exogenous organosulfur metabolites as sulfur source as well. This method is more efficient than consuming inorganic sulfur sources because these organosulfur compounds can be processed into Cys within one or two enzymatic steps. Abundance of glutathione, Met and Cys in host tissues make them ideal sulfur sources for bacteria. Glutathione can be transformed into Cys via two steps: first cleaving the γ -peptide bond releasing glutamate and producing γ -cysteinyl-glycine via γ -glutamyl-transpeptidase, then releasing Cys from glycine via peptidases (Suzuki et al., 2001). Met undergoes recycling reactions to ultimately synthesize Cys and to satisfy sulfur requirement of bacterial pathogens. This recycling procedure contains three steps: first S-adenosyl-methionine (SAM) and the by-product S-adenosyl-homocysteine (SAH) are synthesized from methionine and ATP by SAM synthase. SAH is subsequently degraded into homocysteine by SAH hydrolase. Homocysteine is then converted to cysteine by the reverse transsulfuration pathway via a cystathionine intermediate (Guédon and Martin-Verstraete, 2006).

1.8 Aim of the thesis

Although sulfur deficiency in microbes negatively impacts their plant growth promoting function or leads to a reduced pathogenicity, mechanisms mediating this change are not well understood. Furthermore, most studies have focused on sulfur deficiency of microbes, however it is not clear whether and how modulation of sulfur assimilation of plants affect its susceptibility to pathogen and what key sulfur metabolites affect plant-pathogen interactions. *Burkholderia glumae* is an important crop pathogen which causes a bacterial panicle blight of rice and results in severe yield

loss of rice over the world. Toxoflavin and lipase are known to be major virulence factors of this pathogen (HAM et al., 2011). *B. glumae* also infects other crops, including pepper, eggplant, sesame and tomato, causing bacterial wilt (Jeong et al., 2003). In this study, we used the *Burkholderia glumae* PG1 strain (NCBI Taxonomy ID: 595500) as bacterial pathogen and its sulfur deficient mutants *cysH* and *cysM*, in combination with Arabidopsis Col-0 and plant mutants that are deficient in sulfur homeostasis, to address following questions: (1) Are *cysH* and *cysM* mutants less pathogenic than PG1? If so, what is the underlying mechanism? (2) Are Arabidopsis disrupted in sulfate assimilation pathway more susceptible to attack of pathogens than Col-0? If so, what are determinants that affect plant hosts' response to biotic stress? To answer these two questions, several experiments and cocultivation assays were performed to estimate and quantify pathogenicity, capacity of nutrient uptake and colonization ability. A DNA-based real time PCR method was applied for robust quantification of pathogens abundance inside plant. Discovering the sulfur-related determinants of microbial pathogenicity has significant application potential, since a wide variety of pathogens cause a great loss of productivity of crops and the use of pesticides has resulted in serious environmental problem. Identifying new and different targets of pesticides is thus crucial to increase crop production and sustainable development.

2 Materials and Methods

2.1 Plant materials

The *Arabidopsis thaliana* accession Col-0 was used as the wild-type (WT) for all assays in this thesis and served as the background for the mutants *slim1-1*, *myb28 myb29*, *apr1 apr2*, *sultr1;2*, *apk1 apk2*, *cad2-1*, *gst6* and *gsttatu3* (Table 1). Prior to use, seeds were surface sterilized for 3 hours using vapour-phase sterilization method. Briefly, seeds were exposed to chlorine fumes produced by adding 2.5 ml 37% (v/v) HCl to 12.5% (v/m) sodium hypochlorite in a desiccator dome for 3 h.

Name	Gene	Mutation
<i>cad2-1</i>	AT4G23100	(Cobbett et al., 1998)
<i>apk1 apk2</i>	AT2G14750, AT4G39940	SALK_053427 x SALK_093072 (Mugford et al., 2009)
<i>sultr1;2</i>	AT1G78000	Originating from <i>sel1-8</i> mutants containing a point mutation in the coding sequences of <i>Sultr1;2</i> (Shibagaki et al., 2002)
<i>apr1 apr2</i>	AT4G04610, AT1G62180	<i>apr1 apr2</i> mutants were generated by crossing in our lab. <i>apr1</i> mutants was isolated from tilling, the <i>apr2</i> mutant is the T-DNA insertion line GABI_108G02 (Loudet et al., 2007)
<i>myb28 myb29</i>	AT5G61420, AT5G07690	SALK_136312 x SM_3_34316 (Li et al., 2013)
<i>slim1-1</i>	AT1G73730	a point mutation (Maruyama-Nakashita et al., 2006)
<i>gst6</i>	AT1G02930	SALK_026398
<i>gsttatu3</i>	AT2G29470	SALK_054737

2.2 Bacterial strains and culture conditions

B. glumae PG1 (NCBI Taxonomy ID: 595500) was obtained from Prof. K.-E. Jäger, Heinrich Heine University of Düsseldorf (Gao et al., 2015). Bacterial mutants *cysH* and *cysM* were kindly provided by Dr. Andreas Knapp from Forschungszentrum Jülich (Germany), and generated by disruption of the genes with gentamycin resistance gene. Bacterial cultures rejuvenated from glycerol stocks were grown in Luria–Bertani (LB) medium overnight at 30°C with 200 rpm shaking. Antibiotics were supplemented into the LB medium as followed: 25 µg/mL chloramphenicol for PG1 strain, 25 µg/mL gentamycin for *cysH* and *cysM*. Those overnight cultures were washed with 10 mM MgCl₂ twice for further use.

2.3 Bacterial growth in different sulfur sources

To estimate sulfur assimilation ability of *B. glumae* PG1, *cysH* and *cysM*, a diverse organic and inorganic sulfur-containing chemicals were tested. In this assay, MgSO₄, taurine and 4-Nitrophenyl sulfate potassium salt (PNPS) were used as oxidised sulfur compounds, while cysteine and methionine were applied as reduced sulfur source. LB medium was positive control.

Fresh bacterial strains in LB medium were washed twice with 10 mM MgCl₂ and resuspended to a final OD₆₀₀ of 0.5 in sterile 10 mM MgCl₂ for growth assay. 5 µl of bacterial cultures was added to M9 based minimum salts media containing 25 µg/ml antibiotics and 1 µM of the corresponding sulfur source. Bacteria were grown in a 96-well plate. The final culture volume in each well was 100 µl. Different sulfur-containing compounds were added to the minimal medium without MgSO₄, as the sole sulfur nutrient for bacterial growth. The exact contents of each component in the minimal medium are given in Table 2 and the composition of the media in 96-well plates is given in Table 3 and Table 4. The plate was incubated at 30 °C in a microplate reader (TECAN Infinite[®] 200 PRO) for 48 h. The plate was 3 min continuous shaken followed by 7 min stationary stage. OD₆₀₀ values were measured every 10 min. Growth curves of each bacteria in different sulfur sources were analyzed in R with Growthcurver package (Jacoby et al., 2018).

Table 2 Minimal medium without sulfate (M9)		
Stocks	Dilution factor	Volume to add (ml)
water		34.35
1. M9 salts - 10x Stock	10	5
2. Trace Elements - 1000x Stock	1000	0.05
3. Iron Source - 1000x Stock	1000	0.05
4. Calcium Source - 1000x Stock	1000	0.05
5. Nitrogen Source - NH ₄ Cl - 100x Stock	100	0.5
6. Sulfur Source - MgSO ₄ x 7H ₂ O - 100x Stock	100	0
7. Carbon Source - 10x Stock	10	5
8. Mg substitution - 10 mM MgCl ₂	n/a	5
The information about stock solution used for this minimal medium was in Appendix Table S1.		

Table 3 Stock solution of sulfur sources (0.1 M sulfur)			
Sulfur source	Molecular weight (MW)	Concentration	Mass to add (in 10 ml solution)
MgSO ₄ x 7H ₂ O	246.47	0.1 M	0.246 g
MgCl ₂ x 6H ₂ O	203.30	0.1 M	0.203 g
Cysteine	121.16	0.1 M	0.121 g
Methionine	149.21	0.1 M	0.149 g
Sodium Thiosulfate	158.11	0.05 M	0.079 g
Taurine	125.15	0.1 M	0.125 g
PNPS	257.26	0.1 M	0.257 g
1 µl of each sulfur solution was added to media, the final concentration of sulfur nutrient in each well was 1 mM.			

Table 4 Composition of media with different sulfur sources

	1	2	4	5	6	8	9	10
	LB	MgCl ₂	MgSO ₄	Cysteine	methionine	thiosulfate	taurine	PNPS
A	93 µl LB 1 µl CHL 5 µl PG1 rep1	93 µl M9 1µl MgCl ₂ 1 µl CHL 5 µl PG1 rep1	93 µl M9 1 µl MgSO ₄ 1 µl CHL 5 µl PG1 rep1	93 µl M9 1 µl cysteine 1 µl CHL 5 µl PG1 rep1	93 µl M9 1 µl methionine 1 µl CHL 5 µl PG1 rep1	93 µl M9 1 µl thiosulfate 1 µl CHL 5 µl PG1 rep1	93 µl M9 1 µl taurine 1 µl CHL 5 µl PG1 rep1	93 µl M9 1 µl PNPS 1 µl CHL 5 µl PG1 rep1
B	93 µl LB 1 µl gentamicin 5 µl <i>cysH</i> rep1	93 µl M9 1µl MgCl ₂ 1 µl gentamicin 5 µl <i>cysH</i> rep1	93 µl M9 1 µl MgSO ₄ 1 µl gentamicin 5 µl <i>cysH</i> rep1	93 µl M9 1 µl cysteine 1 µl gentamicin 5 µl <i>cysH</i> rep1	93 µl M9 1 µl methionine 1 µl gentamicin 5 µl <i>cysH</i> rep1	93 µl M9 1 µl thiosulfate 1 µl gentamicin 5 µl <i>cysH</i> rep1	93 µl M9 1 µl taurine 1 µl gentamicin 5 µl <i>cysH</i> rep1	93 µl M9 1 µl PNPS 1 µl gentamicin 5 µl <i>cysH</i> rep1
C	93 µl LB 1 µl gentamicin 5 µl <i>cysM</i> rep1	93 µl M9 1µl MgCl ₂ 1 µl gentamicin 5 µl <i>cysM</i> rep1	93 µl M9 1 µl MgSO ₄ 1 µl gentamicin 5 µl <i>cysM</i> rep1	93 µl M9 1 µl cysteine 1 µl gentamicin 5 µl <i>cysM</i> rep1	93 µl M9 1 µl methionine 1 µl gentamicin 5 µl <i>cysM</i> rep1	93 µl M9 1 µl thiosulfate 1 µl gentamicin 5 µl <i>cysM</i> rep1	93 µl M9 1 µl taurine 1 µl gentamicin 5 µl <i>cysM</i> rep1	93 µl M9 1 µl PNPS 1 µl gentamicin 5 µl <i>cysM</i> rep1
D	93 µl LB 5 µl MgCl ₂	93 µl M9 1µl MgCl ₂ 5 µl MgCl ₂	93 µl M9 1 µl MgSO ₄ 5 µl MgCl ₂	93 µl M9 1 µl cysteine 5 µl MgCl ₂	93 µl M9 1 µl methionine 5 µl MgCl ₂	93 µl M9 1 µl thiosulfate 5 µl MgCl ₂	93 µl M9 1 µl taurine 5 µl MgCl ₂	93 µl M9 1 µl PNPS 5 µl MgCl ₂
E	93 µl LB 1 µl CHL 5 µl PG1 rep2	93 µl M9 1µl MgCl ₂ 1 µl CHL 5 µl PG1 rep2	93 µl M9 1 µl MgSO ₄ 1 µl CHL 5 µl PG1 rep2	93 µl M9 1 µl cysteine 1 µl CHL 5 µl PG1 rep2	93 µl M9 1 µl methionine 1 µl CHL 5 µl PG1 rep2	93 µl M9 1 µl thiosulfate 1 µl CHL 5 µl PG1 rep2	93 µl M9 1 µl taurine 1 µl CHL 5 µl PG1 rep2	93 µl M9 1 µl PNPS 1 µl CHL 5 µl PG1 rep2
F	93 µl LB 1 µl gentamicin 5 µl <i>cysH</i> rep2	93 µl M9 1µl MgCl ₂ 1 µl gentamicin 5 µl <i>cysH</i> rep2	93 µl M9 1 µl MgSO ₄ 1 µl gentamicin 5 µl <i>cysH</i> rep2	93 µl M9 1 µl cysteine 1 µl gentamicin 5 µl <i>cysH</i> rep2	93 µl M9 1 µl methionine 1 µl gentamicin 5 µl <i>cysH</i> rep2	93 µl M9 1 µl thiosulfate 1 µl gentamicin 5 µl <i>cysH</i> rep2	93 µl M9 1 µl taurine 1 µl gentamicin 5 µl <i>cysH</i> rep2	93 µl M9 1 µl PNPS 1 µl gentamicin 5 µl <i>cysH</i> rep2
G	93 µl LB 1 µl gentamicin 5 µl <i>cysM</i> rep1 rep2	93 µl M9 1µl MgCl ₂ 1 µl gentamicin 5 µl <i>cysM</i> rep1 rep2	93 µl M9 1 µl MgSO ₄ 1 µl gentamicin 5 µl <i>cysM</i> rep1 rep2	93 µl M9 1 µl cysteine 1 µl gentamicin 5 µl <i>cysM</i> rep1 rep2	93 µl M9 1 µl methionine 1 µl gentamicin 5 µl <i>cysM</i> rep1 rep2	93 µl M9 1 µl thiosulfate 1 µl gentamicin 5 µl <i>cysM</i> rep1 rep2	93 µl M9 1 µl taurine 1 µl gentamicin 5 µl <i>cysM</i> rep1 rep2	93 µl M9 1 µl PNPS 1 µl gentamicin 5 µl <i>cysM</i> rep1 rep2
H	93 µl LB 5 µl MgCl ₂	93 µl M9 1µl MgCl ₂ 5 µl MgCl ₂	93 µl M9 1 µl MgSO ₄ 5 µl MgCl ₂	93 µl M9 1 µl cysteine 5 µl MgCl ₂	93 µl M9 1 µl methionine 5 µl MgCl ₂	93 µl M9 1 µl thiosulfate 5 µl MgCl ₂	93 µl M9 1 µl taurine 5 µl MgCl ₂	93 µl M9 1 µl PNPS 5 µl MgCl ₂

The media in each well consisted of: 93 µl M9 medium + 1 µl sulfur source + 1 µl antibiotic + 5 µl bacterial suspension. MgCl₂ was the negative control to ensure that the media were not contaminated. CHL is the abbreviation of the antibiotic chloramphenicol. The final concentration of both antibiotics CHL and gentamicin in media was 25 µg/ml.

2.4 Co-cultivation of Col-0 and bacteria strains

Surface sterilized seeds were sown onto square plates containing half strength Murashige Skoog ($\frac{1}{2}$ MS) nutrient solution, supplemented with 0.5% (m/v) sucrose and 0.8% (m/v) agarose. After 3 days of stratification at 4°C in darkness, plates were transferred to a growth chamber (Percival) and incubated vertically under long day conditions (16 h light/ 8 h dark), 120 $\mu\text{E m}^{-2} \text{s}^{-1}$, at 22°C for 7 days. Ten pre-grown seedlings were carefully transferred onto each square plates poured with 50 ml Long Ashton agar medium (Table 5). The Long Ashton medium was mixed with 45 μl of twice-washed *B. glumae* PG1, *cysH* and *cysM* at OD₆₀₀ of 0.05 and the same amount of 10 mM MgCl₂ as control treatment at 42°C before pouring. After 14 days of co-cultivation in the growth chamber as described before, fresh weight of each seedling was determined.

Macroelements	End conc.	stock conc.	stock (g/L)	volume (for 1L medium)
Ca(NO ₃) ₂ x 4H ₂ O	1.5 mM	0.6 M	141.7	2.5 ml
KNO ₃	1 mM	0.4 M	40.4	2.5 ml
KH ₂ PO ₄	0.75 mM	0.3 M	40.8	2.5 ml
MgSO ₄ x 7H ₂ O	0.75 mM	0.3 M	74.0	2.5 ml
Fe-EDTA	0.1 mM	40 mM	14.7	2.5 ml
MnCl ₂ x 4H ₂ O	10 μM	10 mM	1.98	1 ml
H ₃ BO ₃	50 μM	50 mM	3.1	1 ml
ZnCl ₂	1.75 μM	1.75 mM	238.0	1 ml
CuCl ₂	0.5 μM	0.5 mM	67.2	1 ml
Na ₂ MoO ₄	0.8 μM	0.8 mM	164.7	1 ml
KI	1 μM	1 mM	166	1 ml
CoCl ₂ x 6H ₂ O	0.1 μM	0.1 mM	23.8	1 ml
Additives: 0.8 g/L MES hydrate, 8 g/L low EEO agarose				
Macro- and microelements were added from the stock solutions. Low sulfur agarose (Biozym LE Agarose, Biozyme Scientific GmbH, Hessisch Oldendorf, Germany) was used in this medium. The pH of the medium was adjusted to 5.7 with KOH. Agarose was added as the last step.				

2.5 Leaves infiltration

Pre-grown seedlings as described above were transferred individually to 6 cm diameter round pots containing soil and perlites. Seedlings were incubated in growth chamber under short day condition (8 h light/16 h dark) at 22 °C for 4 weeks before syringe infiltration. Plants were covered with lids during the first week in chamber and watered once a week. Overnight cultures of *B. glumae* PG1, *cysH* and *cysM* were washed twice with 10 mM MgCl₂ and adjusted to OD₆₀₀ of 1. To ensure uniformity, four mature rosette leaves in each pot were selected for treatments. Marked leaves were infiltrated by pushing slightly and slowly 1 ml needleless syringe to the upper surface of the leaf. Plungers were slowly pushed to infiltrate the bacterial solution. Infiltration could be confirmed by leaf darkening. Syringe was filled with 0.5-0.6 ml to allow a better control during the infiltration process and to avoid any wound injury to leaves. Around 0.1-0.2 ml bacterial suspension was needed to infiltrate the entire surface of each leaf. 1 to 2 infiltration spots were made to achieve full leaf coverage. Once the infiltration process was completed, absorbent tissue was used to remove the extra pathogen solution. Infiltrated plants from the same treatment group were placed in the same tray and covered with a clear lid. After 3-5 days of incubation, infiltrated leaves were cut and immediately frozen in liquid nitrogen. Samples were stored at -80°C for chlorophyll analysis.

2.6 Chlorophyll measurements

Leaf material was homogenized and ca. 20 mg of leaves were taken for chlorophyll measurement. 1 ml dimethylsulfoxide (DMSO) was used to extract chlorophyll at 60°C and 450 rpm for about 30 min. This hot incubation process finished when leaves turned transparent. Samples were centrifuged and supernatants were transferred to cuvettes for measuring absorbance at 645 nm and 663 nm on a spectrophotometer (Eppendorf BioSpectrometer[®], Germany). Concentration of chlorophyll was calculated by the following equation:

$$\text{Chlorophyll a } (\mu\text{g/ml}) = 12.7 * A_{663} - 2.69 * A_{645};$$

$$\text{Chlorophyll b } (\mu\text{g/ml}) = 22.9 * A_{645} - 4.68 * A_{663};$$

$$\text{Total Chlorophyll } (\mu\text{g/ml}) = 20.21 * A_{645} + 18.02 * A_{663}.$$

2.7 12-well hydroponic system

A 12-well (4*3) hydroponic culture system was established by Dr. Hanna Koprivova, to shorten the growth period of Arabidopsis and to better inoculate bacterial strains.

First, one ml of $\frac{1}{2}$ MS containing 0.5% sucrose was added into the wells of the plate. A sterile square polypropylene micro hole mesh was put onto the surface the medium. Surface sterilized seeds were suspended in 0.1% (m/v) agar liquid and pipetted onto mesh. Each mesh contained 20-30 seeds. The plates were wrapped by aluminum foil and kept in 4°C fridge for 3 days for stratification. Next, plates were transferred to a growth chamber under long day condition (16 h light/8 h dark, $120 \mu\text{E m}^{-2}\text{s}^{-1}$) at 22°C. Plates were uncovered from aluminum foil only after 2.5 days, to promote hypocotyl growth. After 9 days of growth in the chamber, the medium was changed to $\frac{1}{2}$ MS medium without sucrose. At the same day of changing medium, fresh bacterial strains were inoculated in LB medium for the use in the next day. At this stage, the shoots and roots were separated by mesh with roots in the medium and shoots above the mesh without a contact with the media.

Next, bacteria were washed twice with 10 mM MgCl_2 and adjusted to OD_{600} of 0.5. These cultures were further diluted 1000 times. Seven μl of diluted bacterial solution was added to $\frac{1}{2}$ MS medium in each well and co-cultivated with Arabidopsis for 3 days in the growth chamber as described above. Shoots and roots were cut and weighed separated and fast frozen in liquid nitrogen. Samples were stored for measurement of camalexin, anions, thiols (glutathione and Cys), glucosinolates, Pip, SA and gene expression.

2.8 Visualization of H_2O_2 with the DAB staining method

To detect the presence and distribution of hydrogen peroxide (H_2O_2) in Arabidopsis rosette leaves, 3,3'-diaminobenzidine (DAB) staining method was applied. DAB can be oxidized by H_2O_2 in the presence of peroxidases and generate visible dark brown precipitates (Daudi and O'Brien, 2012). Arabidopsis were grown in 12-well hydroponic system and inoculated by *B. glumae* PG1, *cysH* and *cysM* in the hydroponic system as described above. Shoot samples were collected for DAB staining at specific time points, 4 h, 6 h and 8 h after inoculation. A fresh 1 mg/ml DAB solution was generated in a 50 ml falcon tube. 0.2 M HCL was added to the DAB solution to reduce pH to 3.0 and to help dissolve DAB chemical. 25 μl Tween 20 (0.05% v/v) and 2.5 ml of 200 mM Na_2HPO_4 were added to the DAB solution. Finally, a 10 mM Na_2HPO_4 DAB staining solution was

generated and the pH backed up. The DAB solution was covered with aluminum foil since DAB is light-sensitive. $\frac{1}{2}$ MS medium was pipetted out from the 12-well plate and 2 ml DAB solution was added to the wells instead, to ensure that leaves were fully immersed in DAB solution. The plate was gently vacuum infiltrated in a desiccator dome for 5 min to make sure that the DAB was taken up by the leaves. Next, the 12-well plate was covered with aluminum foil and shaken on an orbital shaker for 4-5 h at 80-100 rpm.

Afterwards, the DAB staining solution was replaced by bleaching solution (ethanol: acetic acid: glycerol; 3:1:1) and heated in a boiling water bath at 95°C for 15 min. The bleaching solution was replaced by fresh one and allowed to stand for 30 min at RT. Chlorophyll was bleached out and brown precipitates were remained inside leaves. Samples at this stage were directly visualized for DAB staining and ready for photographing.

Table 6 Preparation of the DAB staining solution in detail
1. Add 50 mg DAB and 45 ml sterile water into 50 ml falcon tubes to make a final 1 mg/ml DAB solution.
2. Add small magnetic stirrer and reduce pH to 3.0 with 0.2 M HCl (to dissolve DAB).
3. Cover tube with aluminum foil since DAB is light-sensitive.
4. Add 25 μ l Tween 20 (0.05% v/v) and 2.5 ml 200 mM Na ₂ HPO ₄ to the stirring DAB solution.
5. This will generate a 10 mM Na ₂ HPO ₄ DAB staining solution and will pull the pH back up again.
Note: Sometimes the DAB will still not be fully dissolved, but usually very high levels of homogeneity in the solution are achieved. The DAB solution is only good for the day, then it should be made fresh. The concentration of DAB solution and time length of staining can be reduced according to plant material.

2.9 Bacterial growth in media containing shoot metabolites

To get a high biomass of Arabidopsis shoots, an updated liquid culture system was applied according to Héту et al. (2005). First, 15-20 surface-sterilized seeds were pipetted onto 2.6 cm diameter steel mesh discs which were lying on square plates filled with $\frac{1}{2}$ MS medium (1% sucrose, 0.1% MES buffer, 0.7 % agar, pH 5.8). Plates were incubated at 4 °C in darkness for 2 days. After that, plates were transferred to a growth chamber for 7 days. The growth condition was the same

as described in subchapter 2.3. Later, plant seedlings anchored to steel disks were transferred to 250 ml Erlenmeyer flasks containing 10 ml of growth medium ($\frac{1}{2}$ MS, 3% sucrose, 0.1% MES buffer, pH 5.8). Plants grew in an incubator at 22 °C and 100 rpm for 7 days. The medium was replaced by 10 ml fresh sucrose containing medium and plants were shaken for another 7 days under the same growth condition. After the fast growth phase, plants were supplied with medium without sucrose for 7 days. Lastly, plants were rinsed twice in 10 mM MgCl₂ after which shoots and roots were easily separated by scissor. Shoots were immediately frozen into liquid nitrogen and stored at -80°C for metabolites extraction.

Arabidopsis shoot metabolites were extracted according to the method updated from Jacoby et al. (2018). Samples were freeze dried in a lyophilizer chamber (Christ Beta 1-8 LD plus, Germany) that was at low pressure and low temperature so the water in the sample can sublime. To extract the metabolites, mortar, pestle, 1.5 ml Eppendorf tubes and micro spoon were pre-cooled with liquid nitrogen. Shoots were ground with a mortar and pestle continuously adding liquid nitrogen. After being ground into powder, shoots were allocated into 1.5 ml Eppendorf tubes for extraction. Metabolites were extracted in hot (75°C) 70% methanol for 10 min with 1500 rpm shaking. Extracts were then centrifuged at 15000 rpm for 10 min. The supernatant was dried in a Speed Vac (Eppendorf Concentrator Plus, Berzdorf, Germany) and metabolites were re-dissolved in MilliQ water. Water solutions of metabolites in Eppendorf tubes were combined together in a falcon tube and sterilized with a 0.22 µm pore size filter. Total organic carbon (TOC) was measure before sterilization.

The metabolites solution described above was used for generating bacterial growth media to mimic conditions of bacterial strains acquiring essential nutrients from their host plants. The growth media was based on 2xM9 formulation with two changes: the carbon source in media was replaced by shoot extracts and 100 mM MgSO₄ as a substitute of MgCl₂ was added to the 2xM9 formulation. Bacterial strains were rejuvenated by looping glycerol stocks into LB medium and incubated at 30°C with 200 rpm shaking overnight. 20 µl of liquid culture were inoculated into LB medium and cultured overnight at the same conditions. Next, bacterial cells were harvested from overnight cultures by centrifuging and rinsed twice in 10 mM MgCl₂. Cultures were adjusted to OD₆₀₀ of 0.5. For growth assays, 5 µl of this bacterial suspension was inoculated into a 96-well plate full with 100 µl media containing shoot extracts. The detail of media formulation was listed in Table 7. The

96-well plates were incubated in a plate reader (TECAN Infinite® 200 PRO). The growth condition was the same as described in subchapter 2.3.

2.10 Bacterial concentration quantification

A DNA-based real-time PCR assay was used for growth quantification of *B. glumae* in *Arabidopsis thaliana* (Ross and Somssich, 2016). Firstly, frozen material was homogenized and extracted by 200 µl of DNA isolation buffer (Table 8). After incubation for 10 min at 65°C and 400 rpm, samples were vortexed gently and then centrifuged for 10 min at 15000 rpm. Supernatant was then transferred to new tube and precipitated with 200 µl of isopropanol. Samples were centrifuged for 10 min; the pellet was dissolved in 100 µl of DNase free water and diluted to 13 ng/µl for quantitative real-time PCR. For qPCR analysis, 1 µl DNA, 4 µl gene-specific primer (*B. glumae* biomass specific primer: Burk1; *A. thaliana* biomass specific primer: INTERACTING PROTEIN OF 41 KDA (*TIP41*) and 5 µl SYBR® Green Supermix (Promega) were mixed. Primers used in this thesis are listed in table 11. The quantitative PCR reaction was performed in a CFX96 Touch™ Real-Time PCR Detection System (Bio-Rad, Munich, Germany) with two technical replicates. The qRT-PCR program is listed in Table 9. The concentration of bacterial PCR product was normalized to the abundance of plant PCR product.

Table 7 Composition of media containing shoot extracts

	LB			Col-0			<i>myb28 myb29</i>			<i>slim1</i>		
	1	2	3	4	5	6	7	8	9	10	11	12
A PG1	95µl LB 5µl PG1	95µl LB 5µl PG1	95µl LB 5µl PG1	26µl Col 5µl PG1 50µl 2xM9 1µl Cys 18µl H ₂ O	26µl Col 5µl PG1 50µl 2xM9 1µl Cys 18µl H ₂ O	26µl Col 5µl PG1 50µl 2xM9 1µl Cys 18µl H ₂ O	37µl <i>myb</i> 5µl PG1 50µl 2xM9 1µl Cys 7µl H ₂ O	37µl <i>myb</i> 5µl PG1 50µl 2xM9 1µl Cys 7µl H ₂ O	37µl <i>myb</i> 5µl PG1 50µl 2xM9 1µl Cys 7µl H ₂ O	35 µl <i>slim</i> 5µl PG1 50µl 2xM9 1µl Cys 9µl H ₂ O	35 µl <i>slim</i> 5µl PG1 50µl 2xM9 1µl Cys 9µl H ₂ O	35 µl <i>slim</i> 5µl PG1 50µl 2xM9 1µl Cys 9µl H ₂ O
B <i>cysH</i>	95µl LB 5µl <i>cysH</i>	95µl LB 5µl <i>cysH</i>	95µl LB 5µl <i>cysH</i>	26µl Col 5µl <i>cysH</i> 50µl 2xM9 1µl Cys 18µl H ₂ O	26µl Col 5µl <i>cysH</i> 50µl 2xM9 1µl Cys 18µl H ₂ O	26µl Col 5µl <i>cysH</i> 50µl 2xM9 1µl Cys 18µl H ₂ O	37µl <i>myb</i> 5µl <i>cysH</i> 50µl 2xM9 1µl Cys 7µl H ₂ O	37µl <i>myb</i> 5µl <i>cysH</i> 50µl 2xM9 1µl Cys 7µl H ₂ O	37µl <i>myb</i> 5µl <i>cysH</i> 50µl 2xM9 1µl Cys 7µl H ₂ O	35 µl <i>slim</i> 5µl <i>cysH</i> 50µl 2xM9 1µl Cys 9µl H ₂ O	35 µl <i>slim</i> 5µl <i>cysH</i> 50µl 2xM9 1µl Cys 9µl H ₂ O	35 µl <i>slim</i> 5µl <i>cysH</i> 50µl 2xM9 1µl Cys 9µl H ₂ O
C <i>cysM</i>	95µl LB 5µl <i>cysM</i>	95µl LB 5µl <i>cysM</i>	95µl LB 5µl <i>cysM</i>	26µl Col 5µl <i>cysM</i> 50µl 2xM9 1µl Cys 18µl H ₂ O	26µl Col 5µl <i>cysM</i> 50µl 2xM9 1µl Cys 18µl H ₂ O	26µl Col 5µl <i>cysM</i> 50µl 2xM9 1µl Cys 18µl H ₂ O	37µl <i>myb</i> 5µl <i>cysM</i> 50µl 2xM9 1µl Cys 7µl H ₂ O	37µl <i>myb</i> 5µl <i>cysM</i> 50µl 2xM9 1µl Cys 7µl H ₂ O	37µl <i>myb</i> 5µl <i>cysM</i> 50µl 2xM9 1µl Cys 7µl H ₂ O	35µl <i>slim</i> 5µl <i>cysM</i> 50µl 2xM9 1µl Cys 9µl H ₂ O	35µl <i>slim</i> 5µl <i>cysM</i> 50µl 2xM9 1µl Cys 9µl H ₂ O	35µl <i>slim</i> 5µl <i>cysM</i> 50µl 2xM9 1µl Cys 9µl H ₂ O
D MgCl ₂	95µl LB 5µl MgCl ₂	95µl LB 5µl MgCl ₂	95µl LB 5µl MgCl ₂	26µl Col 5µl MgCl ₂ 50µl 2xM9 1µl Cys 18µl H ₂ O	26µl Col 5µl MgCl ₂ 50µl 2xM9 1µl Cys 18µl H ₂ O	26µl Col 5µl MgCl ₂ 50µl 2xM9 1µl Cys 18µl H ₂ O	37µl <i>myb</i> 5µl MgCl ₂ 50µl 2xM9 1µl Cys 7µl H ₂ O	37µl <i>myb</i> 5µl MgCl ₂ 50µl 2xM9 1µl Cys 7µl H ₂ O	37µl <i>myb</i> 5µl MgCl ₂ 50µl 2xM9 1µl Cys 7µl H ₂ O	35 µl <i>slim</i> 5µl MgCl ₂ 50µl 2xM9 1µl Cys 9µl H ₂ O	36 µl <i>slim</i> 5µl MgCl ₂ 50µl 2xM9 1µl Cys 9µl H ₂ O	37 µl <i>slim</i> 5µl MgCl ₂ 50µl 2xM9 1µl Cys 9µl H ₂ O
E PG1	95µl LB 5µl PG1	95µl LB 5µl PG1	95µl LB 5µl PG1	31µl Col 5µl PG1 50µl 2xM9 19µl H ₂ O	31µl Col 5µl PG1 50µl 2xM9 19µl H ₂ O	31µl Col 5µl PG1 50µl 2xM9 19µl H ₂ O	44µl <i>myb</i> 5µl PG1 50µl 2xM9 8µl H ₂ O	44µl <i>myb</i> 5µl PG1 50µl 2xM9 8µl H ₂ O	44µl <i>myb</i> 5µl PG1 50µl 2xM9 8µl H ₂ O	42 µl <i>slim</i> 5µl PG1 50µl 2xM9 10µl H ₂ O	42 µl <i>slim</i> 5µl PG1 50µl 2xM9 10µl H ₂ O	42 µl <i>slim</i> 5µl PG1 50µl 2xM9 10µl H ₂ O
F <i>cysH</i>	95µl LB 5µl <i>cysH</i>	95µl LB 5µl <i>cysH</i>	95µl LB 5µl <i>cysH</i>	31µl Col 5µl <i>cysH</i> 50µl 2xM9 19µl H ₂ O	31µl Col 5µl <i>cysH</i> 50µl 2xM9 19µl H ₂ O	31µl Col 5µl <i>cysH</i> 50µl 2xM9 19µl H ₂ O	44µl <i>myb</i> 5µl <i>cysH</i> 50µl 2xM9 8µl H ₂ O	44µl <i>myb</i> 5µl <i>cysH</i> 50µl 2xM9 8µl H ₂ O	44µl <i>myb</i> 5µl <i>cysH</i> 50µl 2xM9 8µl H ₂ O	42 µl <i>slim</i> 5µl <i>cysH</i> 50µl 2xM9 10µl H ₂ O	42 µl <i>slim</i> 5µl <i>cysH</i> 50µl 2xM9 10µl H ₂ O	42 µl <i>slim</i> 5µl <i>cysH</i> 50µl 2xM9 10µl H ₂ O
G <i>cysM</i>	95µl LB 5µl <i>cysM</i>	95µl LB 5µl <i>cysM</i>	95µl LB 5µl <i>cysM</i>	31µl Col 5µl <i>cysM</i> 50µl 2xM9 19µl H ₂ O	31µl Col 5µl <i>cysM</i> 50µl 2xM9 19µl H ₂ O	31µl Col 5µl <i>cysM</i> 50µl 2xM9 19µl H ₂ O	44µl <i>myb</i> 5µl <i>cysM</i> 50µl 2xM9 8µl H ₂ O	44µl <i>myb</i> 5µl <i>cysM</i> 50µl 2xM9 8µl H ₂ O	44µl <i>myb</i> 5µl <i>cysM</i> 50µl 2xM9 8µl H ₂ O	42 µl <i>slim</i> 5µl <i>cysM</i> 50µl 2xM9 10µl H ₂ O	42 µl <i>slim</i> 5µl <i>cysM</i> 50µl 2xM9 10µl H ₂ O	42 µl <i>slim</i> 5µl <i>cysM</i> 50µl 2xM9 10µl H ₂ O
H MgCl ₂	95µl LB 5µl MgCl ₂	95µl LB 5µl MgCl ₂	95µl LB 5µl MgCl ₂	31µl Col 5µl MgCl ₂ 50µl 2xM9 19µl H ₂ O	31µl Col 5µl MgCl ₂ 50µl 2xM9 19µl H ₂ O	31µl Col 5µl MgCl ₂ 50µl 2xM9 19µl H ₂ O	44µl <i>myb</i> 5µl MgCl ₂ 50µl 2xM9 8µl H ₂ O	44µl <i>myb</i> 5µl MgCl ₂ 50µl 2xM9 8µl H ₂ O	44µl <i>myb</i> 5µl MgCl ₂ 50µl 2xM9 8µl H ₂ O	42 µl <i>slim</i> 5µl MgCl ₂ 50µl 2xM9 10µl H ₂ O	42 µl <i>slim</i> 5µl MgCl ₂ 50µl 2xM9 10µl H ₂ O	42 µl <i>slim</i> 5µl MgCl ₂ 50µl 2xM9 10µl H ₂ O

Different volume of shoot extracts solution from plant genotypes was added to ensure that the total organic carbon content in each well was the same.

Table 8 DNA isolation buffer
0.2 M Tris pH 8.0
0.25 M NaCl
0.025 M EDTA pH 8.0
0.5 % SDS

Table 9 qRT-PCR program		
Temp. [°C]	Time [min]	
95	2:00	39x
95	1:15	
59	0:30	
60	0:30	
95	0:30	
59	0:30	
65	0:05	
95	0:5	

2.11 Metabolites analysis

2.11.1 Isolation & quantification of camalexin

Camalexin was extracted and measured as described by Koprivova et al. (2019). Briefly, frozen plant material was crushed by tissue lyser with the help of glass balls. Camalexin was extracted by 200 µl high-performance liquid chromatography (HPLC)-class DMSO at 25 °C and 450 rpm shaking for 20 min. After that, samples were centrifuged at 15000 rpm for 25 min. Supernatants were transferred to new tubes and centrifuged again. The final supernatants were transferred to HPLC vials for further injection. The detail of camalexin measurement by HPLC method was described in Koprivova et al. (2019).

2.11.2 Isolation & quantification of glucosinolates

Glucosinolates were extracted as described by Dietzen et al. (2020). Firstly, columns for glucosinolates isolation were prepared by plugging non-absorbent cotton wool into 1 ml tips. Columns were wet twice with 0.5 ml sterile MilliQ water before adding 0.5 ml DEAE-Sephadex A-25. Columns with the DEAE-Sephadex A-25 layer were washed twice by 0.5 ml sterile MilliQ water and then ready to be used.

Samples were ground in cold tissue lyser blocks and then extracted by 70 °C 70% methanol for 45 min, with the addition of 10 µl sinigrin as internal standard. Samples were cooled down and centrifuged with 15000 rpm for 10 min. Supernatants were added to prepared columns and washed twice with 0.5 ml sterile MilliQ water, and subsequently twice with 0.5 ml of 0.02 M sodium acetate buffer. When columns stopped dropping, 1 ml Eppendorf tubes were placed underneath each column and then 75 µl sulfatase solution was added onto the top surface of DEAE-Sephadex A-25 layer. After overnight incubation, columns were eluted twice with 0.5 ml of sterile MilliQ water and finally with 0.25ml sterile MilliQ water to make sure produced desulfoglucosinolates were eluted completely. Desulfoglucosinolates solution was vortexed, centrifuged and supernatant was transferred to HPLC vials.

Fifty µl desulfoglucosinolates were injected to the Thermo Fisher Scientific Dionex UltiMate 3000 HPLC system equipped with column Spherisorb ODS-2 (250 × 4.6 mm, 5 µm; Waters) and measured at 229 nm UV absorption. Peaks of different desulfoglucosinolates were identified by retention time and quantified by the internal standard method with different response factors corresponding to individual glucosinolates.

2.11.3 Isolation & quantification of low-molecular weight thiols

Arabidopsis were homogenized with glass beads and ca. 20 mg were taken for thiols extraction using 10-fold (W: V) volume of 0.1 M HCL. After 10 min of centrifugation at 4°C, 60 µl supernatant was transferred to Eppendorf tubes containing a mix of 100 µl of 0.25 M CHES-NaOH, pH 9.4 and 35 µl of 100 mM freshly made 0.1 M dithiothreitol (DTT) to reduce disulfides. Samples were incubated for 40 min at room temperature (RT). 5 µl of 25 mM monobromobimane (diluted in acetonitrile) were added to conjugate SH groups of cysteine and glutathione (GSH) for 15 min in dark. 110 µl of 100 mM methanesulfonic acid was added to stop the reaction. The mix was centrifuged at 4°C at 15000 rpm for 20 min and supernatants were transferred into HPLC vials for measurement. Thiols were measured by high-performance liquid chromatography (HPLC) method according to Dietzen et al. 2020 with two changes: excitation changed from 392 nm to 380 nm, detection from 480 nm to 470 nm.

2.11.4 Determination of Pipecolic acid and salicylic acid

Pipecolic acid (Pip) and salicylic acid (SA) were extracted and quantified with the help from the lab of Prof. Dr. Jürgen Zeier. It should be noticed that the whole extraction procedure was performed under cool condition. Arabidopsis shoots were homogenized in cool condition and extracted with 1 ml pre-cooled buffer with internal standard. The mix were then thoroughly vortexed for 5 seconds, shaken for 6 min and centrifuged for 6 min at 4°C. The supernatants were transferred to pre-cooled tubes and the pellets were extracted with 1 ml buffer without internal standard. After vortex, shaking and centrifuge, the supernatants were combined with the one previously collected. A 600 µl aliquot from the combined supernatant was transferred to a pre-cooled 2 ml tubes and dried in a Speed Vac machine Vac (Eppendorf Concentrator Plus, Berzdorf, Germany). Samples should be derivatized before being injected to GC machine (Agilent Technologies) equipped with a fused silica capillary column (ZB-5MS 30 m × 0.25 mm; Zebron, Phenomenex) and a 5975C mass spectrometric detector (Agilent Technologies). Derivatization solutions were added with syringe. 20 µl of pyridine was added to samples and vortexed, following by addition of 20 µl of MSTFA (N-methyl-N-trimethylsilyl trifluoroacetamide) containing 1 % TCMS (chlorotrimethylsilane, v/v). After vortex, 60 µl of n-hexane was added to each sample. Determination of the levels of free SA, conjugated SA and Pip was described in detail by Návarová et al. (2012).

2.12 Gene expression analysis

RNA was isolated by phenol-chlorophorm-isoamylalcohol extraction and precipitated by LiCl. Frozen material was homogenized with glass beads in 500 µl RNA extracted buffer (Table 10) and vortexed for 5 s followed by addition of 500 µl of phenol-chlorophorm-isoamylalcohol mix (25:24:1; v/v). All samples were shaken and rotated for another 5 min after the last sample was finished. Samples were centrifuged at 15000 rpm and room temperature for 25 min. The supernatants were transferred to new tubes containing 500 µl of phenol-chlorophorm-isoamylalcohol mix, vortexed and centrifuged at 15000 rpm for 20 min. This step was repeated a second time and the supernatant was transferred to tubes containing 150 µl of 8 M LiCl to precipitate RNA at -20°C overnight. The next day, samples were centrifuged at 4°C, 15000 rpm for 40 min. 300 µl of MilliQ water was added and samples were shaken at 65 °C, 450 rpm for 10 min to dissolve the RNA pellets. 100 µl of 8 M LiCl was added to re-precipitate RNA at -20°

overnight. The last day, samples were centrifuged at 4°C, 15000 rpm for 40 min. The pellet was washed with 400 µl of 70 % EtOH. After 10 min of centrifugation at the same condition, EtOH was discarded and samples were dried in air. Pellets were dissolved by 30 µl of MilliQ water at 65°C for 20 min. Concentration and purity of RNA were measured using a UV-Vis Spectrophotometer (Nanodrop™, 2000C, Thermo Fisher, Wilmington, Delaware USA).

First-strand cDNA was synthesized from 800 ng of RNA in a 6 µl reaction volume according to the instruction of QuantiTech Reverse Transcription Kit (Qiagen, Crawley, UK). The qPCR reaction was the same as described in bacterial quantification. Expression of genes of interest was normalized to *TIP41* gene using $2^{-\Delta\Delta CT}$ method.

Table 10 RNA isolation buffer (for 200 ml)	
80 mM Tris pH 9.0	1.94 g
5% SDS	50 ml (20 %)
150 mM LiCl	1.2 g
50 mM EDTA	3.72 g
Mix Tris, LiCl and EDTA together and then adjust pH value to 9.0, then make the solution to the final volume of 200 ml.	

Table 11 Oligonucleotides for gene expression analysis by qRT-PCR				
Name	Gene	Forward primer	Reverse primer	Reference
<i>TIP41</i>	AT4G34270	gaactggctgacaatggagtg	atcaactctcagccaaaatcg	(Koprivova et al., 2019b)
<i>Burk1</i>	NR042931	ggaactgcatttgactgg	ctccccacgctttcgtgc	(Koprivova et al., 2019b)
<i>PAL1</i>	AT2G37040	gtgtcgcaacttcagaaggaa	ggcttgtttcttcgtgctt	(Huang et al., 2010)
<i>ALDI</i>	AT2G13810	gtgcaagatcctaccttcccggc	cggtccttgggggtcatagccaga	(Návarová et al., 2012)
<i>ICSI</i>	AT1G74710	gcaagagtgaacatctatattctc	cacaacagctggagttgga	(Park et al., 2007)
<i>PRI</i>	AT2G14610	gtgctcttgttcttcctcg	gcctggttgaacccttag	(Návarová et al., 2012)

2.13 Data analysis

Plots in this thesis were generated in GraphPad Prism (version 9.4.1). All experiments were repeated twice. Experimental results of those two independent repeats were comparable. The presented data was generally from a single biological experiment. Statistical differences between more than two treatments were tested by one-way ANOVA when there was only one independent variable, followed by post-hoc Tukey test at $p \leq 0.05$. Student's *t*-test was used to analysis data within two treatments.

3 Results

3.1 The bacterial *cysH* mutant is deficient in consuming oxidized sulfur sources

The *CysH* and *CysM* are essential genes in sulfur assimilation pathway of bacteria. To be specific, *CysH* gene in *B. glumae* PG1 encodes an enzyme from the APS/PAPS reductase family that reduces activated sulfate in the form of APS to sulfite. The *CysM* gene encodes O-acetyl-L-serine(thiol)-lyase B, which catalyzes the synthesis of S-sulfocysteine (SSC) from thiosulfate and OAS. SSC can be converted to Cys in one step under the catalyzation of thioredoxin/glutaredoxin. To evaluate if mutations in *CysH* or *CysM* gene affect the sulfur assimilation ability of *B. glumae*, three oxidized sulfur sources (MgSO₄, taurine and PNPS) and two reduced sulfur sources (cysteine and methionine) were fed to wild type PG1 strain, *cysH* and *cysM* bacterial mutants at the same final sulfur concentration of 1 μM.

Growth curves were plotted and area under growth curve was computed in R with Growthcurver package. Representative growth curves of bacterial strains fed by different inorganic or organic sulfur sources can be observed in Fig. 3.1A. When fed with taurine (an oxidized sulfur source), OD₆₀₀ value of the *cysH* mutant was stable during the incubation, which means that the bacteria did not proliferate when taurine was the only sulfur source. In contrast, both the *cysM* mutant and PG1 showed a standard growth curve pattern when fed with taurine: from lag phase, exponential phase to stationary phase. PG1 reached the stationary phase later than the *cysM* mutant. The growth curves of PG1, *cysH* and *cysM* grown in media containing MgSO₄ or PNPS were consistent with those from media with taurine. When fed with thiosulfate, cysteine and methionine (reduced sulfur sources), PG1, *cysH* and *cysM* mutants all grew well. These growth curves indicate that the *cysH* mutant is unable to consume oxidized sulfur sources, but is able to effectively utilise reduced sulfur sources. However, sulfur absorption of the *cysM* mutant is not affected and it consumes all sulfur compounds as efficient as PG1. The value of auc_e is the empirical area under the curve which is obtained by summing up the area under the experimental curve from the measurements in the input data. Similar to the growth curve pattern, auc_e value of each bacteria demonstrates that the *cysH* mutant grows slower than PG1 and the *cysM* mutant when an oxidized sulfur compound is the only sulfur source. When a reduced sulfur source is available, PG1, *cysH* and *cysM* mutants grow at the same rate (Fig. 3.1B).

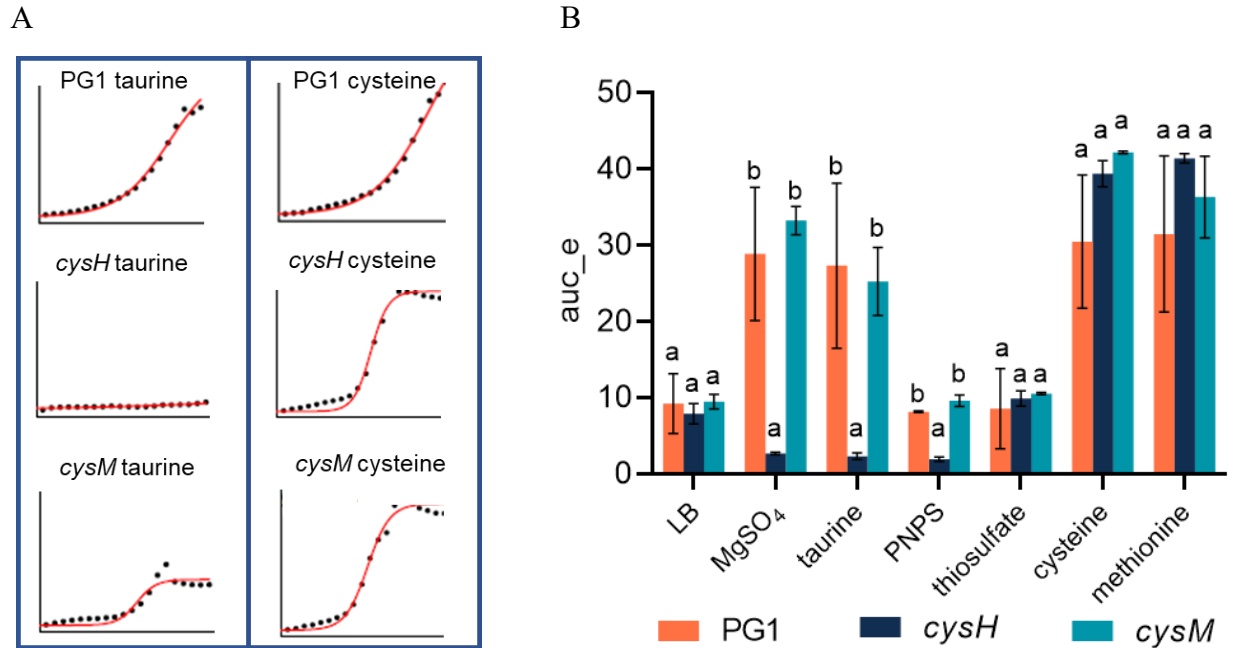


Figure 3.1 *cysH* mutant grows slower than PG1 and *cysM* with oxidized sulfur sources

Bacterial strains were inoculated into M9 minimum media containing glucose as the only carbon source and an exogenous oxidized or reduced compounds as the only sulfur source. They were grown in 96-well plate and incubated in TECAN microplate reader at 30°C for 48 h. During incubation, absorbance value at 600 nm of each well was simultaneously collected every 10 min. Data was analyzed in R with Growthcurver package. (A) Characteristic growth curves of PG1, *cysH* and *cysM* mutants with only one oxidized or reduced sulfur nutrient in media. X-axis represents time and Y-axis represents value of OD₆₀₀. (B) The value of auc_e of bacteria fed with different sulfur chemicals were computed with Growthcurver package in R. Bars represent the mean ± SEM. Different letters above bars denote statistically significant differences between bacterial growth rate fed by the same sulfur source ($P < 0.05$, one-way ANOVA).

3.2 *cysH* and *cysM* mutants have less severe growth inhibitory effect on *Arabidopsis thaliana*

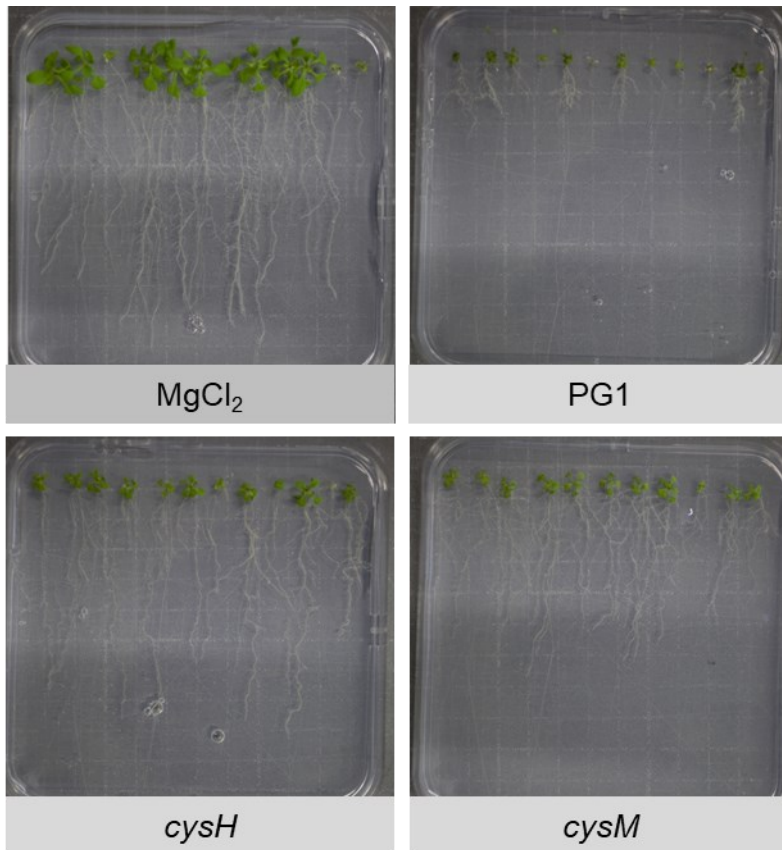
To test whether sulfur assimilation deficiency affects bacterial pathogenicity, PG1, the *cysH* and *cysM* mutants were co-cultivated with Col-0 on square plates containing ½ MS medium for 2 weeks. Fresh weights of *Arabidopsis* and length of the primary root were measured.

All 3 strains, PG1, *cysH* and *cysM* mutants, altered the plant root architecture: bacteria treated roots were shorter than non-treated ones. PG1 treated Col-0 seedlings had the shortest primary root length. The *cysM* mutant-treated Col-0 showed shorter primary root length than the *cysH* mutant

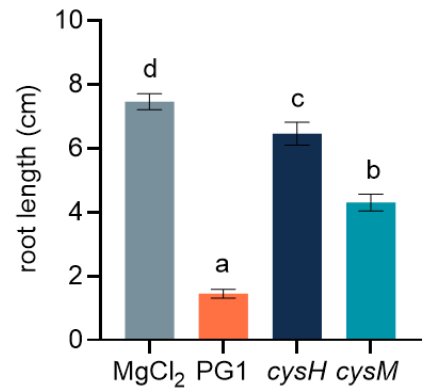
(Fig. 3.2A, Fig. 3.2B). Besides, it can be observed that shoots from the PG1 treated group were slightly smaller than *cysH* and *cysM* shoots, and markedly smaller than the controls. Shoots from plants treated with *cysH* and *cysM* showed no visible alterations in size and color (Fig 2A). Fresh weight of shoots and roots showed the same pattern: bacteria-treated Col-0 grew slower than the control group. However, there was no significant difference in fresh weight between the PG1 treatment and bacterial mutants treatment (Fig. 3.2C).

The growth pattern together with fresh weight data demonstrates that PG1, *cysH* and *cysM* mutants inhibit Col-0 growth. PG1 suppresses root development more severely than *cysH* and *cysM* mutants.

A



B



C

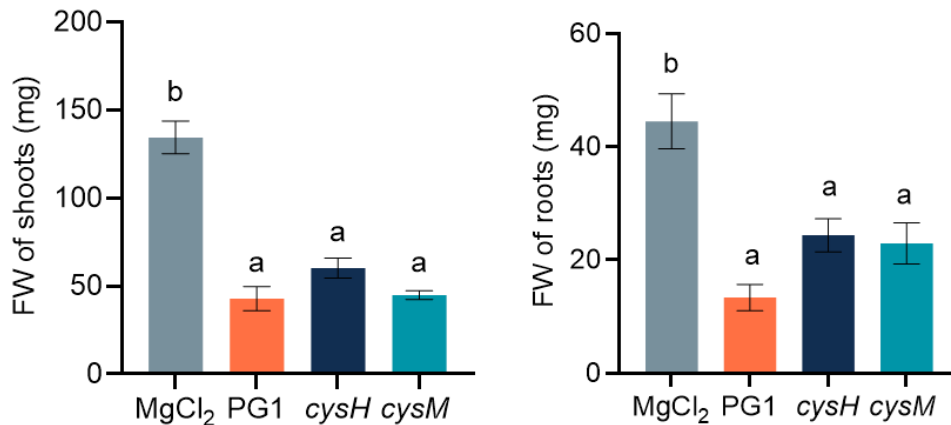


Figure 3.2 PG1, *cysH* and *cysM* inhibit growth of *Arabidopsis* Col-0

Bacterial strains PG1, *cysH* and *cysM* mutants were added to ½ MS medium and poured into square plates. Col-0 was co-cultivated with bacteria on the medium for 2 weeks. Primary root length and fresh weight of plants were recorded. (A) Typical growth of Col-0 co-cultivated with MgCl₂, PG1, *cysH* and *cysM* mutants. (B) Primary root length. (C) Fresh weight of shoots and roots. Bars represent the mean ± SEM of 4 replicates. Different letters represent statistically significant differences of fresh weights between mock control and bacterial treatments ($P < 0.05$, one-way ANOVA).

3.3 PG1 elicits stronger hypersensitive response on *Arabidopsis* leaves than *cysH* and *cysM* mutants

To further examine the pathogenicity of *B. glumae* on *Arabidopsis* and compare it between PG1, *cysH* and *cysM* mutants, a series of experiments was conducted. First, leaves of 4 weeks old *Arabidopsis* grown on soil were infiltrated with bacterial pathogens and the consequent hypersensitive response (HR) was determined. Infected cells undergo rapid programmed cell death called the HR. In our study, part of *B. glumae* infected leaves exhibited obvious HR symptoms, for example yellowish lesion, after 3 days of infiltration.

All three bacterial strains stimulated visible HR response but not extensive necrosis on leaves. Most leaves (11 from 14 leaves) infiltrated with PG1 showed marked yellowish lesion areas. In contrast, only less than a half of the leaves from *cysH* and *cysM* treatments (6 from 14 leaves, 6 from 17 leaves) showed obvious lesions (Fig. 3.3A). To quantify the extent of the HR symptom, we extracted chlorophyll from infiltrated leaves. Less chlorophyll content in leaves corresponds to more lesion elicited by the pathogen infection. PG1 infiltrated leaves contained less chlorophyll than leaves treated by MgCl₂ and the *cysM* mutant. Leaves from *cysH* had also higher chlorophyll

concentration than PG1, but not statistically significant at the chosen P value of 0.05. No significant difference in chlorophyll concentration was observed between *cysH* and *cysM* as well (Fig. 3.3B). The HR symptom indicates that *B. glumae* induces immune response on Arabidopsis and that loss of *CysH* and *CysM* results in lower pathogenicity.

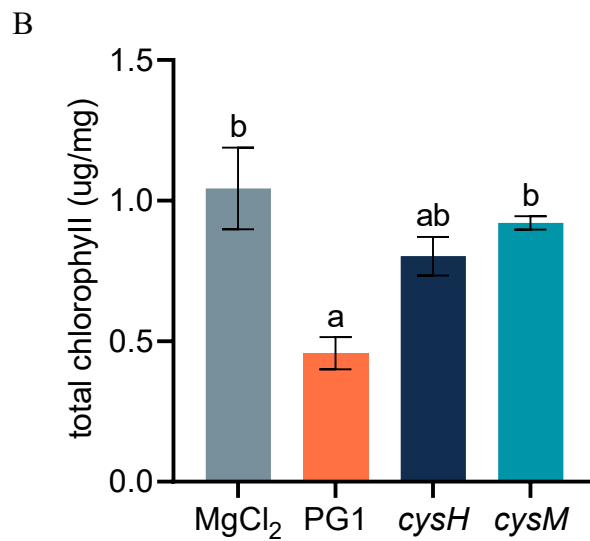


Figure 3.3 PG1 induces larger lesions on Col-0 leaves

Bacterial suspensions were infiltrated into rosette leaves. Leaves were collected for photographing and chlorophyll extraction when no new symptom appeared. (A) Yellowish HR symptom elicited by MgCl₂, PG1, *cysH* and *cysM* mutants. (B) Chlorophyll content of leaves which showed obvious lesion. Bars represent the mean ± SEM. Different letters represent statistically significant differences in chlorophyll between bacterial treatments ($P < 0.05$, one-way ANOVA).

3.4 PG1 triggers stronger initial immune response in Arabidopsis than *cysH* and *cysM* mutants

The earliest responses to pathogen invasion have been defined as Ion flux and a burst of oxygen metabolism that produces reactive oxygen species (ROS). Once being attacked by pathogens, ROS, such as superoxide (O_2^-) and hydrogen peroxide (H_2O_2) are produced, which are in turn required for induction of defense genes and biosynthesis of antimicrobial metabolites, for example camalexin and glucosinolates in Arabidopsis (Scheel, 1998). ROS have been associated with apoptosis of mammalian cells, and have a role in cell death during the HR in plants. In this study, we detected the H_2O_2 level triggered by *B. glumae* invasion with DAB staining method to estimate the strength of immune response triggered by pathogens and compare the pathogenicity difference between *B. glumae* PG1, *cysH* and *cysM* mutants.

Shoots from the 12-well hydroponic culture system were cut and transferred to a new 12-well plate for DAB staining. No DAB staining mark was observed when shoots were dissected 4 h or 8 h after inoculation. Shoots inoculated with bacteria for 6 h showed notable DAB staining marks. No detectable staining mark was found in control leaves (MgCl₂ treatment) at this time point. Most leaves (54 leaves from 72 in total) from the PG1 treated group displayed heavier brown precipitates along the veins and among cells. In contrast, only about 10 leaves from 70 in total from *cysH* and *cysM* groups showed slight brown precipitates on the tip of leaves (Fig. 3.4). These staining results indicate that PG1 induces strikingly stronger initial immune response than *cysH* and *cysM* mutants.

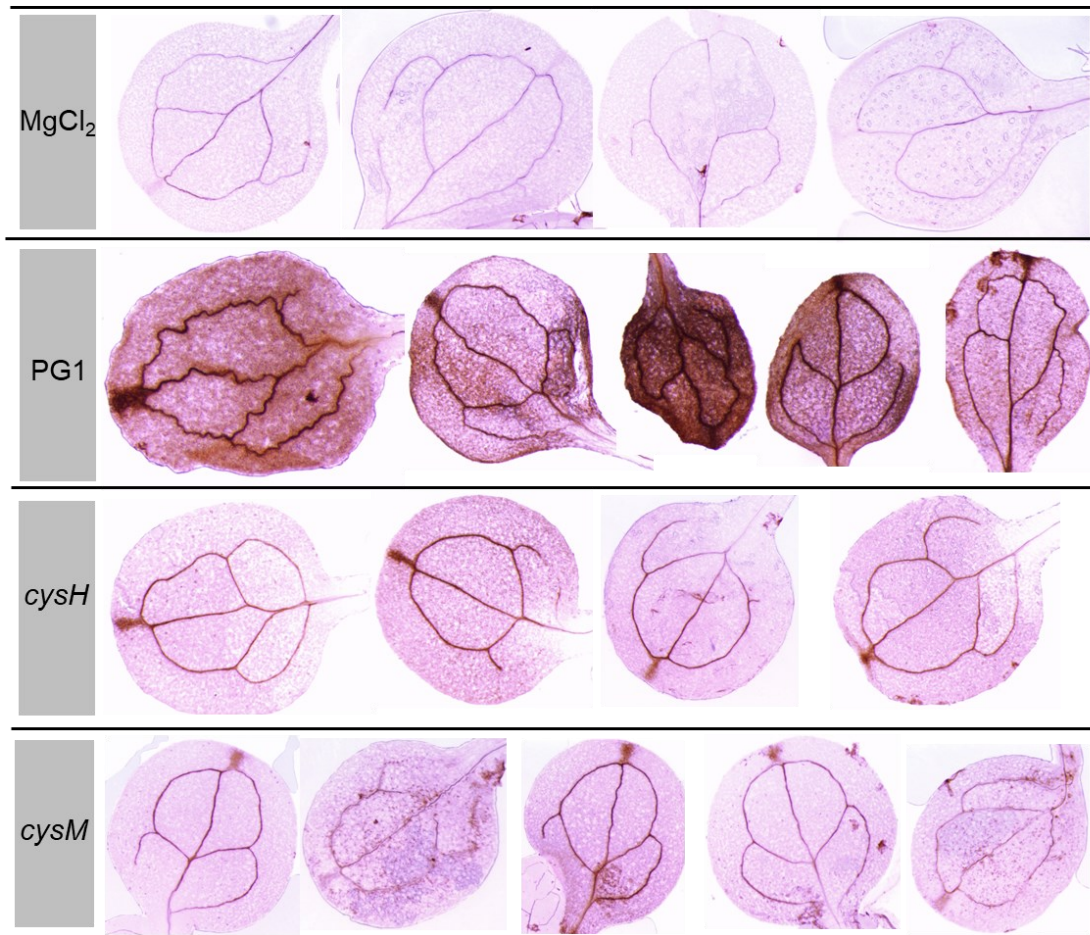


Figure 3.4 PG1 cause stronger Arabidopsis hypersensitive reaction

Arabidopsis Col-0 were incubated with the bacterial strains in the 12-well hydroponic culture system for 4 h, 6 h and 8 h. At those three time points, leaves were cut for DAB staining. Photos represent the staining result 6 hours after inoculation. Dark brown precipitates indicated location and concentration of H_2O_2 .

3.5 *B. glumae* PG1 induces higher level of the phytoalexin camalexin

Camalexin is a dominant phytoalexin of *A. thaliana*, which can be greatly induced by a wide variety of plant pathogens. This phytoalexin has been confirmed to play a positive role in plant resistance to pathogen invasion (Liao et al., 2022). In this assay, we quantified camalexin biosynthesis triggered by *B. glumae* infection to check if the camalexin data is in parallel with the DAB staining result, which will help us better know the pathogenicity difference between PG1, *cysH* and *cysM* mutants.

Camalexin induction level in shoots and roots showed the same pattern: PG1 induced highest camalexin accumulation compared to *cysH* and *cysM* mutants; camalexin content in leaves inoculated with *cysH* and *cysM* mutants were at the same level (Fig. 3.5). Camalexin content of the control plants was repeatedly under detectable level. This result suggests that PG1 stimulates stronger immune response in Col-0 than *cysH* and *cysM*, which means *cysH* and *cysM* lost part of their pathogenicity.

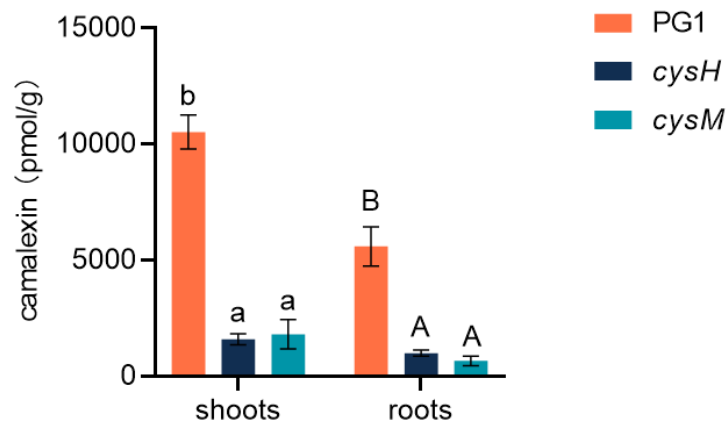


Figure 3.5 Camalexin induction by PG1, *cysH* and *cysM*

Arabidopsis Col-0 were incubated with the bacteria in the 12-well hydroponic system for 3 days. Camalexin was extracted from shoots and roots and analyzed by high-performance liquid chromatography (HPLC). Bars represent the mean \pm SEM. Different letters represent statistically significant differences of camalexin level between bacterial treatments ($P < 0.05$, one-way ANOVA). Small letters and capital letters are assigned to shoots and roots respectively.

3.6 Exogenous cysteine restores pathogenicity of *cysH* and *cysM* mutants

By a series of phenotype experiments and chemical assay, we concluded that *B. glumae* PG1 and its mutants *cysH* and *cysM* have an inhibitory effect on plant growth, cause HR symptoms on leaves and activate immune responses, such as H_2O_2 production and biosynthesis of the antimicrobial compound camalexin. PG1 induces stronger immune responses than *cysH* and *cysM* mutants and *cysH* and *cysM* trigger immune responses at the same level. These results imply that PG1 is more pathogenic than *cysH* and *cysM*, and that sulfur assimilation deficiency has a negative impact on pathogenicity of *cysH* and *cysM*. Even though *cysH* and *cysM* mutants have the same

ability as PG1 to use exogenous reduced sulfur sources in the in-vitro artificial media, it does not mean that they are able to behave as PG1 *in vivo* of host plants, where they encounter more complicate metabolic niches. Thus, we hypothesised that *cysH* and *cysM* mutants are less efficient in taking up sulfur nutrition directly from plants, and this deficiency may explain the pathogenicity loss. To prove this hypothesis, we conducted a shoot metabolite feeding experiment with cysteine complementation. We compared the growth rates of PG1, *cysH* and *cysM* in media containing metabolites extracted from shoots; besides, cysteine was added to media to determine if this exogenous sulfur source will restore growth of *cysH* and *cysM*. Leaf apoplast and cell organelles can serve as nutrient reservoirs for invasive bacterial pathogens. By feeding bacteria with shoot extract, we simulated nutrient niches in plants and had a preliminary insight into how bacteria take up nutrients from plants.

Col-0 shoot extract was applied as the only carbon source to feed bacterial strains. The auc_e result showed that the *cysH* mutant absorbed shoot metabolites distinguishably slower than PG1 and the *cysM* mutant when there was no additional cysteine. The growth rate of *cysH* strikingly increased when exogenous cysteine was applied in media; whereas it only increased the growth rate of PG1 slightly. Interestingly, the *cysM* mutant grew faster than PG1 in the presence or absence of exogenous cysteine supplementation (Fig. 3.6B). The growth rate results indicate that sulfur assimilation deficiency negatively affects the ability of *cysH*, but not *cysM*, to take up nutrients from the plant host, especially when shoot extract is the only carbon and organic sulfur source. Exogenous cysteine provides bacteria with enough organic sulfur and then restores growing the capacity of the *cysH* mutant.

Since cysteine supplementation increased the growth rate of the *cysH* mutant, we therefore hypothesised that additional cysteine could allow bacterial mutants to induce stronger immune response in plants. We added cysteine to the hydroponic culture system after the inoculation of bacteria. *cysH* and *cysM* mutants induced significantly higher camalexin accumulation in the presence of exogenous cysteine than in the absence of cysteine, to the same level as induced by PG1 (Fig. 3.6C). The growth rate results and induction of camalexin biosynthesis proved our hypothesis: the *cysH* mutant is less capable in consuming nutrients from shoot extract than PG1 and the *cysM* mutant and induces weaker immune response than PG1; however, exogenous cysteine, as an organic reduced sulfur source, boosts *cysH* growth rate and then cause stronger

immune response, which means the deficiency to take up nutrients from plant can partly explain the pathogenicity loss.

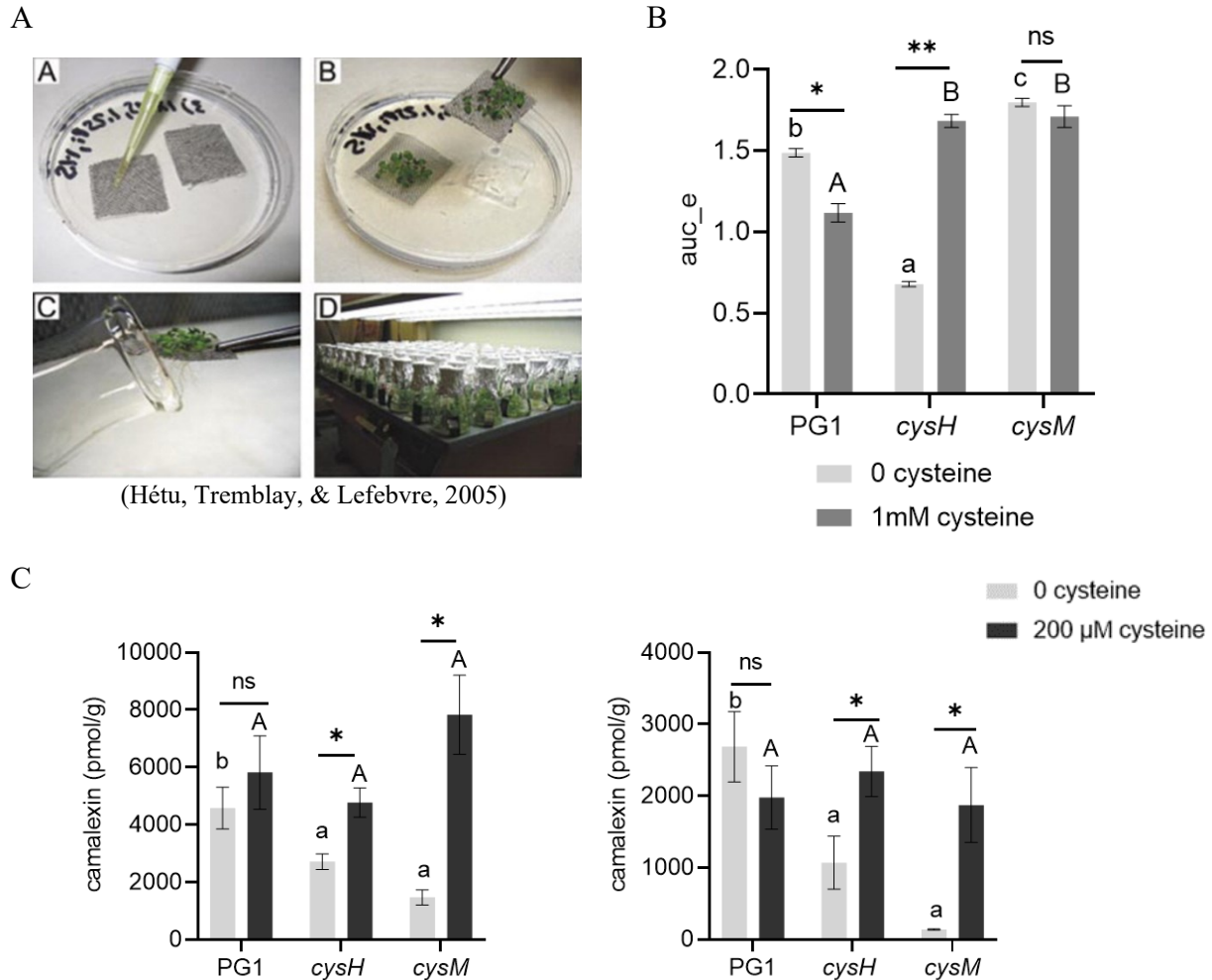


Figure 3.6 Sulfur assimilation deficiency negatively affects nutrient uptake in plant

(A) Procedure of obtaining high biomass plant material used for extracting shoot metabolites. (B) Shoot extract of Col-0 was fed to bacteria as the only carbon source and organic sulfur source. Cysteine was added to media and incubated together with bacteria in a TECAN microplate reader. The auc_e data was plotted in R with Growthcurver package. (C) Cysteine was added to the 12-well hydroponic system after inoculation of bacteria. Camalexin in shoots (left) and roots (right) were analysed. Bars represent the mean \pm SEM. Different letters represent statistically significant differences between bacterial treatments ($P < 0.05$, one-way ANOVA). Capital letters and small letters are assigned to condition with or without cysteine complementation. Asterisks indicate different camalexin induction levels between different cysteine condition of the same treatment (student's t-test, $P < 0.05$).

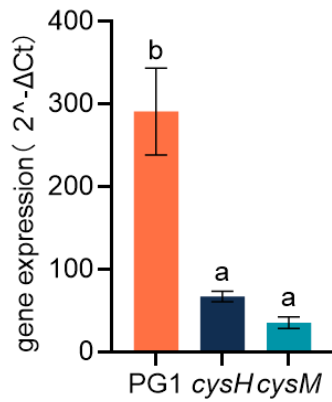
3.7 PG1 has a more robust colonizing ability than *cysH* and *cysM* mutants

By performing in-vitro shoot extract feeding experiment, we confirmed that the *cysH* mutant is defective in taking up nutrients from Arabidopsis and that cysteine added to media boosts its growth rate. Therefore, we hypothesised that PG1, *cysH* and *cysM* mutants were different in their ability to grow inside of the plants; PG1 and the *cysM* mutant may be more robust in inhabiting this niche than the *cysH* mutant. To test this hypothesis, we quantified bacterial concentration inside plants by a qPCR method. This method was proven to be reliable by confirming with traditional plate colony counting method (Appendix S1)

After bacterial inoculation in the 12-well hydroponic system for 3 days, total DNA of plant and bacteria from shoots and roots were extracted. All DNA samples were diluted to the same concentration for further qPCR analysis. Two specific primer pairs targeting a single copy gene from Arabidopsis (*TIP41*) and *B. glumae* (NR042931) were used in this assay. Each copy of DNA represents a single plant cell or bacterial cell. By subtracting the Ct value of the bacterial gene from the Ct value of the plant gene, the relative abundance of bacterial cells can be quantified.

The Δ Ct value showed that the relative concentration of PG1 cells was higher than that of *cysH* and *cysM* mutants cells in both shoots and roots (Fig. 3.7A, 3.7B). This suggests that the PG1 proliferates more and adapts better inside plant niches. For PG1 and the *cysH* mutant, the proliferation ability is consistent with the growth rate in shoot extract media. This means that *cysH* is not only deficient in acquiring nutrients in-vitro but also impaired in adapting to interior niches of plant hosts. The lack of colonization competence leads to less proliferation inside plant followed by a weaker immune response induction, or a lower pathogenicity. In contrast, the *cysM* mutant is able to acquire nutrient from shoot extract as PG1, but is still defective in colonizing interior plant tissue.

A



B

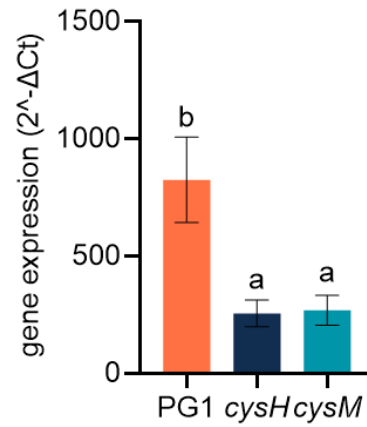


Figure 3.7 Proliferation of PG1 inside plants is notably higher than *cysH* and *cysM*

Relative bacterial abundance in Col-0 shoots (A) and roots (B) was determined by the qPCR-based ΔC_t calculation method. Bars represent the mean \pm SEM. Different letters represent statistically significant differences between bacterial concentration inside the plant ($P < 0.05$, one-way ANOVA).

4 Results

In chapter 3, we conducted a series of experiments to estimate if sulfur assimilation deficiency affects pathogenicity of *cysH* and *cysM* mutants compared to wild type PG1, and to investigate mechanisms underpinning pathogenicity difference between these three strains. The *cysH* mutant is impaired in utilizing oxidized sulfur sources and grows slower than PG1 and the *cysM* mutant in media with shoot extract as the only carbon source. Even though the *cysM* mutant shows the same capability as PG1 to use oxidized sulfur sources and to consume shoot extract, the *cysM* mutant still shows less inhibitory effect on *Arabidopsis* growth and induces reduced immune response compared to PG1 as does the *cysH* mutant. It can be concluded that *cysH* and *cysM* mutants are less adaptive in colonizing inside plants, which results in reduced virulence. This means nutrient uptake competence of pathogens is important for inhabiting inside plant tissues. Plant tissue, for example, phloem, leaf apoplast and cell organelles are abundant with nutrients including sugars, amino acids and organic (Vorholt, 2012). These nutrients inside the plants enable pathogens to grow at high density, consequently to stimulate immune response and eventually to cause disease in an interior space without harsh and fluctuating environmental change. Naturally, we wondered if sulfur-related nutrients alteration inside plants had an impact on immune response to pathogens as well. In this chapter, we tested if modulation of sulfur assimilation in *Arabidopsis* influences its immune response to pathogens, and if so, what were critical metabolites that regulated plant-pathogen interaction.

4.1 Modulation of sulfur assimilation in *Arabidopsis* has an impact on immune response to *B. glumae*

Arabidopsis takes up inorganic sulfate and assimilates it into diverse bio-organic molecules through two ways: either reducing sulfate to sulfide and incorporating it into the skeleton of OAS to form cysteine in the primary sulfur assimilation pathway, or activating stable sulfate to 3'-phosphoadenosine 5'-phosphosulfate (PAPS) and incorporating it into a variety of secondary products (Kopriva et al., 2012). Manipulation of the sulfur assimilation pathway changes sulfur flux through these two branches and alters sulfur metabolism and accumulation of sulfur-containing compounds. To investigate effect of sulfur metabolism on plant immune response, *Arabidopsis* Col-0 and mutants with impaired sulfur assimilation or regulation pathway in both

branches were used in this chapter. Plants and bacterial pathogens were incubated in 12-well hydroponic system for 3 days; camalexin was then extracted from shoots and roots to function as a marker for plant immune response.

Arabidopsis mutant *cad2-1* is deficient in the first step of GSH synthesis pathway and has 15 to 30 % of leaf GSH compared to that in the wild type parental accession Col-0. Besides, *cad2* plant mutant accumulates cysteine. The level of glucosinolates in *apk1 apk2* double mutant is reduced to approximately 20% of that in Col-0. Disruption in *APK1* and *APK2* also leads to great alteration in sulfur metabolism: accumulation of desulfated glucosinolate precursors, and increased level of sulfate, OAS and thiols (Mugford et al., 2009c). Comparing immune response between Col-0, *cad2* and *apk1 apk2* assessed if GSH level might be implicated in immune response. However, camalexin biosynthesis induction pattern was the same in Col-0, *cad2*, and *apk1 apk2*: PG1 triggered significantly higher camalexin accumulation than *cysH* and *cysM* in both shoots and roots (Fig. 4.1A, 4.1B). We compared camalexin concentration of PG1 treatment among Arabidopsis genotypes, and found that *cad2* had slightly lower camalexin biosynthesis than Col-0 and *apk1 apk2* in shoots, but this difference was not observed in roots.

High-affinity sulfate transporter *sultr1;2* is responsible for sulfate uptake from the soil solution. Sulfate contents in the *sultr1;2* mutant plant is ranging from ca. 30 to 65% of the wild-type plant values (Barberon et al., 2008). APR2 is the dominant enzyme in the family of adenosine 5'-phosphosulfate reductase (APR) that converts activated sulfate to sulfite, the first step of sulfate reduction pathway. Sulfur metabolism is perturbed in *apr2* plants with increase in total sulfur and sulfate and decrease in glutathione concentration. Besides, *apr2* does not show typical sulfate starvation phenotype, as cysteine and methionine concentrations increase (Grant et al., 2011). Inactivation of *APR1* reduces APR activity by ca. 20% (Koprivova A and Kopriva S, unpublished). The camalexin induction pattern in Col-0, *sultr1;2* and *apr1 apr2* was comparable: camalexin biosynthesis was higher in PG1 treatment than in bacterial mutants' treatment in both shoots and roots (Fig. 4.1C, 4.1D). In shoots, no difference was observed in PG1-induced camalexin biosynthesis between Col-0 and plant mutants. In contrast, PG1-induced camalexin biosynthesis was notably lower in *sultr1;2* roots compared with that in Col-0 and *apr1 apr2* roots.

According to our previous experiments conducted with Col-0, camalexin induction level displayed the same pattern in shoots and roots: PG1 induced highest camalexin biosynthesis and no difference in camalexin between *cysH* and *cysM* treatments. However, this pattern did not apply

to the plant mutants we assessed here. The picture about sulfur metabolism affecting plant immune response remained inconclusive. To gain a better understanding of the effect of sulfur metabolism on plant immune response, we further screened plant mutants *myb28 myb29* and *slim1-1*, which are deficient in regulation of sulfur metabolism. Double mutant *myb28 myb29* is deficient in aliphatic glucosinolates, which are important for plant defense against insects and pathogens. Besides, glucosinolates are important sulfur-containing secondary metabolites functioning as sulfate donor under sulfur limitation. As a result of *MYB28 MYB29* mutation, tryptophan metabolites, indolelactate, auxin metabolites and glutathione increase (Mostafa et al., 2016). *SLIM1* is a key transcriptional factor regulating plant sulfur assimilation pathway, activating sulfate acquisition, degradation of glucosinolates and enhancing plant growth under sulfur limitation. It was shown by transcriptome data that *SLIM1* participates universally in optimizing transport and internal utilization of sulfate in *Arabidopsis* (Dietzen et al., 2020). Interestingly, PG1 triggered strikingly higher camalexin in shoots of *myb28 myb29* than in Col-0. The camalexin result in *slim1-1* shoots was noteworthy as well: PG1, *cysH* and *cysM* induced the same level of camalexin, which was completely different to the data observed in the other plant mutants (Fig. 4.1E). This complete different camalexin induction pattern in *slim1-1* indicates that sulfur metabolic modulation of plant alters immune response or plant resistance to pathogens. Mutants *gst6* and *gsttau3* involved in glutathione metabolic process were ordered from NASC tested here as well. The reason for screening mutants related to glutathione metabolism was based on RNAseq data. Different expressed genes (DEGs) were identified from *B. glumae*-treated *Arabidopsis* roots and control roots. KEGG pathway analysis of these DEGs with the most significant difference revealed that they are involved in glutathione metabolism pathways, which are catalyzed by ubiquitous glutathione S-transferases (GSTs). Glutathione has been reported to play an important role in protecting plants from biotic and abiotic environmental stress (Xiang et al., 2001; Han et al., 2013). Two highly regulated genes *GST6* and *GSTTAU3* coding GSTs were chosen for further analysis (detail of gene and T-DNA line was listed in Table 1). *GST6* is the sixth *Arabidopsis* GST gene to be isolated and its expression can be induced following treatment with auxin, salicylic acid and H₂O₂ (Chen et al., 1996). *GSTTAU3* encodes glutathione transferase belonging to the tau class of GSTs and is plant specific (Wagner et al., 2002). The study about *GSTTAU3* (also named *GSTU3*) is limited. Homozygous mutants were obtained by PCR genotyping. Camalexin induced by *B. glumae* PG1 and in *gst6* shoot was significantly lower than in Col-0. In both *gst6* and *gsttau3*,

PG1 triggered higher level of camalexin than bacterial mutants (Fig. 4.1F). This result was consistent with camalexin induction pattern in *cad2-1*.

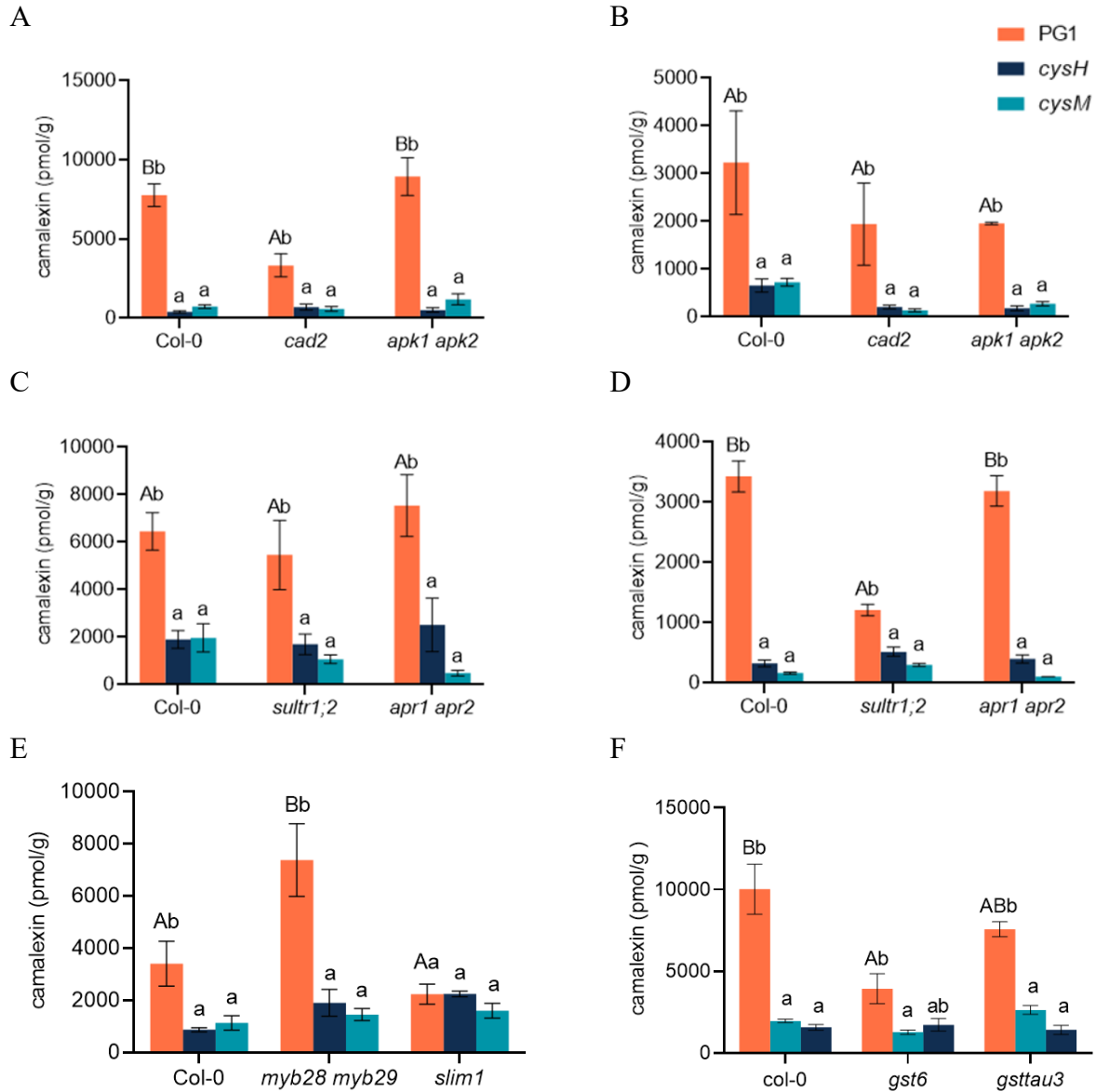


Figure 4.1 Modulation of sulfur assimilation in *Arabidopsis* affects immune response to *B. glumae* PG1

Plants grown in the hydroponic system were used for camalexin analysis. (A), (C), (E) and (F) Camalexin from shoots. (B) and (D) Camalexin from roots. Bars represent the mean \pm SEM. Different letters represent statistically significant differences of camalexin induction between bacterial treatments within the same plant genotype ($P < 0.05$, one-way ANOVA). Capital letters indicate different camalexin biosynthesis induced by PG1 between plant mutants and Col-0.

4.2 Contents of sulfur-containing metabolites in Arabidopsis Col-0, *myb28 myb29* and *slim1-1* do not change upon microbial infection

In the previous subsection, we showed that *myb28 myb29* demonstrates stronger immune response to PG1 than Col-0 in both shoots and roots. Besides, *slim1-1* displayed a new response pattern to pathogen attack: plant defensive compound camalexin was induced at the same level between *B. glumae* PG1 (WT) and bacterial mutants *cysH* and *cysM*. Since *myb28 myb29* and *slim1-1* are both deficient in regulation of sulfur assimilation and in controlling sulfur flux into different metabolites compared with Col-0, we hypothesized that modulation of sulfur-containing metabolites was a potential reason for differences in Arabidopsis immune response between plant mutants. We measured and compared concentration of critical sulfur-containing metabolites in Col-0, *myb28 myb29* and *slim1-1-1* to prove our hypothesis.

We compared the anions contents of shoots within the same plant genotype under various bacterial infestations. In addition to that, we also examined anions content difference between plant genotypes under the same bacterial infestation. When comparing sulfate and phosphate content between pathogens treatment within the same plant genotype, we did not observe any consistent patterns of variation. Even though there was a slight difference between control and bacterial treatments, it was difficult to make clear conclusions (Fig. 4.2A, 4.2C). However, when comparing sulfate content of different plant genotypes inoculated by the same pathogen strain, we surprisingly noted that *cysH* treated plants had lower sulfate content than those inoculated by PG1 and *cysM*. The sulfate content of control treatment was the same between Col-0, *myb28 myb29* and *slim1-1* (Fig. 4.2B). The nitrate level was quite stable among Col-0, *myb28 myb29* and *slim1-1* even under pathogen infection (Fig. 4.2E, 4.2F).

We also quantified important small sulfur containing thiols including glutathione and cysteine in shoots and roots of Col-0, *myb28 myb29* and *slim1-1* to estimate if modulation of sulfur assimilation in Arabidopsis affects thiols status; and if such change in thiols is in accordance with camalexin or not. Cys is a central metabolite in the sulfur assimilation pathway and is also the key substrate for the biosynthesis of glutathione. Glutathione is involved in the plant stress response network that helps plant to maintain intracellular redox environment. In addition, both glutathione and Cys are important for regulating sulfate uptake and activity of APR, a critical enzyme of assimilatory sulfate reduction (Vauclare et al., 2002; Dubreuil-Maurizi and Poinssot, 2012).

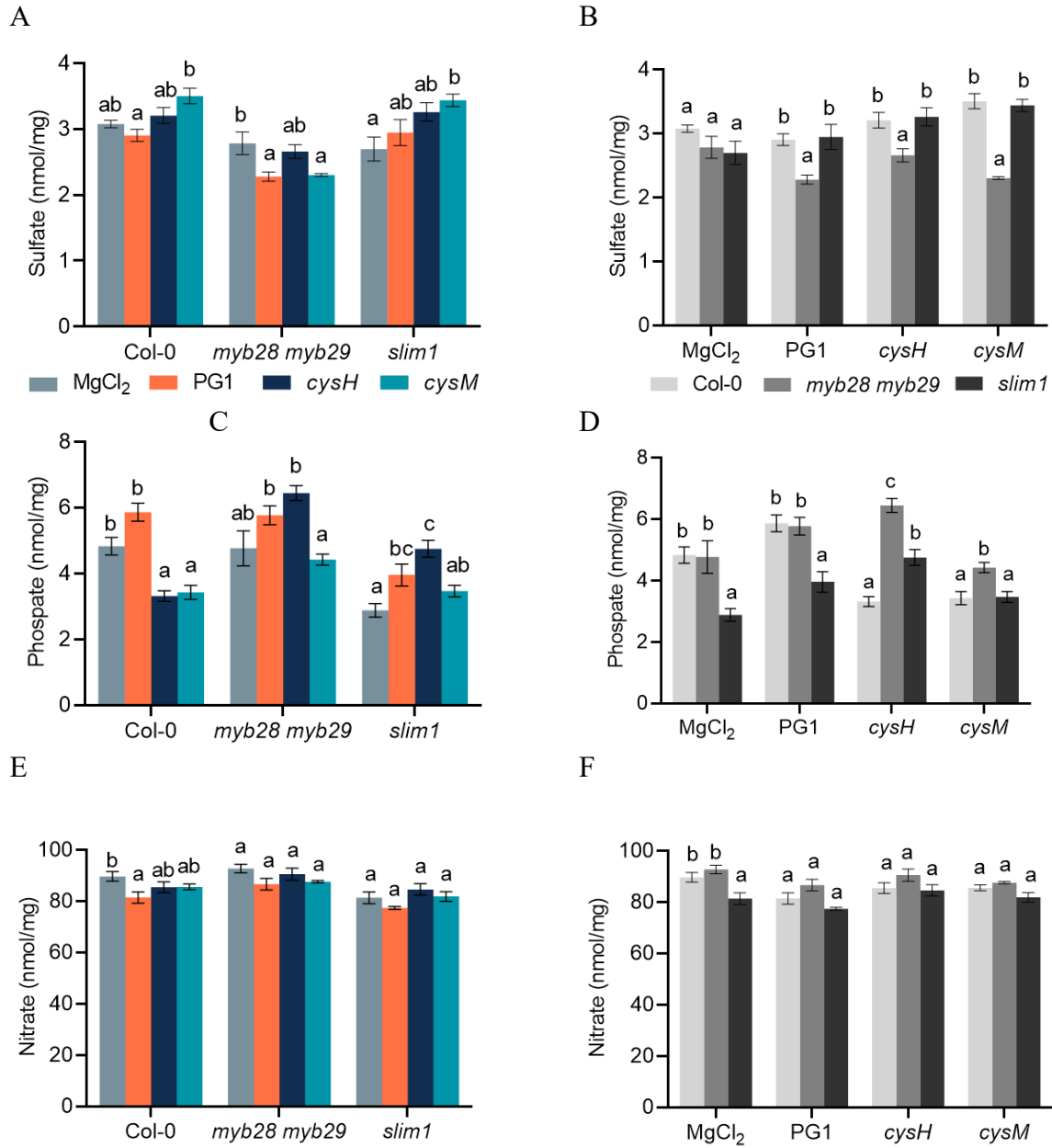
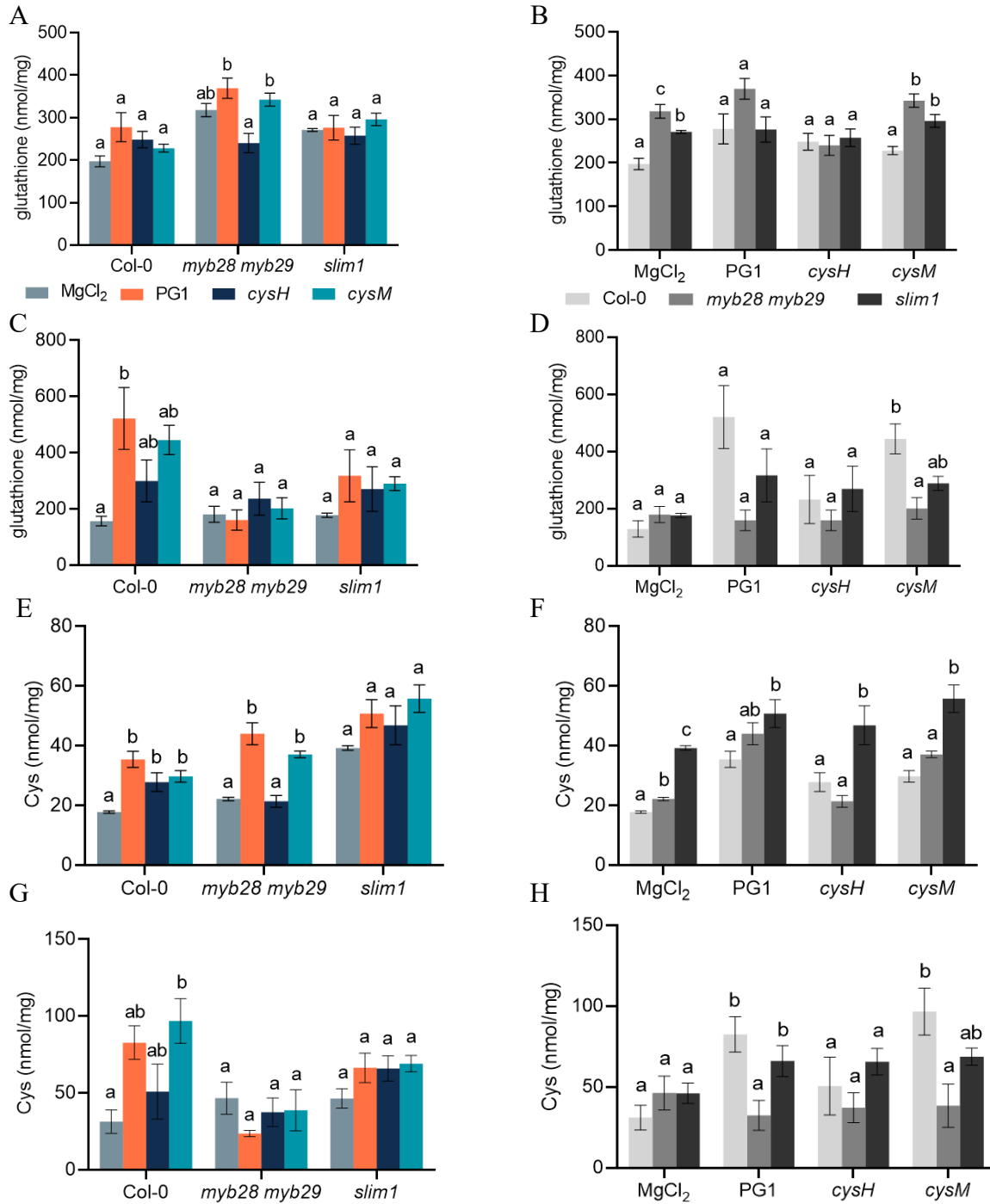


Figure 4.2 Contents of sulfate, phosphate and nitrate display different pattern upon bacterial infection

Plants grown in 12-well hydroponic system were inoculated by the pathogens. After 3 days of incubation, shoots were harvested for anion content analysis. Anions were determined by ion chromatography (IC). Result of anion content was shown in two ways: (A) sulfate, (C) phosphate and (E) nitrate contents were compared within the same plant genotypes under various bacterial treatments; (B), (D) and (F) represented comparison of the same bacterial treatment among plant genotypes. Bars represent mean \pm SEM. Different letters indicate significant difference in anion content between bacterial treatments within the same plant (A, C and E) or between plant genotypes under the same treatment (B, D and F). Data was analysed by One-way ANOVA ($P < 0.05$).



Glutathione and Cys contents of *slim1-1* in shoots and roots were relatively stable upon bacterial infection compared with that of Col-0 and *myb28 myb29* (Fig. 4.3A, 4.3C, 4.3E and 4.3G). Similar to the anion result, thiols concentrations in each plant genotype did not display clear characteristic difference when treated by pathogens and changes in shoots and roots were not identical. A slight difference in glutathione content between bacterial treatments was only observed in the shoot of *myb28 myb29* and in the root in Col-0. Cys content between bacterial treatments showed inconclusive differences in the shoot of *myb28 myb29* and in the root of Col-0. However, overall, the glutathione and Cys content remained constant in *slim1-1* and the root of *myb28 myb29*.

Glucosinolates (GLS), a class of important sulfur-containing primary defense metabolites, were quantified as well. It's interesting to notice that GLS accumulation pattern was different to camalexin induction pattern even though they are both plant defense compounds. GLS storage in both shoots and roots of different bacterial treatment was at the same level within the same plant genotype (Fig. 4.4A, 4.4C). In addition, *myb28 myb29* and *slim1-1* showed lower GLS accumulation compared with Col-0 (Fig. 4.4B, 4.4D).

Taken the metabolite results together, we can draw a conclusion that content of anions, thiols and GLS are not in correlation with camalexin under bacterial treatments. Unlike camalexin which was induced at different level by PG1 (WT) and its mutants, glutathione, Cys and GLS remained relatively stable under different bacterial infection among Col-0, *myb28 myb29* and *slim1-1*. Difference in anions can be observed between bacterial treatments; however, the content changes are not striking. The most interesting observation is that the mutation of *SLIMI* gene has an impact on GLS storage of Arabidopsis in in both shoots and roots: *slim1-1* has reduced GLS content to the same level of *myb28 myb29*. The homeostasis of glutathione and Cys is not altered by loss of *MYB28 MYB29* and *SLIMI*. These findings partly refute our hypothesis that modulation of sulfur-containing metabolites is a potential explanation of differences in Arabidopsis immune response between plant mutants, since anions, thiols and GLS did not show correlation with camalexin and remain stable under pathogens infection.

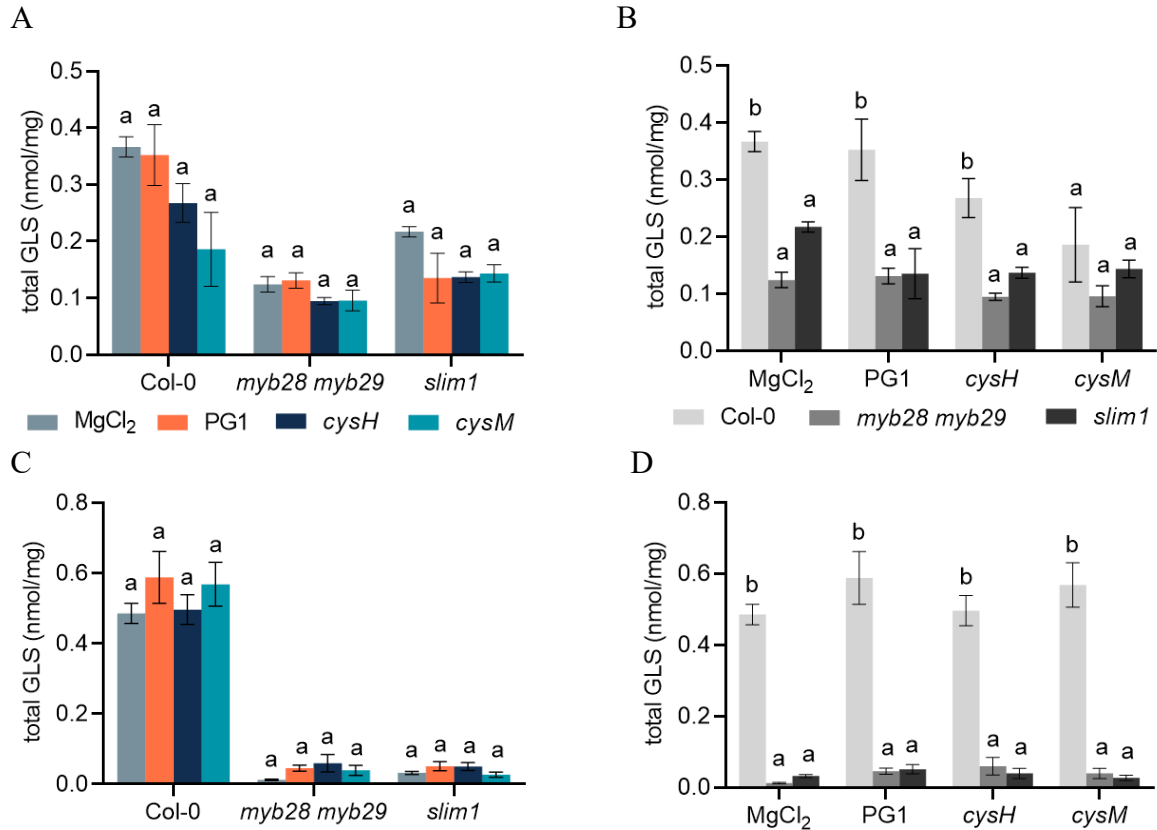


Figure 4.4 The amount of glucosinolates is not altered by pathogenic infection

GLS were extracted from shoots and roots of Col-0, *myb28 myb29* and *slim1-1* and identified by HPLC. (A) and (B) GLS in shoots. (C) and (D) GLS in roots. Bars represent mean \pm SEM. Different letters indicate significant difference of total glucosinolates (GLS) content between bacterial treatments within the same plant (A, C) or between plant genotypes under the same treatment (B, D). Data was analysed by One-way ANOVA ($P < 0.05$).

4.3 *SLIMI* is potentially involved in immune response triggered by *B. glumae*

From the data of GLS content in Col-0, *myb28 myb29* and *slim1-1*, we learned that modulation of sulfur assimilation pathway influences biosynthesis of sulfur-containing metabolites (Fig. 4.4C, 4.4D). In addition, we measured also non-sulfur defense-related small metabolites, pipercolic acid (Pip) and salicylic acid (SA). Pip has been proven to be critical for local resistance to bacterial pathogens and systemic acquired resistance (SAR) in plants; SA is a defense hormone mediating responses against biotrophs and hemi-biotrophs. We surprisingly found that Col-0 and *slim1-1* infected by the *cysH* mutant accumulated significantly more Pip and SA than plants treated by PG1 and the *cysM* mutant. In *myb28 myb29*, PG1 and bacterial mutants induced Pip and SA at the

same level as Col-0 level, but the *cysH* treated plants had slightly higher content of Pip and SA (Fig. 4.5A, 4.5C). There was no significant difference of Pip content between Arabidopsis genotypes when infected with *cysH* and *cysM*. However, it was observed that PG1 treated *slim1-1* had less Pip biosynthesis than Col-0 and *myb28 myb29* (Fig. 4.5B, 4.5D). SA accumulation in Arabidopsis Col-0 WT and mutants showed different pattern: it was observed that *slim1-1* displayed substantially lower SA accumulation than Col-0 and *myb28 myb29* under inoculation of PG1 and the *cysM* mutant; while the decrease after treatment with *cysH* was not statistically significant.

Phenylalanine ammonia-lyase (PAL) is involved in the biosynthesis pathway of SA and responses to biotic and abiotic stress as well (Cools and Ishii, 2002; Olsen et al., 2008). SA can be synthesized from the isochorismate pathway, with the enzyme isochorismate synthase (ICS) involved (Wildermuth et al., 2001). AGD2-LIKE DEFENSE RESPONSE PROTEIN 1 (ALD1) is involved in Pip biosynthesis pathway and regulates defense amplification (Cecchini et al., 2015). PR1 (pathogenesis-related protein 1) is induced in response to a variety of pathogens. The relative expression of *ICS1* under bacterial treatment among Arabidopsis mutants was close to one. We observed no difference of the expression levels of these genes between treatments in the same plant genotype (Fig. 4.6C). The qPCR data showed that the relative expression level of *PAL1* and *PR1* in *slim1-1* inoculated with *B. glumae* PG1 were not statistically different, but slightly lower than in Col-0 (Fig. 4.6B, 4.6F). Furthermore, the relative expression of *ALDI* in *slim1* was below the level of detection in our condition (Fig. 4.6E). Together, these findings indicate that *SLIMI* is involved in the regulation of Pip and SA biosynthesis after inoculation with *B. glumae* and could potentially affect SAR priming of Arabidopsis.

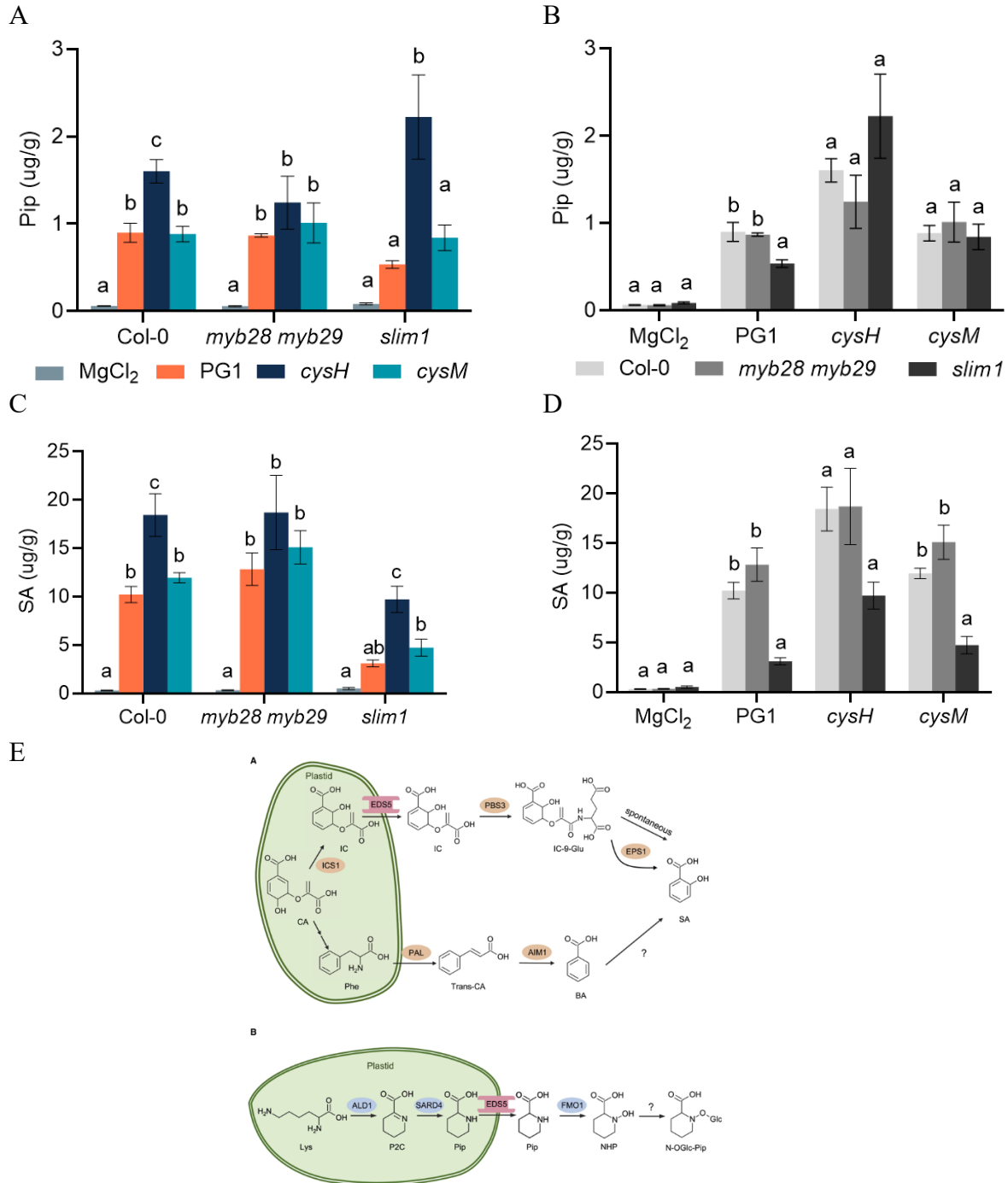


Figure 4.5 Pip and SA accumulation in shoots of Col-0, myb28 myb29 and slim1-1

Shoots from the hydroponic system were harvested for Pip and SA assay after 3 days of bacterial inoculation. (A) and (B) Pip in shoots. (C) and (D) SA in shoots. (E) The Biosynthetic Pathways for Salicylic Acid (SA) and N-Hydroxypipelic Acid (NHP) (Huang et al., 2020). Bars represent mean \pm SEM. Different letters indicate significant difference of Pip and total SA contents between bacterial treatments within the same plant (A, C) or between plant genotypes under the same treatment (B, D). Data was analysed by One-way ANOVA ($P < 0.05$).

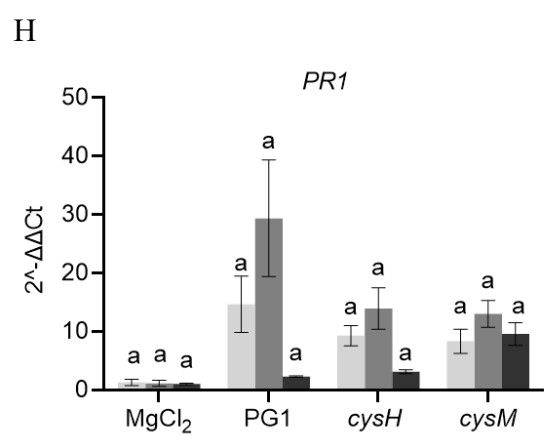
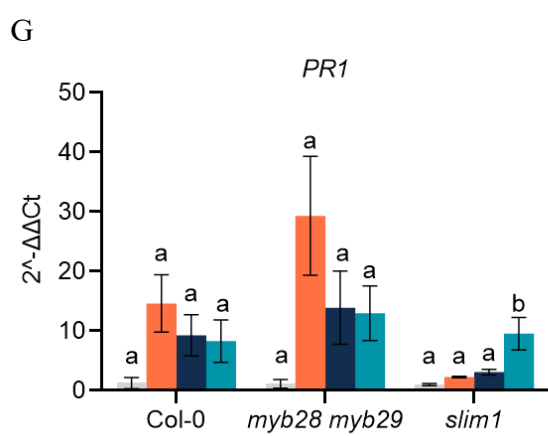
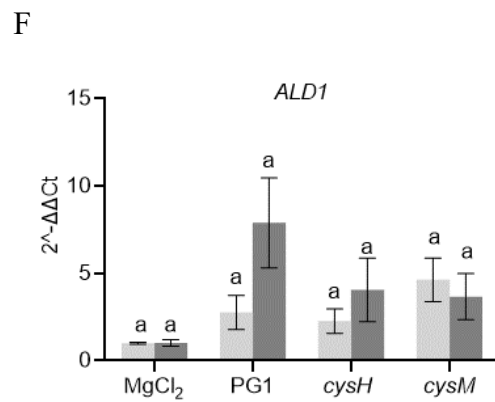
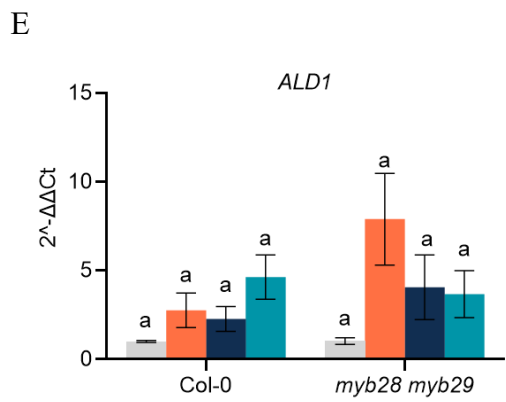
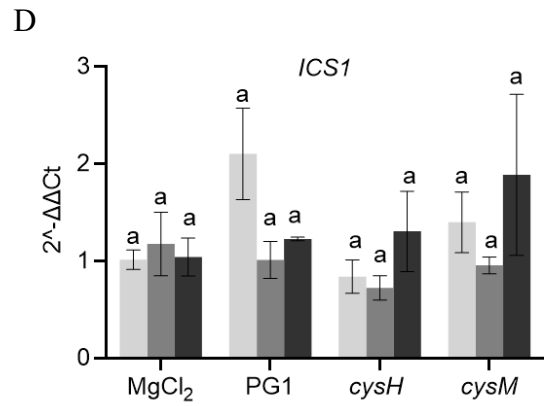
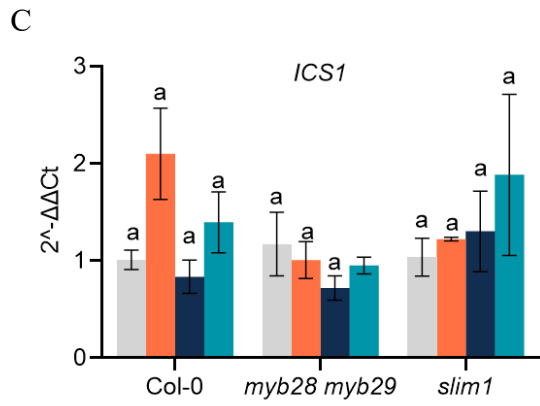
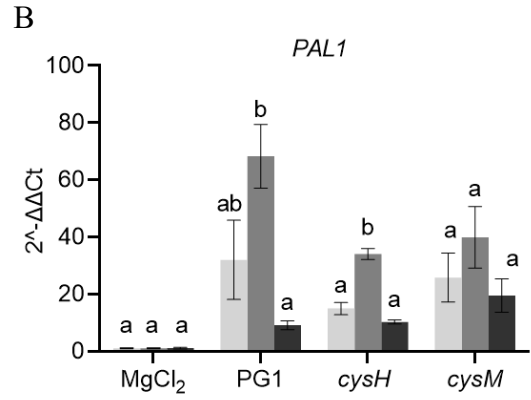
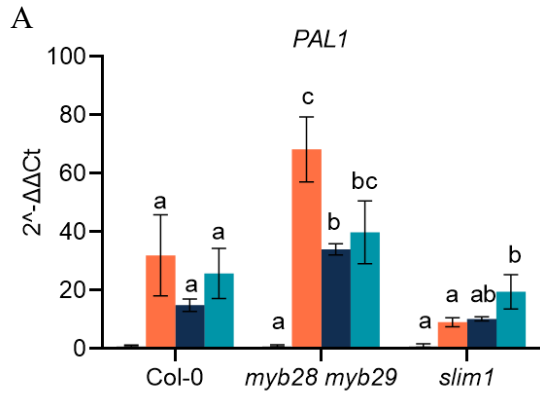


Figure 4.6 Relative expression of genes involved in Pip and SA biosynthesis pathway

Transcription levels of genes involved in SA biosynthesis and SA-triggered immune pathway were assessed by quantitative real-time PCR analysis. Bars represent mean \pm SEM. The housekeeping gene *TIP41* served as reference gene. Gene expression were relative to the respective mock control value.

4.4 *cysH* grows slower than PG1 and *cysM* when fed with shoot extracts of *myb28 myb29* and *slim1-1*

To discover if modulation of sulfur metabolites in plants affects bacterial colonization ability, we estimated the abundance of the bacterial strains inside plants and their growth capacity when fed with shoot metabolites from Arabidopsis.

Auc_e result (the area under growth curve) showed that *B. glumae* PG1 WT and mutants had the same growth rate in LB medium, which offers rich full nutrients. However, compared with PG1 and the *cysM*, the *cysH* mutant displayed obvious deficiency in growth in media containing shoot metabolites as the only carbon source. Besides, shoot metabolites from different plant genotypes did not impact growth of the bacterial strains, i.e., the bacteria grew at the same rate when fed with shoot extracts from Col-0, *myb28 myb29* and *slim1-1* (Fig. 4.7A). This result indicates that modulation of sulfur assimilation pathway of plants does not influence growth rate of bacterial strains in-vitro. Exogenous Cys enhanced the growth of *cysH* significantly to the same level of PG1 and *cysM* (Fig. 4.7B, 4.7C). We surprisingly found that additional Cys inhibited slightly the growth of PG1 and the mutant *cysM* which were in concert with the growth rate result of feeding experiment with Col-0 shoot metabolites (Fig. 4.7B).

Since bacterial strains showed the same ability to consume shoot metabolites from different plant host in vitro, we were wondering if they colonize at the same level inside plant host. To answer this question, we quantified bacterial growth inside plants based on the qPCR method described above. Bacterial abundance in shoots of Col-0 and *slim1-1* showed the same trend: PG1 displayed enhanced bacterial proliferation than *cysH* and *cysM* mutants (Fig. 4.8A). Bacterial concentration in roots of Col-0 was in accordance with that in shoots, but in roots of *slim1-1*, the abundance of *cysM* mutant was the same to that of PG1. Bacterial quantification of PG1, *cysH* and *cysM* mutants was identical in shoots and roots of *myb28 myb29*, and was relatively lower in roots (Fig. 4.8C). It should be noted that the levels of PG1 and the *cysH* mutant were significantly increased in *slim1-1* shoot compared to Col-0 (Fig. 4.8B). The comparison of bacterial proliferation in roots between plant genotypes did not show obvious pattern (Fig. 4.8D).

The ability to take up nutrients from shoot metabolites in-vitro is not parallel to the bacterial concentration in shoots., which means a more comprehensive nutrient uptake activity is happening *in vivo* of host plants during bacterial inhabitation process. Taken the bacterial concentration results together, it can be suggested that *slim1-1* is more susceptible than Col-0.

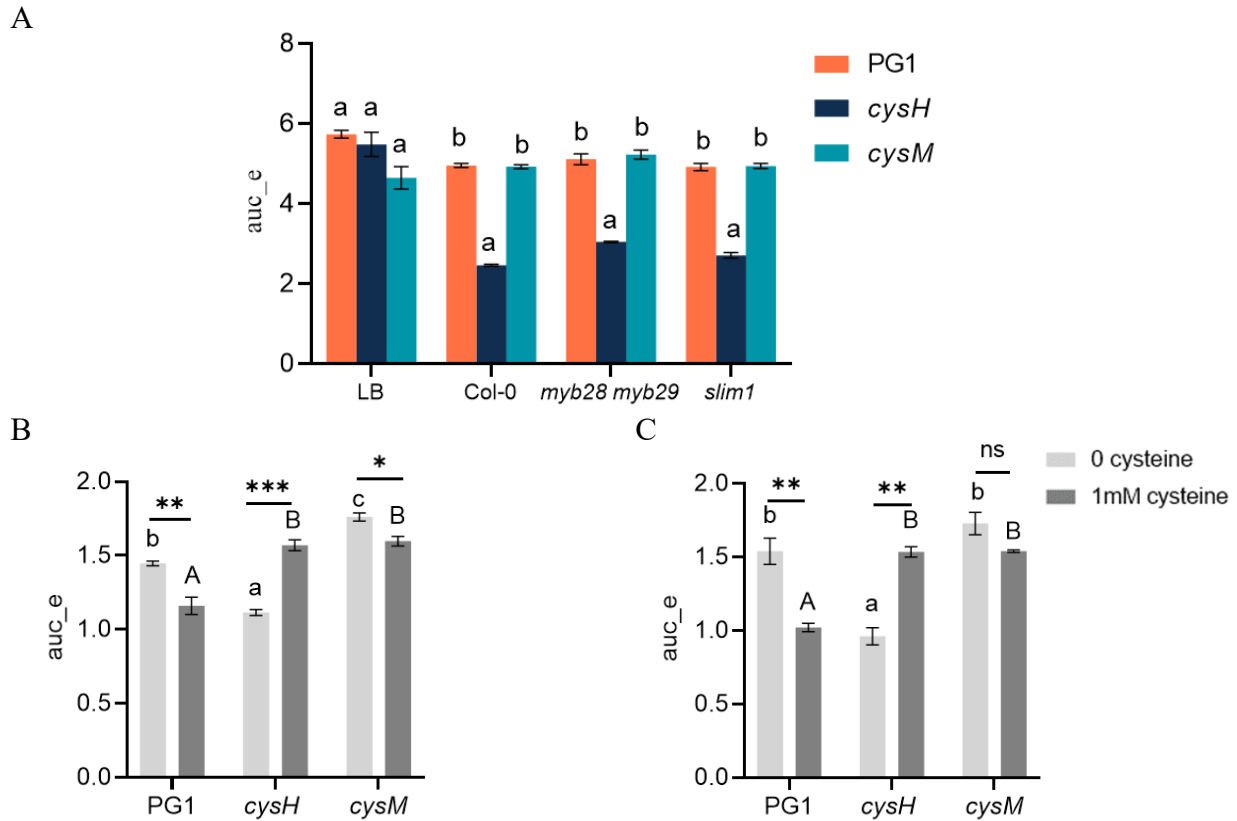


Figure 4.7 The growth rate of bacterial strains in media containing shoot metabolites

(A) Growth rate of PG1, *cysH* and *cysM* when fed with media containing shoot metabolites as the only carbon source. Shoot metabolites from (B) *myb28 myb29* and (C) *slim1-1* were applied in media with or without exogenous Cys. Bars represent the mean \pm SEM. Different letters represent statistically significant differences between bacterial treatments ($P < 0.05$, one-way ANOVA). Capital letters and small letters are assigned to condition with or without cysteine complementation. Asterisks indicate different bacterial growth rates between different cysteine condition of the same treatment (student's t-test, $P < 0.05$).

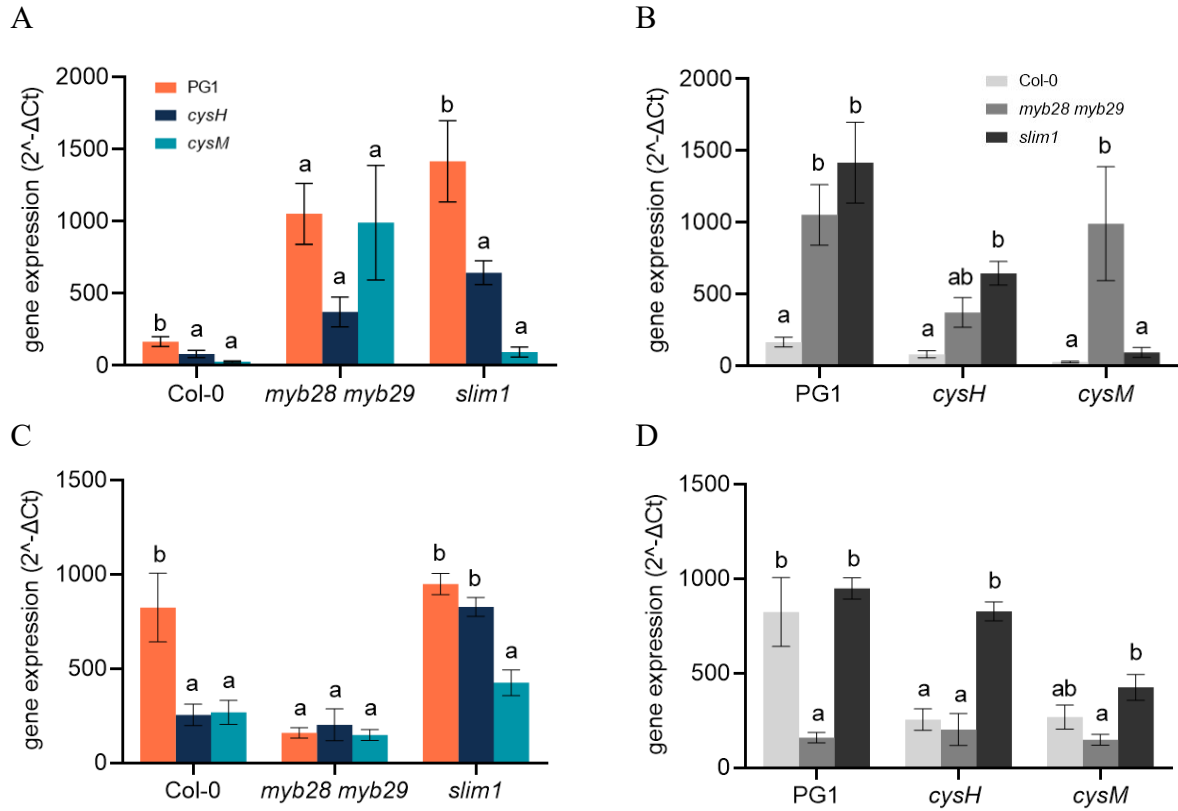


Figure 4.8 Bacterial abundance in shoots and roots of Col-0, *myb28 myb29* and *slim1-1*

Relative bacterial concentration was quantified based on a qPCR gene expression value. (A) and (B) bacterial titer in shoots. (C) and (D) bacterial titer in roots. Bars represent mean \pm SEM. Different letters indicate significant difference of three pathogens concentration within the same plant (A, C) or concentration of the same pathogen strain between plant genotypes (B, D). Data was analysed by One-way ANOVA ($P < 0.05$).

5 Discussion

5.1 Sulfur assimilation pathway affects virulence of *cysH* and *cysM*

B. glumae is a seed-born pathogen that can migrate from the seeds into vegetative tissues and panicles, causing bacterial panicle blight of rice (Ortega and Rojas, 2020). Recent studies showed that *B. glumae* can also invade *Arabidopsis* via roots and consequently induce camalexin accumulation in shoots (Koprivova et al., 2023). Furthermore, an in vitro feeding experiment with camalexin showed that *B. glumae* was resistant to high concentrations of camalexin (10 μ M) (Koprivova et al., 2019). Therefore, *Arabidopsis*-*B. glumae* is a suitable system to evaluate plant-pathogen interactions with modulations of sulfate assimilation. Compared to rice, *Arabidopsis* sulfur metabolism mutants are more accessible. In addition, growing rice in the laboratory is more time consuming than growing *Arabidopsis*.

It has been shown that disruption of Cys biosynthesis in bacterial and fungal pathogens can result in impaired virulence. However, the mechanism behind this Cys deficiency-mediated pathogenicity loss is not well known. In this study, we estimated the effect of sulfate assimilation in *B. glumae* on its pathogenicity and dissected the mechanism underlying from the view of nutrient acquisition. First of all, to explore if sulfur assimilation ability affects pathogenicity of bacteria, we measured fresh weight of *Arabidopsis*, lesions on plant leaves triggered by pathogen infiltration, HR response and camalexin accumulation to determine pathogenicity differences between PG1 and mutants. These physiological and chemical analysis showed that *cysH* and *cysM* mutants induced less severe disease symptoms and responses than PG1, which successfully answered our first question that disruption of sulfate assimilation pathway on *B. glumae* affects its pathogenicity. Recently, some studies on bacterial pathogens have highlighted the importance of Cys biosynthesis pathway in maintain their pathogenicity, consistent with our research that the *B. glumae* sulfur-deficient mutants *cysH* and *cysM* are less pathogenic than WT strain PG1. A CysB regulator in *Ralstonia solanacearum* has been demonstrated to be responsible for Cys synthesis. The *cysB* mutant is Cys auxotroph and fails to grow in minimal medium but grows slightly in host plants. It also fails to wilt tomato plants and remained weakly virulent on tobacco plants. Exogenous Cys fully restores the impaired growth and virulence of *cysB* mutants in both minimal medium and inside host plants (Chen et al., 2022). This Cys biosynthesis-mediated reduced virulence exists in fungal pathogens as well. *Pyricularia oryzae* is a fungal pathogen that causes

blast disease on staple gramineous crops. *P. oryzae* *PoMET3* and *PoMET14* encode the enzyme ATP sulfurylase and APS kinase respectively which are involved in sulfate assimilation and Cys biosynthesis. The deletion of these two genes causes defects of conidiophore formation, Cys and Met auxotroph and limited hyphae extension of *P. oryzae*, which consequently leads to remarkably reduced virulence on rice and barley (Li et al., 2020). *Fusarium oxysporum* f. sp. cubense tropic race 4 (*Foc TR4*) causes an epidemic of banana Fusarium wilt (BFW) worldwide, while *Foc RI* does not cause symptoms of BFW. Comparative analysis of secretory proteins (SPs) in *Foc RI* and *Foc TR4* revealed that *Foc TR4* had a higher proportion of SPs involved in various metabolic pathways, such as cysteine and methionine metabolism, among which cysteine biosynthesis enzyme O-acetylhomoserine (thiol)-lyase (OASTL) was the most abundant root inducible *Foc TR4*-specific SP. Knockout of OASTL resulted in a dramatic loss of pathogenicity in Banana 'Brazil' (Wang et al., 2020a).

The importance of Cys biosynthesis in mediating pathogenicity has been more widely discussed in mammalian pathogens because it is a potential target to develop new antibiotics without risk in rising drug-resistant bacteria. Numerous studies in this field have demonstrated that enzymes involved in Cys biosynthesis and regulation pathway affect the virulence and fitness of microorganisms, using traditional experimental methods or genomic analysis (Akerley et al., 2002; Gebhardt. et al., 2020; Verma and Gupta, 2021). For example, *Paracoccidioides brasiliensis* is a dimorphic fungus. The infective process of this fungus comprises a temperature-dependent morphological switch from the conidia/mycelium phase (environmental temperature around 26°C) to the pathogenic yeast phase at the mammalian host temperature (around 37°C), which is a critical step for the establishment of paracoccidioidomycosis. Experimental result revealed that SconCp, the negative regulator of the inorganic sulfur assimilation pathway, is essential to sustain yeast growth using inorganic sulfur sources only. Importantly, an *in vivo* model of infection validated that the down-regulation of SCONC led to a decreased virulence of *P. brasiliensis* (Menino et al., 2013). CysE is a serine acetyltransferase that catalyzes the synthesis of OAS from L-serine and acetyl coenzyme A (acetyl-CoA), the first committed step of the cysteine biosynthetic pathway. CysK1 and CysK2, function redundantly to catalyze Cys biosynthesis from OAS and sulfide, which is the step downstream of CysE. *Brucella ovis* Δ *cysE* and Δ *cysK1* Δ *cysK2* strains have a fitness defect in stationary phase, terminates growth at a lower density than the WT and are sensitive to exogenous oxidative stress. Besides, these phenotypes can be restored by cysteine or

glutathione (Varesio et al., 2021). In our study, we also demonstrated that exogenous Cys in the hydroponic system triggered higher levels of camalexin induction by *cysH* and *cysM*, which emphasized the importance of Cys nutrition in eliciting host immune response.

A limitation of these studies is that most researches only described distinct disease symptoms caused by WT strain and sulfur deficient mutants or Cys auxotroph knockouts. However, the details of the effect of lost Cys synthesis on plant-pathogens interactions underpinning reduced virulence has not been studied in detail, which means that it is not clear if impaired virulence is only due to slower growth in host tissues or whether Cys auxotrophy affects virulence factors directly. By now, a limited literature has shown that Cys auxotrophy has extensive impact on bacterial transcriptome, especially a sulfur-rich host environment could contribute to the transcription of genes related to putative virulence factors such as flagella, phospholipase, and hemolysin (Anderson et al., 2019).

5.2 Reduced nutrition acquirement and bacterial proliferation in plant niches partly explain attenuated pathogenicity of mutants *cysH* and *cysM*

It has been reported that pathogens are able to inhabit phyllosphere, apoplast and cytosol in plants and obtain nutrients including carbon sources such as glucose and fructose, organic acids and amino acids from these nutrient niches (S. and D., 2000; Leveau and Lindow, 2001; Rico and Preston, 2008; Vorholt, 2012). Microbial access to host nutrients and proliferation within the host are fundamental and a prerequisite for diseases infection by pathogens. It has been shown that some Cys auxotrophic bacterial or fungal strains are unable to grow on minimal medium, but are able to colonize plants and insects and induce disease symptoms (Scully and Bidochka, 2009; Klee et al., 2019; Chen et al., 2022), suggesting that they can take up the essential Cys from *in vivo* plant niches. The study on a series of auxotrophic mutants of *Erwinia amylovora* showed that auxotrophic mutant growth in apple fruitlet medium had a modest positive correlation with virulence in apple fruitlet tissues. This finding was confirmed by inoculating apple tree shoot with a representative subset of auxotrophs (Klee et al., 2019). This study suggests that the capacity of auxotrophic bacteria to actively obtain metabolites from the host environment and from tissue extracts has substantial impact on their virulence.

In our study, the *in vitro* feeding experiment using various sulfur-containing compounds in minimal media (Fig. 3.1) showed that the *cysH* mutant is not able to use oxidized sulfur sources, while the *cysM* can use both oxidized and reduced sulfur sources as the WT PG1. Not only PG1 and the *cysM*, but also the *cysH*, were able to grow when these bacteria were fed with the shoot extract in minimal media, an experimental setup that mimicked the metabolic milieu of the Arabidopsis shoot habitat. It appears that Cys and other vital nutrients for bacterial survival can be obtained from Arabidopsis shoot tissues. According to the *auc_e* data from the shoot extract feeding experiment, the *cysM* mutant and PG1 had the same ability to obtain nutrients, whereas the *cysH* exhibits a reduced ability to acquire nutrients from shoot metabolites. Exogenous cysteine completely recovered the slowed growth of the *cysH* mutant in the media containing shoot extracts (Fig. 3.6B). This suggests that PG1 and the *cysM* mutant can assimilate enough sulfate from the shoot extract to generate sufficient Cys to support their growth, whereas the *cysH* mutant cannot and must obtain Cys directly. Exogenous Cys increased the camalexin induction of the *cysH* and *cysM* mutants to the same level as that triggered by PG1, demonstrating the importance of sufficient Cys for the pathogenicity of *B. glumae*. Numerous studies have also demonstrated that exogenous Cys, Met, or Leucine are able to boost growth and restore impaired phenotypes in auxotrophic mutants, indicating the importance of amino acids biosynthesis and ability to use exogenous amino acids in maintaining virulence of pathogens (Saint-Macary et al., 2015; Que et al., 2020). In summary, the two feeding experiments conducted in this study provided evidence that the *cysH* mutant has a Cys auxotrophic property and a diminished capacity to absorb nutrients from host metabolites. In addition, the *cysM* mutant harbours the same ability as PG1 to utilize nutrients *in vitro*.

It is interesting to note that despite having the same capacity as PG1 to absorb nutrients *in vitro*, the disease parameters caused by the *cysM* were less severe than those caused by PG1. In contrast to the *cysM* mutant, the growth of PG1 and the auxotrophic mutant *cysH* *in vitro* had a modestly positive correlation with their virulence in Arabidopsis, which was a result within our expectation. Together, these findings demonstrate that bacteria's ability to acquire nutrients *in vitro* is unrelated to their pathogenicity. By examining the concentration of bacteria inside plants, which can be a proxy for *in vivo* nutrient acquisition capacity, we were able to ascertain whether pathogenicity is correlated with it. In Arabidopsis, the relative concentration of the *cysH* and *cysM* mutants was noticeably lower than that of PG1, which was consistent with the level of camalexin induction and

the results of the DAB staining. This finding indicates that pathogenicity of bacteria is positively correlated with the capacity for proliferation inside host plants. Since endophytic populations, not epiphytic populations, are probably responsible for disease induction, it makes sense that the capacity to grow endophytically may directly influence the potential for pathogenesis (Beattie and Lindow, 1995).

Instead of the conventional plate counting method, we used a qPCR-based technique in this study for robust growth quantification of bacteria in planta. The relative concentration of bacteria determined by the Ct value from qPCR result was parallel to the result of conventional colony counting, demonstrating the robustness and reliability of the qPCR-based method. The study of Ross and Somssich (2016) served as an inspiration for the methodology. This method is better suited for routine experiments and larger-scale analyses than the conventional time-consuming plate counting method, which requires that samples be processed right away after collection. For this qPCR-based method, samples can be stored at -80°C and be analysed when convenient.

5.3 Differences between the *cysH* and the *cysM*

The feeding experiment demonstrated that the *cysH* mutant did not grow on minimal media containing only oxidized sulfur sources such as sulfate, taurine and PNPS. As far as is currently known, the PAPS reduction to sulfite, which occurs in the first part of the sulfate assimilation pathway, only involves the *CysH* gene. This well explains the Cys-auxotrophic property of the *cysH* mutant. The Cys biosynthesis from sulfide and OAS fails in the *cysH* mutant as a result of the subsequent sulfate reduction being blocked. The *CysM* gene encodes enzyme O-acetylserine sulfhydrylase B (OASS-B). In *E. coli*, the OASS-B catalyzes the conversion of thiosulfate and OAS into S-sulfocysteine (SSC), which is reductively divided into Cys and sulfite with the involvement of NADPH and enzymes thioredoxins (Trx) and glutaredoxins (Grx). It is an alternative pathway of Cys biosynthesis in addition to the primary pathway through CysK (Nakatani et al., 2012). This thiosulfate assimilation pathway also occurs in other bacteria, such as *Salmonella typhimurium* (Nakamura et al., 1983). Based on these two Cys synthesis pathways, it can be speculated that the *cysM* mutant is able to use both oxidized and reduced sulfur sources, but not thiosulfate. The feeding experiment confirmed the hypothesis only partly: the *cysM* mutant thrived on sulfate, taurine, Cys and Met, but grew well also on thiosulfate. It is unclear whether a CysM-independent thiosulfate assimilation pathway exists in *B. glumae*. However, it was

demonstrated in *E. coli* that the *cysM* mutant could accumulate Cys and sulfide to the same level as WT when thiosulfate was served as the sole sulfur source. This suggests that the initial part of the thiosulfate to sulfite (SO_3^{2-}) conversion, which is partially mediated by thiosulfate sulfurtransferase (GlpE); and the latter part might be shared with the final part of the known sulfate assimilation pathway [sulfite \rightarrow sulfide (S^{2-}) \rightarrow L-cysteine (Kawano et al., 2017)]. Considering that the *cysM* mutant of *B. glumae* is able to use thiosulfate as the sole sulfur source, it indicates that it harbours a CysM-independent thiosulfate assimilation pathway similar to *E. coli*.

The *cysH* and *cysM* mutants also show differences in their ability to grow on shoot extracts: in media containing Col-0, *myb28 myb29* or *slim1-1* shoot extracts as the sole sources of carbon and sulfur, the growth rate of *cysH* mutants is significantly slower than that of *cysM*. This difference can be compensated by additional cysteine. It remains unclear whether Cys is the only component responsible for this difference, or whether *cysH* and *cysM* also differ in their ability to acquire and assimilate other nutrients. To our knowledge, this is the first experiment that shows substrate preference of bacterial mutants with genes deleted for the sulfur assimilation pathway in host plant shoot extracts. In fact, substrate preference is not a new concept, especially in rhizomicrobiome studies at the metabolic level. A growing body of literature demonstrates that the taxonomic composition of the rhizosphere microbiome can be shaped by plant-derived molecules. A preference by rhizosphere bacteria for consumption of plant root exudates such as aromatic organic acids, flavonoids was observed (Zhalnina et al., 2018; Yu et al., 2021a). Exometabolomic profiling of bacterial strains cultivated with Arabidopsis root extract indicates that root-resident strains have a stronger ability to take up metabolites than *E. coli* (Jacoby et al., 2018). The combination of these plant exudation properties and microbial substrate uptake traits interact to yield the patterns of microbial community assembly (Jacoby and Kopriva, 2019). These studies imply that substrate preference is an important property for microbiome to successfully inhabit and thrive in a certain environment.

However, little is known about how mutants deficient in essential nutrient biosynthesis react to a mix of nutrients, for example plant tissue extracts. Here, we were surprised to note that bacterial mutants *cysH* and *cysM* behaved significantly differently when grown on shoot extract. The initial expectation was that *cysH* and *cysM* would be able to use shoot metabolites to the same extent since a diversity of metabolites from the host plants may provide sufficient nutrients to meet the need of *cysH* and *cysM*. However, the experimental results were different and *cysH* was growing

significantly slower than *cysM*. Sulfate is an important sulfur source for bacteria, which can be reduced and ultimately incorporated into Cys, Met, glutathione and other essential organic active compounds to sustain full growth of bacteria. The *cysH* mutant fails to reduce PAPS to SO_3^{2-} , the first part of sulfate assimilation pathway, thereby blocking the biosynthesis of Cys and other crucial organic sulfur-containing metabolites. It can be expected that Cys, Met or glutathione in plant apoplast and other tissues are not sufficient to sustain full growth of the *cysH* mutant. It can also be expected that the *cysJ* mutant deficient in sulfite reductase would not grow well on shoot extract whereas the *cysE* mutant deficient in the serineacetyltransferase (SAT) activity would.

This shows that it is of great interest to quantify the ability of taking up shoot metabolites, since bacterial strains capable to display endophytic lifestyle definitely have to cope with dynamic metabolic niches in host plant and achieve trophic dominance from the inside niches. Dissecting adaptation and substrates preferences of bacterial mutants to shoot metabolites will help us to decipher the mechanisms underlying the loss of pathogenicity and plant-bacteria interactions at the metabolic level, and discover important and indispensable metabolites for disease development. To achieve this goal, exometabolomics of bacteria grown on shoot extracts can be profiled to further explore plant-microbe trophic interactions.

Another notable difference between the strains is the inconsistency between the ability of the *cysM* mutant to absorb nutrients *in vitro* and its reduced proliferation *in vivo*, which is contrast to the *cysH*. This inconsistency may be explained from two aspects: first, it is probably due to the fact that shoot extracts cannot fully reflect the nutritional environment and the metabolic profile in plants due to the limitation of extraction method; second, the dynamic and complex *in vivo* niches of plants cannot be replicated in *in vitro* feeding experiments. To be more specific for the first aspect, the main goal of the shoot extracts in most studies is to obtain the maximum number of metabolites or ideally all the metabolites present in the sample. Due to the presence of a wide range of metabolites in very different concentrations and with very different polarities, it is not possible to extract them with a single solvent system (Verpoorte et al., 2008; Kim and Verpoorte, 2010). For example, a series of solvents was tested for the extraction of Arabidopsis and these extracts were subsequently analysed by NMR. The metabolic profiles of the extracts obtained with different polar solvents were quite different: principal component analysis data showed that metabolites extracted with MeOH-water (1:1) were more enriched in carbohydrates, amino acids, and organic acids, and less on flavonoid phenylpropanoids; while metabolites extracted with

acetone–MeOH (1 : 1) contained relatively more flavonoids and less carbohydrates, amino acids, and organic acids (Verpoorte et al., 2007). This indicates that the MeOH-water solvent used in this study could not extract all metabolites in *Arabidopsis* shoots, thus our shoot extracts do not fully reflect the metabolic and nutritional compounds in the plant. Regarding the second aspect, we know that pH and redox environments, dynamic regulation of metabolomes, and immune responses characterize plant ecological niches and cannot be adequately mimicked in vitro experiments. However, these factors may have an impact on bacteria surviving inside plants. To address this issue, GFP-labeled bacteria can be applied to monitor bacterial infection, localization, activity, and movement *in vivo* through fluorescence microscopy. It has been reported that one of the GFP variants, GFPuv, which can be expressed from a stable and broad-host-range plasmid vector, pDSK-GFPuv, is visible not only at the cellular level under a fluorescence microscope, but also at the whole-plant level to the naked eye under long-wavelength UV light. Application of this GFPuv enables a real-time monitoring of bacterial infection in living plant tissues. Furthermore, the presence of pDSK-GFPuv did not significantly affect the growth and virulence of pathogens *in vitro* or *in vivo* (Wang et al., 2007).

5.4 Regulation of sulfate assimilation pathway in *Arabidopsis* affects camalexin induction pattern by *B. glumae*

Recent research demonstrated that bacterial and plant sulfur metabolism were coordinately changed upon colonization of the beneficial bacterium *Enterobacter sp. SAI87*, attenuating salt stress for host plants (Andrés-Barrao et al., 2021). This study indicates the importance of both bacterial and plant sulfur metabolism in mutualistic plant-bacteria interactions. We have utilized, to our knowledge for the first time, both bacterial and plant sulfur metabolic mutants to investigate sulfur metabolism-mediated plant-pathogen interactions, with pathogenicity and plant susceptibility concerned. After analysis of the effect of manipulation of bacterial sulfate assimilation on the interaction between PG1 and *Arabidopsis*, we investigated whether disruption of sulfate assimilation and its regulation in plants affects their susceptibility to this pathogen. Therefore, several *Arabidopsis* mutants for genes involved in sulfate assimilation or regulation were examined to compare their immune response to the infection of *B. glumae* PG1, *cysH* and *cysM*. Camalexin was measured as a parameter indicating disease resistance of *Arabidopsis* exposed to pathogen challenge. In Col-0, *cad2*, *apk1 apk2*, *sultr1;2*, *apr1 apr2*, *gst6* and *gsttau3*,

B. glumae PG1 triggered higher camalexin biosynthesis than bacterial mutants *cysH* and *cysM*. However, surprisingly, there was little difference in the level of camalexin induction by PG1 among these Arabidopsis mutants. This shows that the susceptibility of these Arabidopsis mutants to the pathogen was not significantly altered. It also suggests that neither higher nor lower sulfate content in *apr1 apr2* and *sultr1;2* respectively, affects the interactions with *B. glumae*, which is somewhat surprising in the light of the results with the *cysH* mutant, as its slower growth indicated sulfate being a prevalent source of sulfur for the bacteria.

Notably, *myb28 myb29* treated with PG1 showed significantly higher camalexin accumulation than that of Col-0. MYB28 and MYB29 are important key regulators of methionine-derived aliphatic glucosinolates biosynthesis, while the biosynthesis of camalexin is closely connected with indolic glucosinolates, sharing the common precursor indole-3-acetaldoxime (IAOx). Sønderby et al. (2007) showed that transcript levels for the indolic glucosinolates regulatory MYB factors are not altered in plants that over-express MYB28, MYB29, or MYB76 and indolic glucosinolates levels were not affected in the *myb28 myb29* double knockout mutant in comparison to the WT. In addition, transcriptome analysis revealed that genes encoding enzymes involved in the biosynthesis of tryptophan, camalexin and indolic glucosinolates were simultaneously induced in response to biotic stress (Schlaeppli et al., 2010; Yang et al., 2020). Based on these two findings, we cannot speculate that the accumulation of camalexin in *myb28 myb29* could be due to the reduced sulfur flux into aliphatic glucosinolates or elevation of IAOx. A possible explanation could be that *myb28 myb29* accumulates higher levels of camalexin to restore compromised plant resistance caused by reduced aliphatic glucosinolates. This interpretation is partially supported by the reduced accumulation of total glucosinolates in *myb28 myb29*. Aliphatic glucosinolates are important for disease resistance in plants. Researchers have shown that isothiocyanates derived from aliphatic glucosinolates, indolic glucosinolates and camalexin all play roles in defense of Arabidopsis against the pathogenic *Sclerotinia sclerotiorum*. Mutant plant lines deficient in camalexin, indole, or aliphatic glucosinolate biosynthesis were hypersusceptible to *S. sclerotiorum* (Stotz et al., 2011). Plants lacking the aliphatic glucosinolate pathway were unable to attenuate the expression of type III secretion system (TTSS) genes of *P. syringae* and exhibited increased susceptibility to the pathogen (Wang et al., 2020b). Sulforaphane (4-methylsulfinylbutylisothiocyanate), a natural product derived from aliphatic glucosinolates, has been shown to inhibit host-free growth of *Pseudomonas* in Arabidopsis plants (Fan et al., 2011).

Therefore, reduced aliphatic glucosinolates may lead to hypersusceptivity in *myb28 myb29* after *B. glumae* PG1 infection. *myb28 myb29* may increase the accumulation of camalexin, another antibacterial compound to rescue compromised plant immune response. However, this hypothesis is conflict with the camalexin result of *apk1 apk2* mutant, which has even less glucosinolates biosynthesis as in *myb28 myb29*. While the levels of both aliphatic and indolic glucosinolates are reduced approximately fivefold in *apk1 apk2* compared with WT plants (Mugford et al., 2009), the camalexin accumulation in *apk1 apk2* treated by PG1 was not significantly higher than that of Col-0. This conflict between *apk1 apk2* and *myb28 myb29* reveals an unexpectedly complex interconnection between camalexin and glucosinolates, especially under biotic stress. Another noteworthy discovery is that the abundance of the bacteria PG1, *cysH*, and *cysM* in the *myb28 myb29* was the same, unlike in Col-0 and *slim1-1*. This suggests that changes in sulfur metabolism in the host plant can impact the acquisition and colonization of nutrients by bacteria. This result highlights the complex interplay between plants and pathogens and the role of sulfur metabolism in shaping this invasion procedure.

Surprisingly, camalexin was induced at the same level in *slim1-1* by *B. glumae* PG1, *cysH* and *cysM* mutants, which was quite different from Col-0 and other Arabidopsis mutants tested in this study. This finding will be discussed in the next subsection. Patterns of camalexin induction observed from Col-0, *myb28 myb29* and *slim1-1* suggest that perturbation of regulation of sulfur metabolism in Arabidopsis affects immune response to pathogenic challenge. It is of great interest to discover the comprehensive alteration of sulfur flux into primary and secondary sulfur metabolism under pathogen challenge among Arabidopsis genotypes.

5.5 SLIM1 is involved in the regulation of Arabidopsis defense response

Compared to the other Arabidopsis mutants examined in this study, *slim1-1* showed a completely different pattern of camalexin induction after the infection with *B. glumae* PG1, *cysH* and *cysM*. The same level of camalexin induced by PG1 and bacterial mutants suggests that *slim1-1* may be less responsive to biotic stress. The finding that PG1-induced SA and Pip accumulation in *slim1-1* to a lower degree than in Col-0 is consistent with this hypothesis. In addition, the relative gene expression of *PAL1* and *PR1* in PG1-treated *slim1-1* was slightly lower than that in Col-0, suggesting that SLIM1 has an impact on salicylate regulated defense response. PAL1 is an

inducible enzyme that catalyzes the first step in the biosynthesis of salicylic acid (SA), an essential signal involved in plant defense and systemic acquired resistance (Chaman et al., 2003). A study in pepper plants (*Capsicum annuum*) showed that *PAL1*-silenced plants exhibited increased susceptibility to the infection of virulent and avirulent *Xanthomonas campestris* pv. *Vesicatoria* (Xcv). Reactive oxygen species (ROS) induction, hypersensitive cell death, SA accumulation, and induction of PAL activity were significantly impaired in *PAL1* mutants (Kim and Hwang, 2014). SA is an important mobile defense signalling molecule that promotes immunity against biotic stress (Kniskern et al., 2007; Lu, 2009). It plays a crucial role in enhancing local immune responses and inducing systemic acquired resistance (SAR) (Lawton et al., 1995). In addition, number of studies revealed the role of Pip as a long-distance signal that orchestrating SAR and local resistance responses (Kim et al., 2020). Pip accumulates in inoculated Arabidopsis leaves, in petiole exudates from inoculated leaves, and in leaves distal to the site of inoculation (Návarová et al., 2012). This allows Pip to prepare distal plant leaves for future pathogen attack by preactivating multiple stages of defense signaling. Summarizing the results of SA, Pip accumulation, and related gene expression in *slim1-1*, we propose that SLIM1 may play a role in modulating plant SAR. SLIM1 transcription factor has a key role in regulating plant response to sulfur deficiency (Maruyama-Nakashita et al., 2006; Dietzen et al., 2020). In addition to sulfur deficiency, SLIM1 has been shown to act in response and resistance to heavy metal cadmium and arsenic, probably through altering redox status (Yamaguchi et al., 2020; Jobe et al., 2021). Furthermore, we discovered three DEGs significantly down-regulated in *slim1-1* mutant that overlap with genes involved in SA regulation (data source is from Dietzen et al., 2020), namely *SARD1*, *DMR6* and *DLO1*. *SARD1* (*systemic acquired resistance deficient 1*; AT1G73805) is a key regulator for ICS1 induction and SA synthesis. It was reported that the growth of *Pseudomonas syringae* pv. *maculicola* (*Pma*) ES4326 pathogen was enhanced in *sard1*, SA levels and expression of PR1 were dramatically reduced as well (Wang et al., 2011). *DMR6* (*downy mildew resistant 6*; AT5G24530) encodes salicylic acid 5-hydroxylase (S5H) that converts SA into its inactive form, 2,5-DHBA. It is a plant susceptibility (S) gene that facilitates pathogen infection and displays a substrate inhibition property that may enable automatic control of its enzyme activities (Zhang et al., 2017; Thomazella et al., 2021). *DLO1* (*DMR6-like oxygenase 1*, AT4G10500) is strongly activated and co-expressed with *DMR6* during pathogen attack. The *dmr6-3_dlo1* double mutant is completely resistant to downy mildew *Hyaloperonospora arabidopsidis* which can be linked to high level of SA

(Zeilmaker et al., 2015). The regulation of these distinct genes by SLIM1 suggest its role in maintaining SA stability. However, its function in the plant immune response has not been recognised, yet. Further research is needed to understand the function of SLIM1 in plant defense signaling. This will be achieved by assessing the response of *slim1-1* to pathogens at both transcriptional and metabolomic levels, not just on inoculated leaves, but also on distal leaves. This will give us a better understanding of the versatility of SLIM1 and increase our knowledge of this factor.

5.6 Camalexin, glucosinolates and pipecolic acid demonstrated different accumulation pattern following bacterial infection

In this study, we evaluated the accumulation of camalexin, glucosinolates and pipecolic acid (Pip) after infection with bacterial pathogens. Interestingly, we noted that they were accumulated in different patterns. Camalexin plays an important role in plant immune response to *B. glumae* invasion, as Arabidopsis maintained fairly low levels of camalexin in the absence of biotic stress, and once Arabidopsis was infected with the PG1, camalexin accumulated at high levels. The *B. glumae* PG1 induced more camalexin than bacterial mutants in sulfate accumulation in Col-0. As for glucosinolates, their levels were maintained stable after pathogenic infection and no difference was observed between bacterial treatments and mock control. Both camalexin and glucosinolates are important antimicrobial compounds of plants. Plant mutants deficient in camalexin, or indolic or aliphatic glucosinolates biosynthesis were hypersusceptible to pathogen challenge (Sanchez-Vallet et al., 2010; Stotz et al., 2011). It will be interesting to understand why these metabolites display different accumulation patterns under biotic stress.

One hypothesis is that glucosinolates biosynthesis is not sensitive to the infection of non-host *B. glumae*, as glucosinolates concentration were at the same level in both mock control and bacteria-treated plants. However, a number of studies have shown that Arabidopsis confers immunity to non-adapted pathogens. For example, PEN2, a myrosinase, accumulates underneath powdery mildew contact sites to initiate the hydrolysis of indole glucosinolates, to release potential antimicrobial products (Lipka et al., 2005; Bednarek et al., 2009). It was reported that both adapted and non-adapted isolates of *Plectosphaerella cucumerina* triggered the accumulation of Trp-derived indolic glucosinolates in Arabidopsis. Mutation of *CYP79B2* and *CYP79B3* renders Arabidopsis fully susceptible to non-adapted *P. cucumerina* isolates, and super-susceptible to an

adapted *P. cucumerina* isolate (Sanchez-Vallet et al., 2010). These findings may refute the hypothesis. However, it is normal that different pathogens induce different defense metabolites accumulation in Arabidopsis. For example, the transcript levels of genes associated with aliphatic glucosinolates biosynthesis that were elevated following infection of *Sclerotinia sclerotiorum* were not influenced by infection with the closely related pathogen *B. cinerea*. In contrast, *B. cinerea* strongly induced camalexin biosynthetic genes (Stotz et al., 2011). In our study, it may be the case that *B. glumae* triggers camalexin accumulation more than glucosinolates. The central question is how defense-responsive genes are regulated, how sulfur metabolism-related pathways react to different stages of host–pathogen interactions, and how sulfur-responsive transcription factors such as MYBs, SULTRs, WRKYs and SLIM1 regulate the diverse responses related to sulfur metabolisms to different pathogens.

A plausible explanation for the glucosinolates accumulation pattern may be that glucosinolates and camalexin act at different stages of infection. The transcription profiles during the early stage of *Agrobacterium* infection showed that several genes involved in indole glucosinolates biosynthesis and hydrolysis and the camalexin biosynthesis pathway were up-regulated, whereas genes involved in aliphatic glucosinolates biosynthesis pathway were generally down-regulated. Indeed, hydrolysis products of indolic glucosinolates had an inhibitory impact on *Agrobacterium* transient transformation efficiency of Arabidopsis seedlings at the early stage of infection. Certain indolic and aliphatic glucosinolates were reduced in Arabidopsis seedlings after *Agrobacterium* infection, while the accumulation of camalexin was a key factor during the later stage to inhibit tumor development on Arabidopsis inflorescence stalks (Shih et al., 2018). This study suggests that camalexin and glucosinolates can synergistically and coordinately exert different functions at different stages of pathogenic infection. These studies are beyond the scope of this work and await future investigations.

Another surprising finding of this study is that Pip and SA, two mobile signal that mediate SAR in response to pathogens, were significantly induced in Col-0 and *slim1-1* by the Cys auxotrophic *cysH*, but not by fully virulent PG1. Plants deficient in Pip or SA biosynthesis pathway can be applied to gain insights into whether and how Pip and SA regulate plant susceptibility to *B. glumae* PG1 and the *cysH* mutant.

5.7 Conclusions and outlook

Sulfur-induced resistance has obtained awareness because sulfur-containing metabolites are important for plant defense against a variety of biotic and abiotic stress. Pathogens have evolved strategies to consume these metabolites, support their own growth inside plants and overcome plants immunity (Wang et al., 2022). It is interesting to decipher how regulation of sulfur metabolism affects plant-pathogen interactions to shed light on environmentally friendly strategy for fighting against pathogens, increasing crop yield. Our study addressed two questions, the first was whether modulation of the sulfate assimilation pathway of *B. glumae* has an impact on its pathogenicity. Through a range of morphological and physiological experiments, we found that the *cysH* mutant deficient in sulfate reduction and the *cysM* mutant with a depletion in the thiosulfate assimilation pathway, have impaired pathogenicity, which was coordinated to their reduced ability to proliferate inside plants. We also found that the *cysH* mutant partially lost the ability to take up from host plants. These results confirm the frequently cited concept of sulfur-induced resistance and point out the importance of sulfur-containing compounds for plant-bacteria interactions at the metabolic level. The second question was whether changes in plant sulfur metabolism affect susceptibility and immune response to pathogens. Arabidopsis mutants impaired in sulfate assimilation and regulation pathway were evaluated. Camalexin, Pip and SA accumulation levels, along with relative gene expression values indicate the possibility that SLIM1, which is known to be a central regulator of many sulfur deficiency responsive genes, is involved in the regulation of plant immune response. Further experiments are required to investigate the immune pathway regulated by SLIM1, which will increase the knowledge on SLIM1's function. Importantly, this study is, to our knowledge, the first attempt to combine both bacterial and plant mutants to investigate how manipulation of sulfur metabolism and the ability to metabolize sulfur compounds affect pathogenicity and plant susceptibility. The interaction between several Arabidopsis mutants of sulfur metabolism and *B. glumae* deficient in sulfate assimilation pathway reveals comprehensive regulation of sulfur flux into camalexin and glucosinolates and orchestrated biosynthesis of defense compounds upon pathogen attack. Here we used the noxious rice pathogen *B. glumae* in Arabidopsis hydroponic system and showed that impaired sulfate assimilation pathway negatively affects its pathogenicity, which increases our knowledge about factors influencing virulence and could be potentially implemented for crop security.

Although we addressed these two initial questions, the underlying mechanisms affecting pathogenicity have not yet been fully unraveled. To decipher information about plant nutrient uptake as well as dynamic plant immune response during infection, Dual RNA-seq can be performed to profile gene expression simultaneously in pathogen and host plants during infection. It has been demonstrated that both bacterial and plant sulfur metabolism were coordinately regulated during interaction, which might explain the mechanism underlying which beneficial microbes mitigate salt stress to host plants (Andrés-Barrao et al., 2021). Therefore, monitoring the dynamics in metabolic pathways would also be a powerful approach to identify key factors and biotic processes involved in plant–pathogen interactions. GFP-labeling bacteria and isotope-labeling sulfur can be used to monitor plant-microbial interactions *in vivo* and investigate metabolite exchange. The exometabolism of bacteria grown on a nutrient mix can also be studied to better understand substrate preferences of WT bacteria and sulfur deficient mutants, and to identify dominant metabolites that limit bacterial growth in planta.

References

- Abuyusuf M, Robin AHK, Lee J-H, Jung H-J, Kim H-T, Park J-I, Nou I-S** (2018) Glucosinolate Profiling and Expression Analysis of Glucosinolate Biosynthesis Genes Differentiate White Mold Resistant and Susceptible Cabbage Lines. *Int J Mol Sci.* doi: 10.3390/ijms19124037
- Aires A, Mota VR, Saavedra MJ, Monteiro AA, Simões M, Rosa EAS, Bennett RN** (2009) Initial in vitro evaluations of the antibacterial activities of glucosinolate enzymatic hydrolysis products against plant pathogenic bacteria. *J Appl Microbiol* **106**: 2096–2105
- Akerley BJ, Rubin EJ, Novick VL, Amaya K, Judson N, Mekalanos JJ** (2002) A genome-scale analysis for identification of genes required for growth or survival of *Haemophilus influenzae*. *Proc Natl Acad Sci U S A* **99**: 966–971
- Anderson MT, Mitchell LA, Sintsova A, Rice KA, Mobley HLT** (2019) Sulfur Assimilation Alters Flagellar Function and Modulates the Gene Expression Landscape of *Serratia marcescens*. doi: 10.1128/mSystems.00285-19
- Andréasson E, Jørgensen LB, Höglund AS, Rask L, Meijer J** (2001) Different myrosinase and idioblast distribution in *Arabidopsis* and *Brassica napus*. *Plant Physiol* **127**: 1750–1763
- Andrés-Barrao C, Alzubaidy H, Jalal R, Mariappan KG, de Zélicourt A, Bokhari A, Artyukh O, Alwutayd K, Rawat A, Shekhawat K, et al** (2021) Coordinated bacterial and plant sulfur metabolism in *Enterobacter* sp. SA187-induced plant salt stress tolerance. *Proc Natl Acad Sci U S A.* doi: 10.1073/pnas.2107417118
- Barberon M, Berthomieu P, Clairotte M, Shibagaki N, Davidian JC, Gosti F** (2008) Unequal functional redundancy between the two *Arabidopsis thaliana* high-affinity sulphate transporters *SULTR1;1* and *SULTR1;2*. *New Phytol* **180**: 608–619
- Beattie GA, Lindow SE** (1995) The secret life of foliar bacterial pathogens on leaves. *Annu Rev Phytopathol* **33**: 145–172
- Bednarek P** (2012) Sulfur-Containing Secondary Metabolites from *Arabidopsis thaliana* and other Brassicaceae with Function in Plant Immunity. *ChemBioChem* **13**: 1846–1859
- Bednarek P, Piślewska-Bednarek M, Ver Loren van Themaat E, Maddula RK, Svatoš A, Schulze-Lefert P** (2011) Conservation and clade-specific diversification of pathogen-inducible tryptophan and indole glucosinolate metabolism in *Arabidopsis thaliana* relatives. *New Phytol* **192**: 713–726
- Bloem E, Haneklaus S, Schnug E** (2014) Milestones in plant sulfur research on sulfur-induced-resistance (SIR) in Europe. *Front Plant Sci* **5**: 779
- Bloem E, Riemenschneider A, Volker J, Papenbrock J, Schmidt A, Salac I, Haneklaus S, Schnug E** (2004) Sulphur supply and infection with *Pyrenopeziza brassicae* influence L-cysteine desulphydrase activity in *Brassica napus* L. *J Exp Bot* **55**: 2305–2312

- Borlinghaus J, Albrecht F, Gruhlke MCH, Nwachukwu ID, Slusarenko AJ** (2014) Allicin: Chemistry and Biological Properties. *Molecules* **19**: 12591
- Boubakri H, Wahab MA, Chong J, Gertz C, Gandoura S, Mliki A, Bertsch C, Soustre-Gacougnolle I** (2013) Methionine elicits H₂O₂ generation and defense gene expression in grapevine and reduces *Plasmopara viticola* infection. *J Plant Physiol* **170**: 1561–1568
- Browne LM, Conn KL, Ayert WA, Tewari JP** (1991) The camalexins: New phytoalexins produced in the leaves of *camelina sativa* (cruciferae). *Tetrahedron* **47**: 3909–3914
- Buchner P, Takahashi H, Hawkesford MJ** (2004) Plant sulphate transporters: co-ordination of uptake, intracellular and long-distance transport. *J Exp Bot* **55**: 1765–1773
- Cecchini NM, Jung HW, Engle NL, Tschaplinski TJ, Greenberg JT** (2015) ALD1 Regulates Basal Immune Components and Early Inducible Defense Responses in *Arabidopsis*. *Mol Plant Microbe Interact* **28**: 455–466
- Celenza JL, Quiel JA, Smolen GA, Merrikk H, Silvestro AR, Normanly J, Bender J** (2005) The *Arabidopsis* ATR1 Myb transcription factor controls indolic glucosinolate homeostasis. *Plant Physiol* **137**: 253–262
- Chaman ME, Copaja S V, Argandoña VH** (2003) Relationships between salicylic acid content, phenylalanine ammonia-lyase (PAL) activity, and resistance of barley to aphid infestation. *J Agric Food Chem* **51**: 2227–2231
- Chaturvedi R, Shah J** (2007) Salicylic acid in plant disease resistance. *Salicylic Acid A Plant Horm* 335–370
- Chen M, Zhang W, Han L, Ru X, Cao Y, Hikichi Y, Ohnishi K, Pan G, Zhang Y** (2022) A CysB regulator positively regulates cysteine synthesis, expression of type III secretion system genes, and pathogenicity in *Ralstonia solanacearum*. *Mol Plant Pathol* **23**: 679–692
- Chen S, Glawischnig E, Jørgensen K, Naur P, Jørgensen B, Olsen C-E, Hansen CH, Rasmussen H, Pickett JA, Halkier BA** (2003) CYP79F1 and CYP79F2 have distinct functions in the biosynthesis of aliphatic glucosinolates in *Arabidopsis*. *Plant J* **33**: 923–937
- Chen W, Chao G, Singh KB** (1996) The promoter of a H₂O₂-inducible, *Arabidopsis* glutathione S-transferase gene contains closely linked OBF- and OBP1-binding sites. *Plant J* **10**: 955–966
- Chen YC, Holmes EC, Rajniak J, Kim JG, Tang S, Fischer CR, Mudgett MB, Sattely ES** (2018) N-hydroxy-pipecolic acid is a mobile metabolite that induces systemic disease resistance in *Arabidopsis*. *Proc Natl Acad Sci U S A* **115**: E4920–E4929
- Cheng X, Etalo DW, van de Mortel JE, Dekkers E, Nguyen L, Medema MH, Raaijmakers JM** (2017) Genome-wide analysis of bacterial determinants of plant growth promotion and induced systemic resistance by *Pseudomonas fluorescens*. *Environ Microbiol* **19**: 4638–4656
- Chhajed S, Mostafa I, He Y, Abou-Hashem M, El-Domiaty M, Chen S** (2020) Glucosinolate Biosynthesis and the Glucosinolate–Myrosinase System in Plant Defense. *Agron* 2020, Vol 10, Page 1786 **10**: 1786
- Chun SC, Chandrasekaran M** (2019) Chitosan and chitosan nanoparticles induced expression of pathogenesis-

- related proteins genes enhances biotic stress tolerance in tomato. *Int J Biol Macromol* **125**: 948–954
- Cobbett CS, May MJ, Howden R, Rolls B** (1998) The glutathione-deficient, cadmium-sensitive mutant, *cad2-1*, of *Arabidopsis thaliana* is deficient in γ -glutamylcysteine synthetase. *Plant J* **16**: 73–78
- Cools HJ, Ishii H** (2002) Pre-treatment of cucumber plants with acibenzolar-S-methyl systemically primes a phenylalanine ammonia lyase gene (PAL1) for enhanced expression upon attack with a pathogenic fungus. *Physiol Mol Plant Pathol* **61**: 273–280
- Cooper RW, Resende MLV, Flood J, Rowan MG, Beale MH, Potter U** (1996) Detection and cellular localization of elemental sulphur in disease-resistant genotypes of *Theobroma cacao*. *Nat* 1996 3796561 **379**: 159–162
- Daudi A, O'Brien J** (2012) Detection of Hydrogen Peroxide by DAB Staining in *Arabidopsis* Leaves. *BIO-PROTOCOL*. doi: 10.21769/BIOPROTOC.263
- Delmotte N, Knief C, Chaffron S, Innerebner G, Roschitzki B, Schlapbach R, Von Mering C, Vorholt JA** (2009) Community proteogenomics reveals insights into the physiology of phyllosphere bacteria. *Proc Natl Acad Sci U S A* **106**: 16428–16433
- Denoux C, Galletti R, Mammarella N, Gopalan S, Werck D, De Lorenzo G, Ferrari S, Ausubel FM, Dewdney J** (2008) Activation of Defense Response Pathways by OGs and Flg22 Elicitors in *Arabidopsis* Seedlings. *Mol Plant* **1**: 423–445
- Dietzen C, Koprivova A, Whitcomb SJ, Langen G, Jobe TO, Hoefgen R, Kopriva S** (2020) The Transcription Factor EIL1 Participates in the Regulation of Sulfur-Deficiency Response. *Plant Physiol* **184**: 2120–2136
- Dubreuil-Maurizi C, Poinssot B** (2012) Role of glutathione in plant signaling under biotic stress. *Plant Signal Behav* **7**: 210–212
- Durrant WE, Dong X** (2004) Systemic acquired resistance. *Annu Rev Phytopathol* **42**: 185–209
- Escudero V, Torres MÁ, Delgado M, Sopeña-Torres S, Swami S, Morales J, Muñoz-Barríos A, Mélida H, Jones AM, Jordá L, et al** (2019) Mitogen-activated protein kinase phosphatase 1 (MKP1) negatively regulates the production of reactive oxygen species during *Arabidopsis* immune responses. *Mol Plant-Microbe Interact* **32**: 464–478
- Fahey JW, Zalcemann AT, Talalay P** (2001) The chemical diversity and distribution of glucosinolates and isothiocyanates among plants. *Phytochemistry* **56**: 5–51
- Fan J, Crooks C, Creissen G, Hill L, Fairhurst S, Doerner P, Lamb C** (2011) *Pseudomonas sax* genes overcome aliphatic isothiocyanate-mediated non-host resistance in *Arabidopsis*. *Science* **331**: 1185–1188
- Ferelli AMC, Boltén S, Szczesny B, Micallef SA** (2020) *Salmonella enterica* Elicits and Is Restricted by Nitric Oxide and Reactive Oxygen Species on Tomato. *Front Microbiol* **11**: 391
- Fodor J, Gullner G, Ádám AL, Barna B, Kömives T, Király Z** (1997) Local and Systemic Responses of Antioxidants to Tobacco Mosaic Virus Infection and to Salicylic Acid in Tobacco (Role in Systemic Acquired

- Resistance). *Plant Physiol* **114**: 1443–1451
- Frerigmann H, Gigolashvili T** (2014) MYB34, MYB51, and MYB122 distinctly regulate indolic glucosinolate biosynthesis in *Arabidopsis thaliana*. *Mol Plant* **7**: 814–828
- Frerigmann H, Glawischnig E, Gigolashvili T** (2015) The role of MYB34, MYB51 and MYB122 in the regulation of camalexin biosynthesis in *Arabidopsis thaliana*. *Front. Plant Sci.* **6**:
- Frerigmann H, Piślewska-Bednarek M, Sánchez-Vallet A, Molina A, Glawischnig E, Gigolashvili T, Bednarek P** (2016) Regulation of Pathogen-Triggered Tryptophan Metabolism in *Arabidopsis thaliana* by MYB Transcription Factors and Indole Glucosinolate Conversion Products. *Mol Plant* **9**: 682–695
- Gao R, Krysciak D, Petersen K, Utpatel C, Knapp A, Schmeisser C, Daniel R, Voget S, Jaeger K-E, Streit WR** (2015) Genome-wide RNA sequencing analysis of quorum sensing-controlled regulons in the plant-associated *Burkholderia glumae* PG1 strain. *Appl Environ Microbiol* **81**: 7993–8007
- Gebhardt MJ, Gallagher LA, Jacobson RK, Usacheva EA, Peterson LR, Zurawski D V., Shuman HA** (2015) Joint Transcriptional Control of Virulence and Resistance to Antibiotic and Environmental Stress in *Acinetobacter baumannii*. *MBio*. doi: 10.1128/MBIO.01660-15
- Gigolashvili T, Berger B, Mock HP, Müller C, Weisshaar B, Flügge UI** (2007a) The transcription factor HIG1/MYB51 regulates indolic glucosinolate biosynthesis in *Arabidopsis thaliana*. *Plant J* **50**: 886–901
- Gigolashvili T, Kopriva S** (2014) Transporters in plant sulfur metabolism. *Front Plant Sci* **5**: 442
- Gigolashvili T, Yatusевич R, Berger B, Müller C, Flügge UI** (2007b) The R2R3-MYB transcription factor HAG1/MYB28 is a regulator of methionine-derived glucosinolate biosynthesis in *Arabidopsis thaliana*. *Plant J* **51**: 247–261
- Gilbert SM, Clarkson DT, Cambridge M, Lambers H, Hawkesford MJ** (1997) SO42- Deprivation Has an Early Effect on the Content of Ribulose-1,5-Bisphosphate Carboxylase/Oxygenase and Photosynthesis in Young Leaves of Wheat. *Plant Physiol* **115**: 1231–1239
- Grant K, Carey NM, Mendoza M, Schulze J, Pilon M, Pilon-Smits EAH, Van Hoewyk D** (2011) Adenosine 5'-phosphosulfate reductase (APR2) mutation in *Arabidopsis* implicates glutathione deficiency in selenate toxicity. *Biochem J* **438**: 325–335
- Guédon E, Martin-Verstraete I** (2006) Cysteine Metabolism and Its Regulation in Bacteria. *Amin Acid Biosynth ~ Pathways, Regul Metab Eng* 195–218
- Gullner G, Zechmann B, Künstler A, Király L** (2017) The signaling roles of glutathione in plant disease resistance. *Glutathione Plant Growth, Dev Stress Toler* 331–357
- Gust AA, Biswas R, Lenz HD, Rauhut T, Ranf S, Kemmerling B, Götz F, Glawischnig E, Lee J, Felix G, et al** (2007) Bacteria-derived peptidoglycans constitute pathogen-associated molecular patterns triggering innate immunity in *Arabidopsis*. *J Biol Chem* **282**: 32338–32348

- Gutierrez Boem FH, Prystupa P, Ferraris G** (2007) Seed Number and Yield Determination in Sulfur Deficient Soybean Crops. <http://dx.doi.org/101080/01904160601055095> **30**: 93–104
- HAM JH, MELANSON RA, RUSH MC** (2011) Burkholderia glumae: next major pathogen of rice? *Mol Plant Pathol* **12**: 329–339
- Han Y, Chaouch S, Mhamdi A, Queval G, Zechmann B, Noctor G** (2013) Functional analysis of arabidopsis mutants points to novel roles for glutathione in coupling H₂O₂ to activation of salicylic acid accumulation and signaling. *Antioxidants Redox Signal* **18**: 2106–2121
- Hansen CH, Wittstock U, Olsen CE, Hick AJ, Pickett JA, Halkier BA** (2001) Cytochrome p450 CYP79F1 from arabidopsis catalyzes the conversion of dihomomethionine and trihomomethionine to the corresponding aldoximes in the biosynthesis of aliphatic glucosinolates. *J Biol Chem* **276**: 11078–11085
- Harada E, Kusano T, Sano H** (2000) Differential Expression of Genes Encoding Enzymes Involved in Sulfur Assimilation Pathways in Response to Wounding and Jasmonate in *Arabidopsis thaliana*. *J Plant Physiol* **156**: 272–276
- Hayat Q, Hayat S, Irfan M, Ahmad A** (2010) Effect of exogenous salicylic acid under changing environment: A review. *Environ Exp Bot* **68**: 14–25
- He Y, Xu J, Wang X, He X, Wang Y, Zhou J, Zhang S, Meng X** (2019) The Arabidopsis Pleiotropic Drug Resistance Transporters PEN3 and PDR12 Mediate Camalexin Secretion for Resistance to Botrytis cinerea. *Plant Cell* **31**: 2206–2222
- Hétu M-F, Tremblay LJ, Lefebvre DD** (2005) High root biomass production in anchored *Arabidopsis* plants grown in axenic sucrose supplemented liquid culture. *Biotechniques* **39**: 345–349
- Hirai MY, Fujiwara T, Awazuhara M, Kimura T, Noji M, Saito K** (2003) Global expression profiling of sulfur-starved Arabidopsis by DNA microarray reveals the role of O-acetyl-l-serine as a general regulator of gene expression in response to sulfur nutrition. *Plant J* **33**: 651–663
- Hirai MY, Sugiyama K, Sawada Y, Tohge T, Obayashi T, Suzuki A, Araki R, Sakurai N, Suzuki H, Aoki K, et al** (2007) Omics-based identification of Arabidopsis Myb transcription factors regulating aliphatic glucosinolate biosynthesis. *Proc Natl Acad Sci U S A* **104**: 6478–6483
- Horbach R, Navarro-Quesada AR, Knogge W, Deising HB** (2011) When and how to kill a plant cell: infection strategies of plant pathogenic fungi. *J Plant Physiol* **168**: 51–62
- Houhou M, Joutei KA, Louhalia S** (2018) Biomass production, chlorophyll content and morphological parameters are affected by sulfur deficiency in *Eruca sativa* L. *Int J Ecol Environ Sci* **44**: 67–75
- Huang J, Gu M, Lai Z, Fan B, Shi K, Zhou Y-H, Yu J-Q, Chen Z** (2010) Functional analysis of the Arabidopsis PAL gene family in plant growth, development, and response to environmental stress. *Plant Physiol* **153**: 1526–1538

- Huang W, Wang Y, Li X, Zhang Y** (2020) Biosynthesis and Regulation of Salicylic Acid and N-Hydroxypipicolinic Acid in Plant Immunity. *Mol Plant* **13**: 31–41
- Hull AK, Vij R, Celenza JL** (2000) Arabidopsis cytochrome P450s that catalyze the first step of tryptophan-dependent indole-3-acetic acid biosynthesis. *Proc Natl Acad Sci U S A* **97**: 2379–2384
- Imssande J** (1998) Iron, sulfur, and chlorophyll deficiencies: A need for an integrative approach in plant physiology. *Physiol Plant* **103**: 139–144
- Iwai T, Miyasaka A, Seo S, Ohashi Y** (2006) Contribution of ethylene biosynthesis for resistance to blast fungus infection in young rice plants. *Plant Physiol* **142**: 1202–1215
- J. GM, M. CD, Shweta S, V. ZD, Lev B, A. SH** (2020) GigC, a LysR Family Transcription Regulator, Is Required for Cysteine Metabolism and Virulence in *Acinetobacter baumannii*. *Infect Immun* **89**: e00180-20
- Jacobs JM, Babujee L, Meng F, Milling A, Allen C** (2012) The in planta transcriptome of *Ralstonia solanacearum*: conserved physiological and virulence strategies during bacterial wilt of tomato. *MBio*. doi: 10.1128/MBIO.00114-12
- Jacoby RP, Kopriva S** (2019) Metabolic niches in the rhizosphere microbiome: new tools and approaches to analyse metabolic mechanisms of plant–microbe nutrient exchange. *J Exp Bot* **70**: 1087–1094
- Jacoby RP, Martyn A, Kopriva S** (2018) Exometabolomic Profiling of Bacterial Strains as Cultivated Using *Arabidopsis* Root Extract as the Sole Carbon Source. *Mol Plant-Microbe Interact* **31**: 803–813
- Jeong Y, Kim J, Kim S, Kang Y, Nagamatsu T, Hwang I** (2003) Toxoflavin produced by *Burkholderia glumae* causing rice grain rot is responsible for inducing bacterial wilt in many field crops. *Plant Dis* **87**: 890–895
- Jobe TO, Yu Q, Hauser F, Xie Q, Meng Y, Maassen T, Kopriva S, Schroeder JI** (2021) The SLIM1 transcription factor is required for arsenic resistance in *Arabidopsis thaliana*. *FEBS Lett* **595**: 1696–1707
- Jost R, Altschmied L, Bloem E, Bogs J, Gershenzon J, Hähnel U, Hänsch R, Hartmann T, Kopriva S, Kruse C, et al** (2005) Expression profiling of metabolic genes in response to methyl jasmonate reveals regulation of genes of primary and secondary sulfur-related pathways in *Arabidopsis thaliana*. *Photosynth Res* **86**: 491–508
- Kawano Y, Onishi F, Shiroyama M, Miura M, Tanaka N, Oshiro S, Nonaka G, Nakanishi T, Ohtsu I** (2017) Improved fermentative l-cysteine overproduction by enhancing a newly identified thiosulfate assimilation pathway in *Escherichia coli*. *Appl Microbiol Biotechnol* **101**: 6879–6889
- Khan MS, Haas FH, Samami AA, Gholami AM, Bauer A, Fellenberg K, Reichelt M, Hänsch R, Mendel RR, Meyer AJ, et al** (2010) Sulfite reductase defines a newly discovered bottleneck for assimilatory sulfate reduction and is essential for growth and development in *Arabidopsis thaliana*. *Plant Cell* **22**: 1216–1231
- Kies PJ, Hammer ND** (2022) A Resourceful Race: Bacterial Scavenging of Host Sulfur Metabolism during Colonization. *Infect Immun*. doi: 10.1128/IAI.00579-21/ASSET/EA35CCDF-DBA8-4090-89A0-C2BC53F7DD36/ASSETS/IMAGES/LARGE/IAI.00579-21-F002.JPG

- Kim DS, Hwang BK** (2014) An important role of the pepper phenylalanine ammonia-lyase gene (PAL1) in salicylic acid-dependent signalling of the defence response to microbial pathogens. *J Exp Bot* **65**: 2295–2306
- Kim HK, Verpoorte R** (2010) Sample preparation for plant metabolomics. *Phytochem Anal* **21**: 4–13
- Kim Y, Gilmour SJ, Chao L, Park S, Thomashow MF** (2020) Arabidopsis CAMTA Transcription Factors Regulate Picecolic Acid Biosynthesis and Priming of Immunity Genes. *Mol Plant* **13**: 157–168
- Klee SM, Sinn JP, Finley M, Allman EL, Smith PB, Aimufua O, Sittler V, Lehman BL, Krawczyk T, Peter KA, et al** (2019) *Erwinia amylovora* Auxotrophic Mutant Exometabolomics and Virulence on Apples. *Appl Environ Microbiol*. doi: 10.1128/AEM.00935-19
- Kliebenstein DJ, Rowe HC, Denby KJ** (2005) Secondary metabolites influence Arabidopsis/Botrytis interactions: variation in host production and pathogen sensitivity. *Plant J* **44**: 25–36
- Kniskern JM, Traw MB, Bergelson J** (2007) Salicylic Acid and Jasmonic Acid Signaling Defense Pathways Reduce Natural Bacterial Diversity on Arabidopsis thaliana. *Mol Plant-Microbe Interact* **20**: 1512–1522
- Kopriva S** (2006) Regulation of sulfate assimilation in Arabidopsis and beyond. *Ann Bot* **97**: 479–495
- Kopriva S, Mugford SG, Baraniecka P, Lee B-R, Matthewman CA, Koprivova A** (2012) Control of sulfur partitioning between primary and secondary metabolism in Arabidopsis. *Front Plant Sci* **3**: 163
- Kopriva S, Mugford SG, Matthewman C, Koprivova A** (2009) Plant sulfate assimilation genes: Redundancy versus specialization. *Plant Cell Rep* **28**: 1769–1780
- Koprivova A, North KA, Kopriva S** (2008) Complex signaling network in regulation of adenosine 5'-phosphosulfate reductase by salt stress in Arabidopsis roots. *Plant Physiol* **146**: 1408–1420
- Koprivova A, Schuck S, Jacoby RP, Klinkhammer I, Welter B, Leson L, Martyn A, Nauen J, Grabenhorst N, Mandelkow JF, et al** (2019a) Root-specific camalexin biosynthesis controls the plant growth-promoting effects of multiple bacterial strains. *Proc Natl Acad Sci* **116**: 15735–15744
- Koprivova A, Schuck S, Jacoby RP, Klinkhammer I, Welter B, Leson L, Martyn A, Nauen J, Grabenhorst N, Mandelkow JF, et al** (2019b) Root-specific camalexin biosynthesis controls the plant growth-promoting effects of multiple bacterial strains. *Proc Natl Acad Sci U S A* **116**: 15735–15744
- Koprivova A, Schwier M, Volz V, Kopriva S** (2023) Shoot-root interaction in control of camalexin exudation in Arabidopsis. *J Exp Bot*. doi: 10.1093/jxb/erad031
- Koroleva OA, Davies A, Deeken R, Thorpe MR, Tomos AD, Hedrich R** (2000) Identification of a New Glucosinolate-Rich Cell Type in Arabidopsis Flower Stalk. *Plant Physiol* **124**: 599–608
- Kruszka D, Sawikowska A, Kamalabai Selvakesavan R, Krajewski P, Kachlicki P, Franklin G** (2020) Silver nanoparticles affect phenolic and phytoalexin composition of Arabidopsis thaliana. *Sci Total Environ*. doi: 10.1016/J.SCITOTENV.2019.135361

- Lappartient AG, Vidmar JJ, Leustek T, Glass ADM, Touraine B** (1999) Inter-organ signaling in plants: regulation of ATP sulfurylase and sulfate transporter genes expression in roots mediated by phloem-translocated compound. *Plant J* **18**: 89–95
- Lawton K, Weymann K, Friedrich L, Vernooij B, Uknes S, Ryals J** (1995) Systemic acquired resistance in *Arabidopsis* requires salicylic acid but not ethylene. *MPMI-Molecular Plant Microbe Interact* **8**: 863–870
- Lensmire JM, Hammer ND** (2019) Nutrient sulfur acquisition strategies employed by bacterial pathogens. *Curr Opin Microbiol* **47**: 52–58
- Leustek T, Martin MN, Bick JA, Davies JP** (2003) PATHWAYS AND REGULATION OF SULFUR METABOLISM REVEALED THROUGH MOLECULAR AND GENETIC STUDIES. <https://doi.org/10.1146/annurev.arplant511141> **51**: 141–165
- Li Y, Li R, Sawada Y, Boerzhijin S, Kuwahara A, Sato M, Hirai MY** (2021) Abscisic acid-mediated induction of FLAVIN-CONTAINING MONOOXYGENASE 2 leads to reduced accumulation of methylthioalkyl glucosinolates in *Arabidopsis thaliana*. *Plant Sci.* doi: 10.1016/J.PLANTSCI.2020.110764
- Li Y, Sawada Y, Hirai A, Sato M, Kuwahara A, Yan X, Hirai MY** (2013a) Novel insights into the function of *Arabidopsis* R2R3-MYB transcription factors regulating aliphatic glucosinolate biosynthesis. *Plant Cell Physiol* **54**: 1335–1344
- Li Y, Sawada Y, Hirai A, Sato M, Kuwahara A, Yan X, Hirai MY** (2013b) Novel insights into the function of *Arabidopsis* R2R3-MYB transcription factors regulating aliphatic glucosinolate biosynthesis. *Plant Cell Physiol* **54**: 1335–1344
- Li Y, Wu M, Yu Q, Su ZZ, Dong B, Lu JP, Lin FC, Liao QS, Liu XH** (2020) PoMet3 and PoMet14 associated with sulfate assimilation are essential for conidiogenesis and pathogenicity in *Pyricularia oryzae*. *Curr Genet* **66**: 765–774
- Liao A, Li L, Wang T, Lu A, Wang Z, Wang Q** (2022) Discovery of Phytoalexin Camalexin and Its Derivatives as Novel Antiviral and Antiphytopathogenic-Fungus Agents. *J Agric Food Chem* **70**: 2554–2563
- Lithgow JK, Hayhurst EJ, Cohen G, Aharonowitz Y, Foster SJ** (2004) Role of a Cysteine Synthase in *Staphylococcus aureus*. *J Bacteriol* **186**: 1579–1590
- Loudet O, Saliba-Colombani V, Camilleri C, Calenge F, Gaudon V, Koprivova A, North KA, Kopriva S, Daniel-Vedele F** (2007) Natural variation for sulfate content in *Arabidopsis thaliana* is highly controlled by APR2. *Nat Genet* 2007 397 **39**: 896–900
- Lu H** (2009) Dissection of salicylic acid-mediated defense signaling networks. *Plant Signal Behav* **4**: 713–717
- Madloo P, Lema M, Francisco M, Soengas P** (2019) Role of Major Glucosinolates in the Defense of Kale Against *Sclerotinia sclerotiorum* and *Xanthomonas campestris* pv. *campestris*. *Phytopathology®* **109**: 1246–1256
- Malhi SS, Gan Y, Raney JP** (2007) Yield, Seed Quality, and Sulfur Uptake of Brassica Oilseed Crops in Response

to Sulfur Fertilization. *Agron J* **99**: 570–577

Martin GB, Bogdanove AJ, Sessa G (2003) Understanding the functions of plant disease resistance proteins. *Annu Rev Plant Biol* **54**: 23–61

Maruyama-Nakashita A, Nakamura Y, Tohge T, Saito K, Takahashi H (2006) Arabidopsis SLIM1 Is a Central Transcriptional Regulator of Plant Sulfur Response and Metabolism. *Plant Cell* **18**: 3235–3251

Melotto M, Underwood W, He SY (2008) Role of stomata in plant innate immunity and foliar bacterial diseases. *Annu Rev Phytopathol* **46**: 101–122

Mendgen K, Hahn M (2002) Plant infection and the establishment of fungal biotrophy. *Trends Plant Sci* **7**: 352–356

Menino JF, Saraiva M, Gomes-Rezende J, Sturme M, Pedrosa J, Castro AG, Ludovico P, Goldman GH, Rodrigues F (2013) *P. brasiliensis* virulence is affected by SconC, the negative regulator of inorganic sulfur assimilation. *PLoS One*. doi: 10.1371/JOURNAL.PONE.0074725

Mikkelsen MD, Hansen CH, Wittstock U, Halkier BA (2000) Cytochrome P450 CYP79B2 from Arabidopsis catalyzes the conversion of tryptophan to indole-3-acetaldoxime, a precursor of indole glucosinolates and indole-3-acetic acid. *J Biol Chem* **275**: 33712–33717

Miura K, Tada Y (2014) Regulation of water, salinity, and cold stress responses by salicylic acid. *Front Plant Sci* **5**: 4

Mostafa I, Zhu N, Yoo MJ, Balmant KM, Misra BB, Dufresne C, Abou-Hashem M, Chen S, El-Domiaty M (2016) New nodes and edges in the glucosinolate molecular network revealed by proteomics and metabolomics of Arabidopsis myb28/29 and cyp79B2/B3 glucosinolate mutants. *J Proteomics* **138**: 1–19

Mugford SG, Yoshimoto N, Reichelt M, Wirtz M, Hill L, Mugford ST, Nakazato Y, Noji M, Takahashi H, Kramell R, et al (2009a) Disruption of Adenosine-5'-Phosphosulfate Kinase in Arabidopsis Reduces Levels of Sulfated Secondary Metabolites. *Plant Cell* **21**: 910–927

Mugford SG, Yoshimoto N, Reichelt M, Wirtz M, Hill L, Mugford ST, Nakazato Y, Noji M, Takahashi H, Kramell R, et al (2009b) Disruption of adenosine-5'-phosphosulfate kinase in Arabidopsis reduces levels of sulfated secondary metabolites. *Plant Cell* **21**: 910–927

Mugford SG, Yoshimoto N, Reichelt M, Wirtz M, Hill L, Mugford ST, Nakazato Y, Noji M, Takahashi H, Kramell R, et al (2009c) Disruption of adenosine-5'-phosphosulfate kinase in Arabidopsis reduces levels of sulfated secondary metabolites. *Plant Cell* **21**: 910–927

Nafisi M, Goregaoker S, Botanga CJ, Glawischnig E, Olsen CE, Halkier BA, Glazebrook J (2007) Arabidopsis Cytochrome P450 Monooxygenase 71A13 Catalyzes the Conversion of Indole-3-Acetaldoxime in Camalexin Synthesis. *Plant Cell* **19**: 2039–2052

Nakai Y, Maruyama-Nakashita A (2020) Biosynthesis of Sulfur-Containing Small Biomolecules in Plants. *Int J Mol Sci* 2020, Vol 21, Page 3470 **21**: 3470

- Nakamura T, Kon Y, Iwahashi H, Eguchi Y** (1983) Evidence that thiosulfate assimilation by *Salmonella typhimurium* is catalyzed by cysteine synthase B. *J Bacteriol* **156**: 656–662
- Nakatani T, Ohtsu I, Nonaka G, Wiriathanawudhiwong N, Morigasaki S, Takagi H** (2012a) Enhancement of thioredoxin/glutaredoxin-mediated L-cysteine synthesis from S-sulfocysteine increases L-cysteine production in *Escherichia coli*. *Microb Cell Fact* **11**: 1–9
- Nakatani T, Ohtsu I, Nonaka G, Wiriathanawudhiwong N, Morigasaki S, Takagi H** (2012b) Enhancement of thioredoxin/glutaredoxin-mediated L-cysteine synthesis from S-sulfocysteine increases L-cysteine production in *Escherichia coli*. *Microb Cell Fact* **11**: 1–9
- Návarová H, Bernsdorff F, Döring A-C, Zeier J** (2012) Pipecolic Acid, an Endogenous Mediator of Defense Amplification and Priming, Is a Critical Regulator of Inducible Plant Immunity. *Plant Cell* **24**: 5123 LP – 5141
- Nguyen NH, Trotel-Aziz P, Clément C, Jeandet P, Baillieul F, Aziz A** (2022a) Camalexin accumulation as a component of plant immunity during interactions with pathogens and beneficial microbes. *Planta* **255**: 116
- Nguyen NH, Trotel-Aziz P, Villaume S, Rabenoelina F, Clément C, Baillieul F, Aziz A** (2022b) Priming of camalexin accumulation in induced systemic resistance by beneficial bacteria against *Botrytis cinerea* and *Pseudomonas syringae* pv. *tomato* DC3000. *J Exp Bot* **73**: 3743–3757
- Noctor G, Mhamdi A, Chaouch S, Han Y, Neukermans J, Marquez-Garcia B, Queval G, Foyer CH** (2012) Glutathione in plants: an integrated overview. *Plant Cell Environ* **35**: 454–484
- Nomura H, Komori T, Uemura S, Kanda Y, Shimotani K, Nakai K, Furuichi T, Takebayashi K, Sugimoto T, Sano S, et al** (2012) Chloroplast-mediated activation of plant immune signalling in *Arabidopsis*. *Nat Commun*. doi: 10.1038/NCOMMS1926
- Olsen KM, Lea US, Slimestad R, Verheul M, Lillo C** (2008) Differential expression of four *Arabidopsis* PAL genes; PAL1 and PAL2 have functional specialization in abiotic environmental-triggered flavonoid synthesis. *J Plant Physiol* **165**: 1491–1499
- Ortega L, Rojas CM** (2020) Bacterial Panicle Blight and *Burkholderia glumae*: From Pathogen Biology to Disease Control. *Phytopathology*® **111**: 772–778
- Park SW, Kaimoyo E, Kumar D, Mosher S, Klessig DF** (2007) Methyl salicylate is a critical mobile signal for plant systemic acquired resistance. *Science* **318**: 113–116
- Poveda J, Eugui D, Velasco P** (2020) Natural control of plant pathogens through glucosinolates: an effective strategy against fungi and oomycetes. *Phytochem Rev* **19**: 1045–1059
- Que Y, Yue X, Yang N, Xu Z, Tang S, Wang C, Lv W, Xu L, Talbot NJ, Wang Z** (2020) Leucine biosynthesis is required for infection-related morphogenesis and pathogenicity in the rice blast fungus *Magnaporthe oryzae*. *Curr Genet* **66**: 155–171
- Qutob D, Kemmerling B, Brunner F, Kufner I, Engelhardt S, Gust AA, Luberacki B, Seitz HU, Stahl D, Rauhut**

- T, et al** (2006) Phytotoxicity and Innate Immune Responses Induced by Nep1-Like Proteins. *Plant Cell* **18**: 3721–3744
- Rahantaniaina MS, Tuzet A, Mhamdi A, Noctor G** (2013) Missing links in understanding redox signaling via thiol/disulfide modulation: How is glutathione oxidized in plants? *Front Plant Sci* **4**: 477
- Resurreccion AP, Makino A, Bennett J, Mae T** (2001) Effects of sulfur nutrition on the growth and photosynthesis of rice. *Soil Sci Plant Nutr* **47**: 611–620
- Ristova D, Kopriva S** (2022) Sulfur signaling and starvation response in Arabidopsis. *iScience* **25**: 104242
- Ross A, Somssich IE** (2016) A DNA-based real-time PCR assay for robust growth quantification of the bacterial pathogen *Pseudomonas syringae* on *Arabidopsis thaliana*. *Plant Methods*. doi: 10.1186/s13007-016-0149-z
- Rouached H, Wirtz M, Alary R, Hell R, Arpat AB, Davidian JC, Fourcroy P, Berthomieu P** (2008) Differential Regulation of the Expression of Two High-Affinity Sulfate Transporters, SULTR1.1 and SULTR1.2, in Arabidopsis. *Plant Physiol* **147**: 897–911
- Saint-Macary ME, Barbisan C, Gagey MJ, Frelin O, Beffa R, Lebrun MH, Droux M** (2015) Methionine Biosynthesis is Essential for Infection in the Rice Blast Fungus *Magnaporthe oryzae*. *PLoS One* **10**: 1–22
- Sanchez-Vallet A, Ramos B, Bednarek P, López G, Piślewska-Bednarek M, Schulze-Lefert P, Molina A** (2010) Tryptophan-derived secondary metabolites in *Arabidopsis thaliana* confer non-host resistance to necrotrophic *Plectosphaerella cucumerina* fungi. *Plant J* **63**: 115–127
- Sarosh BR, Sivaramakrishnan S, Shetty HS** (2005) Elicitation of defense related enzymes and resistance by L-methionine in pearl millet against downy mildew disease caused by *Sclerospora graminicola*. *Plant Physiol Biochem PPB* **43**: 808–815
- Scheel D** (1998) Resistance response physiology and signal transduction. *Curr Opin Plant Biol* **1**: 305–310
- Scheerer U, Haensch R, Mendel RR, Kopriva S, Rennenberg H, Herschbach C** (2010) Sulphur flux through the sulphate assimilation pathway is differently controlled by adenosine 5'-phosphosulphate reductase under stress and in transgenic poplar plants overexpressing gamma-ECS, SO, or APR. *J Exp Bot* **61**: 609–622
- Schlaeppli K, Abou-Mansour E, Buchala A, Mauch F** (2010) Disease resistance of *Arabidopsis* to *Phytophthora brassicae* is established by the sequential action of indole glucosinolates and camalexin. *Plant J* **62**: 840–851
- Schuhegger R, Nafisi M, Mansourova M, Petersen BL, Olsen CE, Svatos A, Halkier BA, Glawischnig E** (2006) CYP71B15 (PAD3) catalyzes the final step in camalexin biosynthesis. *Plant Physiol* **141**: 1248–1254
- Scully LR, Bidochka MJ** (2009) An alternative insect pathogenic strategy in an *Aspergillus flavus* auxotroph. *Mycol Res* **113**: 230–239
- Sekowska A, Kung H-F, Danchin A** (2000) Sulfur metabolism in *Escherichia coli* and related bacteria: facts and fiction. *J Mol Microbiol Biotechnol* **2**: 145–177

- Shibagaki N, Rose A, McDermott JP, Fujiwara T, Hayashi H, Yoneyama T, Davies JP** (2002) Selenate-resistant mutants of *Arabidopsis thaliana* identify Sultr1;2, a sulfate transporter required for efficient transport of sulfate into roots. *Plant J* **29**: 475–486
- Shih P-Y, Chou S-J, Müller C, Halkier BA, Deeken R, Lai E-M** (2018) Differential roles of glucosinolates and camalexin at different stages of *Agrobacterium*-mediated transformation. *Mol Plant Pathol* **19**: 1956–1970
- Sønderby IE, Geu-Flores F, Halkier BA** (2010) Biosynthesis of glucosinolates--gene discovery and beyond. *Trends Plant Sci* **15**: 283–290
- Sønderby IE, Hansen BG, Bjarnholt N, Ticconi C, Halkier BA, Kliebenstein DJ** (2007) A Systems Biology Approach Identifies a R2R3 MYB Gene Subfamily with Distinct and Overlapping Functions in Regulation of Aliphatic Glucosinolates. *PLoS One* **2**: e1322
- Spoel SH, Loake GJ** (2011) Redox-based protein modifications: the missing link in plant immune signalling. *Curr Opin Plant Biol* **14**: 358–364
- Stotz HU, Sawada Y, Shimada Y, Hirai MY, Sasaki E, Kruschke M, Brown PD, Saito K, Kamiya Y** (2011) Role of camalexin, indole glucosinolates, and side chain modification of glucosinolate-derived isothiocyanates in defense of *Arabidopsis* against *Sclerotinia sclerotiorum*. *Plant J* **67**: 81–93
- Suzuki H, Kamatani S, Kim ES, Kumagai H** (2001) Aminopeptidases A, B, and N and dipeptidase D are the four cysteinylglycinases of *Escherichia coli* K-12. *J Bacteriol* **183**: 1489–1490
- T. S, M. L, P. S, E. CM, P. V** (2015) In Vitro Activity of Glucosinolates and Their Degradation Products against Brassica-Pathogenic Bacteria and Fungi. *Appl Environ Microbiol* **81**: 432–440
- Tahir J, Watanabe M, Jing HC, Hunter DA, Tohge T, Nunes-Nesi A, Brotman Y, Fernie AR, Hoefgen R, Dijkwel PP** (2013) Activation of R-mediated innate immunity and disease susceptibility is affected by mutations in a cytosolic O-acetylserine (thiol) lyase in *Arabidopsis*. *Plant J* **73**: 118–130
- Takahashi H, Kopriva S, Giordano M, Saito K, Hell R** (2011a) Sulfur Assimilation in Photosynthetic Organisms: Molecular Functions and Regulations of Transporters and Assimilatory Enzymes. <https://doi.org/10.1146/annurev-arplant-042110-103921> **62**: 157–184
- Takahashi H, Kopriva S, Giordano M, Saito K, Hell R** (2011b) Sulfur Assimilation in Photosynthetic Organisms: Molecular Functions and Regulations of Transporters and Assimilatory Enzymes. *Annu Rev Plant Biol* **62**: 157–184
- Thomazella DP de T, Seong K, Mackelprang R, Dahlbeck D, Geng Y, Gill US, Qi T, Pham J, Giuseppe P, Lee CY, et al** (2021) Loss of function of a DMR6 ortholog in tomato confers broad-spectrum disease resistance. *Proc Natl Acad Sci* **118**: e2026152118
- Trdá L, Boutrot F, Ciaverie J, Brulé D, Dorey S, Poinssot B** (2015) Perception of pathogenic or beneficial bacteria and their evasion of host immunity: pattern recognition receptors in the frontline. *Front Plant Sci*. doi:

- Vanetten HD, Mansfield JW, Bailey JA, Farmer EE** (1994) Two Classes of Plant Antibiotics: Phytoalexins versus Phytoanticipins. *Plant Cell* **6**: 1191–1192
- Varesio LM, Fiebig A, Crosson S** (2021) *Brucella ovis* Cysteine Biosynthesis Contributes to Peroxide Stress Survival and Fitness in the Intracellular Niche. *Infect Immun.* doi: 10.1128/IAI.00808-20
- Vauclare P, Kopriva S, Fell D, Suter M, Sticher L, Von Ballmoos P, Krähenbühl U, Den Camp RO, Brunold C** (2002) Flux control of sulphate assimilation in *Arabidopsis thaliana*: adenosine 5'-phosphosulphate reductase is more susceptible than ATP sulphurylase to negative control by thiols. *Plant J* **31**: 729–740
- Verma D, Gupta V** (2021) New insights into the structure and function of an emerging drug target CysE. *3 Biotech* **11**: 373
- Verpoorte R, Choi YH, Kim HK** (2007) NMR-based metabolomics at work in phytochemistry. *Phytochem Rev* **6**: 3–14
- Verpoorte R, Choi YH, Mustafa NR, Kim HK** (2008) Metabolomics: back to basics. *Phytochem Rev* **7**: 525–537
- Vorholt JA** (2012) Microbial life in the phyllosphere. *Nat Rev Microbiol* 2012 1012 **10**: 828–840
- Wagner U, Edwards R, Dixon DP, Mauch F** (2002) Probing the diversity of the *Arabidopsis* glutathione S-transferase gene family. *Plant Mol Biol* **49**: 515–532
- Wang D, Peng C, Zheng X, Chang L, Xu B, Tong Z** (2020a) Secretome Analysis of the Banana Fusarium Wilt Fungi Foc R1 and Foc TR4 Reveals a New Effector OASTL Required for Full Pathogenicity of Foc TR4 in Banana. *Biomolecules.* doi: 10.3390/biom10101430
- Wang K, Kang L, Anand A, Lazarovits G, Mysore KS** (2007) Monitoring in planta bacterial infection at both cellular and whole-plant levels using the green fluorescent protein variant GFPuv. *New Phytol* **174**: 212–223
- Wang L, Tsuda K, Truman W, Sato M, Nguyen L V, Katagiri F, Glazebrook J** (2011) CBP60g and SARD1 play partially redundant critical roles in salicylic acid signaling. *Plant J* **67**: 1029–1041
- Wang W, Liu J, Mishra B, Mukhtar MS, McDowell JM** (2022) Sparking a sulfur war between plants and pathogens. *Trends Plant Sci* **27**: 1253–1265
- Wang W, Yang J, Zhang J, Liu Y-X, Tian C, Qu B, Gao C, Xin P, Cheng S, Zhang W, et al** (2020b) An *Arabidopsis* Secondary Metabolite Directly Targets Expression of the Bacterial Type III Secretion System to Inhibit Bacterial Virulence. *Cell Host Microbe* **27**: 601-613.e7
- Wildermuth MC, Dewdney J, Wu G, Ausubel FM** (2001) Isochorismate synthase is required to synthesize salicylic acid for plant defence. *Nature* **414**: 562–565
- Wingate VPM, Lawton MA, Lamb CJ** (1988) Glutathione Causes a Massive and Selective Induction of Plant Defense Genes. *Plant Physiol* **87**: 206–210

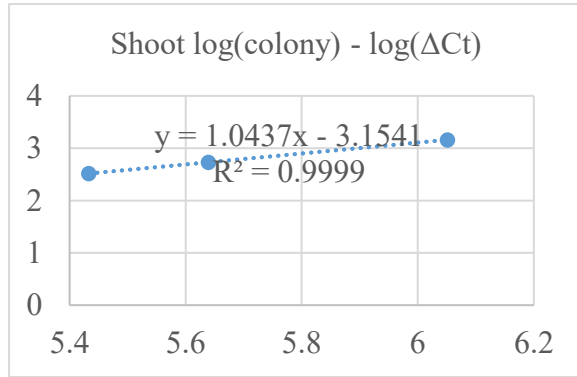
- Wittstock U, Halkier BA** (2000) Cytochrome P450 CYP79A2 from *Arabidopsis thaliana* L. Catalyzes the conversion of L-phenylalanine to phenylacetaldoxime in the biosynthesis of benzylglucosinolate. *J Biol Chem* **275**: 14659–14666
- Wu L, Chen H, Curtis C, Fu ZQ** (2014) Go in for the kill: How plants deploy effector-triggered immunity to combat pathogens. *Virulence* **5**: 710–721
- Xiang C, Werner BL, Christensen EM, Oliver DJ** (2001) The Biological Functions of Glutathione Revisited in *Arabidopsis* Transgenic Plants with Altered Glutathione Levels. *Plant Physiol* **126**: 564–574
- Yamaguchi C, Khamsalath S, Takimoto Y, Suyama A, Mori Y, Ohkama-Ohtsu N, Maruyama-Nakashita A** (2020) SLIM1 Transcription Factor Promotes Sulfate Uptake and Distribution to Shoot, Along with Phytochelatin Accumulation, Under Cadmium Stress in *Arabidopsis thaliana*. *Plants* (Basel, Switzerland). doi: 10.3390/plants9020163
- Yang L, Zhang Y, Guan R, Li S, Xu X, Zhang S, Xu J** (2020) Co-regulation of indole glucosinolates and camalexin biosynthesis by CPK5/CPK6 and MPK3/MPK6 signaling pathways. *J Integr Plant Biol* **62**: 1780–1796
- Yoshimoto N, Inoue E, Watanabe-Takahashi A, Saito K, Takahashi H** (2007) Posttranscriptional regulation of high-affinity sulfate transporters in *Arabidopsis* by sulfur nutrition. *Plant Physiol* **145**: 378–388
- Yu P, He X, Baer M, Beirinckx S, Tian T, Moya YAT, Zhang X, Deichmann M, Frey FP, Bresgen V, et al** (2021a) Plant flavones enrich rhizosphere Oxalobacteraceae to improve maize performance under nitrogen deprivation. *Nat plants* **7**: 481–499
- Yu Z, She M, Zheng T, Diepeveen D, Islam S, Zhao Y, Zhang Y, Tang G, Zhang Y, Zhang J, et al** (2021b) Impact and mechanism of sulphur-deficiency on modern wheat farming nitrogen-related sustainability and gliadin content. *Commun Biol* **4**: 945
- Zechmann B** (2020) Subcellular Roles of Glutathione in Mediating Plant Defense during Biotic Stress. *Plants* **9**: 1–21
- Zeilmaker T, Ludwig NR, Elberse J, Seidl MF, Berke L, Van Doorn A, Schuurink RC, Snel B, Van den Ackerveken G** (2015) DOWNY MILDEW RESISTANT 6 and DMR6-LIKE OXYGENASE 1 are partially redundant but distinct suppressors of immunity in *Arabidopsis*. *Plant J* **81**: 210–222
- Zhalnina K, Louie KB, Hao Z, Mansoori N, Da Rocha UN, Shi S, Cho H, Karaoz U, Loqué D, Bowen BP, et al** (2018) Dynamic root exudate chemistry and microbial substrate preferences drive patterns in rhizosphere microbial community assembly. *Nat Microbiol* **3**: 470–480
- Zhang Y, Zhao L, Zhao J, Li Y, Wang J, Guo R, Gan S, Liu C-J, Zhang K** (2017) S5H/DMR6 Encodes a Salicylic Acid 5-Hydroxylase That Fine-Tunes Salicylic Acid Homeostasis. *Plant Physiol* **175**: 1082–1093
- Zhao J, Williams CC, Last RL** (1998) Induction of *Arabidopsis* Tryptophan Pathway Enzymes and Camalexin by Amino Acid Starvation, Oxidative Stress, and an Abiotic Elicitor. *Plant Cell* **10**: 359–370

Supplemental data

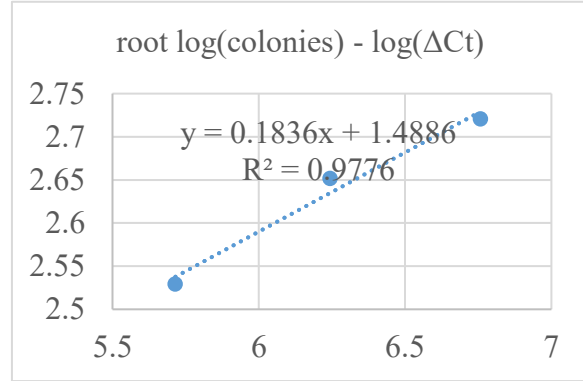
Table S1 Stock solution used for minimal medium				
Compound	MW	Stock conc (M)	Mass to add (g)	Final conc (M) - once diluted in media
1. M9 salts - 10x stock, 400 ml				
Na ₂ HPO ₄ x 2 H ₂ O	177.99	0.477505036	16.99822428	0.047750504
KH ₂ PO ₄	136.09	0.220442354	6	0.022044235
NaCl	58.44	0.085557837	1	0.008555784
2. Trace Elements - 1000x Stock, 1000 ml				
MnCl ₂ x 4H ₂ O	197.91	0.01	1.9791	0.00001
H ₃ BO ₃	61.83	0.05	3.0915	0.00005
ZnCl ₂	136.3	0.00175	0.238525	0.00000175
CuCl ₂	134.45	0.0005	0.067225	0.0000005
Na ₂ MoO ₄	205.92	0.0008	0.164736	0.0000008
KI	166	0.001	0.166	0.000001
CoCl ₂ x 6H ₂ O	237.93	0.0001	0.023793	0.0000001
3. Iron Source - 1000x Stock, 200 ml				
Fe-EDTA	367.05	0.05	3.6705	0.00005
4. Calcium Source - 1000x Stock, 200 ml				
CaCl ₂ x H ₂ O	147.01	0.1	2.9402	0.0001
5. Nitrogen Source - NH₄Cl - 100x Stock, 200 ml				
NH ₄ Cl	53.49	2	21.396	0.02
6. Sulfur Source - MgSO₄x7H₂O - 100x Stock, 200 ml				
MgSO ₄ x 7H ₂ O	246.47	0.1	4.9294	0.001
7. Carbon Source - 10x Stock, 400 ml				
Glucose	180.1	0.5	36.02	0.05

Table S2 Comparison analysis of two quantification methods for bacterial growth rates

A



B



To relate the qPCR results to the bacteria titre, and to ensure that qPCR value is able to represent bacteria concentration, bacterial concentration of shoots and roots was assessed through two ways in parallel: routinely used plate counting method and the qPCR-based method. The colonies and Δ Ct value were correlated well.

List of abbreviations

Col-0	Arabidopsis ecotype Columbia-0
<i>cad2</i>	<i>CADMIUM-SENSITIVE 2</i> mutant
MYB	R2R3-MYB transcription factor family
APS	Adenosine 5'-phosphosulfate
APK	APS kinase
PAPS	3'-phosphoadenosine 5'-phosphosulfate
SiR	Sulfite Reductase
OAS	<i>O</i> -acetylserine
OAS-TL	<i>O</i> -acetylserine (thiol) lyase
SAT	Serine acetyltransferase
SULTR	Sulfate transporter
APR	Adenosine 5'-phosphosulfate reductase
SLIM1	Sulfur limitation 1
GST6	Glutathione S-transferase 6
GSTTU3	Glutathione S-transferase tau 3 (GSTU3)
ROS	Reactive oxygen species
DAB	3,3'-Diamino-benzidin
<i>Pst</i>	<i>Pseudomonas syringae</i> pv. <i>tomato</i> DC3000
Pip	Pipecolic acid
SA	Salicylic acid
JA	Jasmonic acid
ET	Ethylene
Cys	Cysteine
Met	Methionine
GLS	Glucosinolates
ITCs	Isothiocyanates
SSC	S-sulfocysteine
PT1	Pattern-triggered immunity

ET1	Effector-triggered immunity
SAR	Systemic acquired resistance
HR	Hypersensitive response
ISR	Induced systemic resistance
PAL	Phenylalanine ammonia-lyase 1
ICS1	Arabidopsis isochlorogenic acid synthase 1
ALD1	AGD2-like defense response protein 1
PR	pathogenesis-related
PCD	Programmed cell death
DNA	Deoxyribonucleic acid
T-DNA	Transfer DNA
cDNA	Complementary DNA
RNA	Ribonucleic acid
PCR	Polymerase chain reaction
HPLC	High-performance liquid chromatography
qRT-PCR	Reverse transcription–quantitative PCR (qPCR)
GFP	Green fluorescent protein
EDTA	Ethylenediaminetetraacetic acid
EtOH	Ethanol
MeOH	Methanol
IAOx	Indole-3-acetaldoxime
LB	Lysogenic broth medium
M9	Minimal medium
Min	Minutes
DPI	Days post inoculation
HPLC	High-performance liquid chromatography

List of tables and figures

Table 1	Arabidopsis mutant lines used in this study
Table 2	Minimal medium without sulfate (M9)
Table 3	Stock solution of sulfur sources (0.1 M sulfur)
Table 4	Composition of media with different sulfur sources
Table 5	Composition of modified Long Ashton medium
Table 6	Preparation of the DAB staining solution in detail
Table 7	Composition of media containing shoot extracts
Table 8	DNA isolation buffer
Table 9	qRT-PCR program
Table 10	RNA isolation buffer (for 200 ml)
Table 11	Oligonucleotides for gene expression analysis by qRT-PCR
Table S1	Stock solution used for minimal medium
Table S2	Comparison analysis of two quantification methods for bacterial growth rates
Figure 1.1	Scheme of plant sulfate assimilation
Figure 1.2	Regulatory pathways and components under sulfur deficiency condition of Arabidopsis
Figure 1.3	Sulfur assimilation and L-cysteine biosynthesis pathway in <i>Escherichia coli</i>
Figure 3.1	<i>cysH</i> mutant grows slower than PG1 and <i>cysM</i> with oxidized sulfur sources
Figure 3.2	PG1, <i>cysH</i> and <i>cysM</i> inhibit growth of Arabidopsis Col-0
Figure 3.3	PG1 induces lesions on Col-0 leaves
Figure 3.4	PG1 cause heavier Arabidopsis plant cell death than <i>cysH</i> and <i>cysM</i>
Figure 3.5	Camalexin induction by PG1, <i>cysH</i> and <i>cysM</i>
Figure 3.6	Sulfur assimilation deficiency negatively affects nutrient uptake in plant
Figure 3.7	Proliferation of PG1 inside plants is notably higher than <i>cysH</i> and <i>cysM</i>
Figure 4.1	Modulation of sulfur assimilation in <i>Arabidopsis</i> affects immune response to <i>B. glumae</i> PG1
Figure 4.2	Contents of sulfate, phosphate and nitrate display different pattern upon bacterial infection
Figure 4.3	Thiols (glutathione and cysteine) content in shoots and roots

Figure 4.4	The amount of GLS is not altered by pathogenic infection
Figure 4.5	Pip and SA accumulation in shoots of Col-0, <i>myb28 myb29</i> and <i>slim1</i>
Figure 4.6	Relative expression of genes involved in Pip and SA biosynthesis pathway
Figure 4.7	The growth rate of bacterial strains in media containing shoot metabolites
Figure 4.8	Bacterial abundance in shoots and roots of Col-0, <i>myb28 myb29</i> and <i>slim1</i>

Acknowledgement

This thesis not only reflects my research results and hard work over the past three years, but also summarizes the support and assistance of my supervisor, PhD colleagues, technicians, and others from external of our lab.

First of all, I would like to express my deepest gratitude to my supervisor Prof. Dr. Stanislav Kopriva. He is a nice and responsible mentor. He gave me extensive instructions on my project, including offering me a great opportunity to work on this interesting project, preparing the outline, discussing the developments of the project and supporting my writing. He motivated me a lot when I am stressed, especially during the Corona epidemic. Without his motivation, I couldn't think I can be better. We met regularly to discuss the progress of the project. At the meeting, he answered my questions and guided the direction of the project. He nicely offered me a chance to participate an international conference in Ireland, where I met people work on a diverse of Arabidopsis-related projects and broadened my horizon.

Secondly, I would like to thank Dr. Hanna Koprivova in our lab. She was a great help when I first came to the lab. She patiently and carefully taught me the experimental methods and gave me feedback on my experimental results. Also, she is a responsible person providing support to a lot of tasks in the lab.

Furthermore, my PhD colleagues in the lab have definitely provided a lot of help from the start of my project to the end of the work, especially helped me a lot with editing my thesis. This kind of help is not only about experiments and researches, but also about supporting me when I am stressed. They provide me sound advice and tips based on their own practical experience. We had great times together, which will be a treasure for me. Thank you, Melina Schwier, José Maria López Ramos, Ivan Zenzen, Raissa Krone. Without you, the life of PhD will be hard. The technicians Sabine Ambrosius, Irene Klinkhammer and Bastian Welter have also been great at patiently answering my questions when something is unclear. Without them, I couldn't adapt to the lab so fast and so well. I would like to also thank Dr. Richard P. Jacoby, who taught me great method about high-biomass culture of Arabidopsis and extracting metabolites from shoots and roots. I also appreciate help external our lab: Nicole Mantke helped me measure total carbon, Prof. Dr. Jürgen Zeier and Ms. Karin Kiefer helped me measure Pip and SA. I would like to express my thanks to Prof. Dr. Alga Zuccaro, Dr. Johana Stadtel geb. Misas Villamil, who are members of my TAC and gave me nice suggestions on my project.

Finally, my family and friends provided me a lot of company and encouragement during the past three years, we hiked together and enjoyed the nature of Germany, without them the life in Germany wouldn't be colorful.

This research is funded by Deutsche Forschungsgemeinschaft and my living in Germany is supported by the Chinese Scholarship Council.



Erklärung

Erklärung zur Dissertation

gemäß der Promotionsordnung vom 12. März 2020

„Hiermit versichere ich an Eides statt, dass ich die vorliegende Dissertation selbstständig und ohne die Benutzung anderer als der angegebenen Hilfsmittel und Literatur angefertigt habe. Alle Stellen, die wörtlich oder sinngemäß aus veröffentlichten und nicht veröffentlichten Werken dem Wortlaut oder dem Sinn nach entnommen wurden, sind als solche kenntlich gemacht. Ich versichere an Eides statt, dass diese Dissertation noch keiner anderen Fakultät oder Universität zur Prüfung vorgelegen hat; dass sie - abgesehen von unten angegebenen Teilpublikationen und eingebundenen Artikeln und Manuskripten - noch nicht veröffentlicht worden ist sowie, dass ich eine Veröffentlichung der Dissertation vor Abschluss der Promotion nicht ohne Genehmigung des Promotionsausschusses vornehmen werde. Die Bestimmungen dieser Ordnung sind mir bekannt. Darüber hinaus erkläre ich hiermit, dass ich die Ordnung zur Sicherung guter wissenschaftlicher Praxis und zum Umgang mit wissenschaftlichem Fehlverhalten der Universität zu Köln gelesen und sie bei der Durchführung der Dissertation zugrundeliegenden Arbeiten und der schriftlich verfassten Dissertation beachtet habe und verpflichte mich hiermit, die dort genannten Vorgaben bei allen wissenschaftlichen Tätigkeiten zu beachten und umzusetzen. Ich versichere, dass die eingereichte elektronische Fassung der eingereichten Druckfassung vollständig entspricht.“

Teilpublikationen:

CHEN, Li
Köln, 26.01.2023



Curriculum Vitae

Li Chen

1st of June 1993, Born in Xiantao, China, chenli315@mails.ucas.ac.cn

Bernkasteler Straße 52, 50969, Köln, Germany

Education

Doctorate	University of Cologne, Institute of Plant Sciences, Cologne, Germany
Since September of 2019	Thesis: Alteration of sulfur assimilation pathway in plants and pathogens affect immune resistance and pathogenicity Supervisor: Prof. Dr. Stanislav Kopriva
Master of Science	University of Chinese Academy of Sciences, Beijing, China
October 2015 - June 2018	Thesis: The role of gut-associated bacteria of <i>Dendroctonus valens</i> in overcoming abietic acid defense of its host pine trees Supervisor: Prof. Dr. Jianghua Sun
Bachelor of Technology	Hubei University of Technology, Wuhan, China
October 2011 – June 2015	Thesis: Effects of four antibiotics and their combination to gut-associated microbiota abundance of <i>Dendroctonus valens</i> Supervisor: Prof. Dr. Jianghua Sun

Publications

-
1. Jacoby RP, **Chen L**, Schwier M, Koprivova A, Kopriva S (2020) Recent advances in the role of plant metabolites in shaping the root microbiome. F1000Research. doi: 10.12688/F1000RESEARCH.21796.1
 2. Cao Q, Wickham JD, **Chen L**, Ahmad F, Lu M, Sun J (2018) Effect of Oxygen on Verbenone Conversion From cis-Verbenol by Gut Facultative Anaerobes of *Dendroctonus valens*. Front Microbiol 9: 464
 3. Cheng C, Wickham JD, **Chen L**, Xu D, Lu M, Sun J (2018) Bacterial microbiota protect an invasive bark beetle from a pine defensive compound. Microbiome 6: 132

4. Xu L, Lu M, Xu D, **Chen L**, Sun J (2016) Sexual variation of bacterial microbiota of *Dendroctonus valens* guts and frass in relation to verbenone production. *J Insect Physiol* 95: 110–117

26.01.2023, Köln